Supporting Information

Sequential multicomponent catalytic synthesis of pyrrole-3-carboxaldehydes: Evaluation for antibacterial and antifungal activities along with docking studies

Nisar A. Mir,[a] Panduga Ramaraju,[a] Satheeshvarma Vanaparthi,[a] Sachin Choudhary,[a] Rajnish P. Singh,[b] Preetika Sharma,[c] Rajni Kant,[c] Rajpal Singh,[d] Murugesan Sankaranarayanan,[e] and Indresh Kumar*[a]

[a]*Department of Chemistry, Birla Institute of Technology & Science, Pilani 333 031, India*

[b]*Department of Biological Science, Birla Institute of Technology & Science, Pilani*

[c]*X-ray Crystallography Laboratory, Post-Graduate Department of Physics & Electronics, University of Jammu, India*

[d]*Research & Development Centre in Pharmaceutical Science and Applied Chemistry, Bharati Vidyapeeth Deemed University, Erandawane, Pune, India*

[e]*Department of Pharmacy, Birla Institute of Technology & Science, Pilani*

Corresponding Email: indresh.kumar@pilani.bits-pilani.ac.in, indresh.chemistry@gmail.com

Table of Contents

Synthesis of 4-Oxo-4-phenylbutanal (4a):[1]

To a stirred solution of crushed Magnesium turnings (0.56 g, 23.2 mmol, 2.0 equiv.) in dry THF (10.0 mL) was added a solution of bromobenzene (1.81 g, 11.6 mmol, 1.0 equiv.) in dry THF (10.0 mL) dropwise using syringe at room temperature slowly for one hour under inert atmosphere. This in situ prepared Grignard reagent solution was cooled to 0 °C and added dropwise to the stirred solution of γ-butyrolactone (1.0 g, 11.6 mmol, 1.0 equiv.) in dry THF (10.0 mL) at 0 °C through cannula over 30 minutes. The combined reaction mixture was stirred at 0 °C for additional 2 h, and quench by saturated NH_4Cl solution (15.0 mL) and stirred with EtOAc (20.0 mL). The organic layer was separated, and aqueous layer was again extracted with EtOAc (10.0 mL), the combined extracts were washed with brine (15.0 mL), dried over Na_2SO_4, filtered, and concentrated in vacuo. The residue was purified by silica gel (100-200 mesh) column chromatography (Hexane: EtOAc, 20:1 to 5:1) to give the desired 4-Hydroxy-1-phenylbutan-1-one as a white semi-solid (1.30 g, 68% yield).

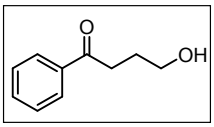

White semi-solid, ^{1}H NMR (400 MHz, $CDCl_3$) δ 1.89-1.96 (m, 2H), 3.05 (t, *J* = 7.0 Hz, 2H), 3.65 (t, *J* = 6.2 Hz, 2H), 3.98 (bs, 1H), 7.42 (d, *J* = 7.8 Hz, 2H), 7.52 (t, *J* = 7.4 Hz, 1H), 7.92 (d, *J* = 7.2 Hz, 2H); ^{13}C NMR (100 MHz, $CDCl_3$) δ 26.53, 34.71, 62.32, 126.12 (2C), 128.12 (2C), 132.65, 146.82, 200.31; IR (KBr)/cm^{-1} 3379, 2939, 1766, 1172, 1033; HRMS (ESI-TOF) *m/z*: [M + H$^+$] Calcd for $C_{10}H_{12}O_2$ 165.0916; Found 165.0921.

Next, 4-Hydroxy-1-phenylbutan-1-one (0.5 g, 3.0 mmol, 1 equiv.) was stirred with pyridinium chlorochromate (PCC) (0.98 g, 4.6 mmol, 1.5 equiv.) and celite (0.25 g) in dichloromethane (4.0 mL) for 3 h at room temperature. After completion, reaction was filtered over a pad of Na_2SO_4, and concentrated in vacuo. The residue was purified by column chromatography (Hexane:EtOAc = 90:10 to 70:30) to give the desired product keto-aldehyde **(4a)** as a yellow oily liquid (0.272 g, 55% yield).

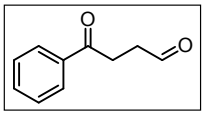

Yellow liquid, ^{1}H NMR (400 MHz, $CDCl_3$) δ 2.79-2.97 (m, 2H), 3.31 (t, *J* = 6.3Hz, 2H), 7.40-7.48 (m, 2H), 7.57 (t, *J* = 7.5 Hz, 1H), 7.98 (d, *J* = 7.6 Hz, 2H),

9.90 (s, 1H); 13C NMR (100 MHz, $CDCl_3$) δ 30.97, 37.54, 128.00 (2C), 128.60 (2C), 133.27, 136.37, 197.83, 200.70; IR (KBr)/cm^{-1} 2923,1728, 1681, 1211, 979, 694; HRMS (ESI-TOF) *m/z*: [M + H^+] Calcd for $C_{10}H_{10}O_2$ 163.0759; Found 163.0763.

Similarly, all other 1,4-ketoaldehydes were prepared by following this protocol.

Mechanism details:

Based on our initial study and literature precedents on proline **1** catalysed Mannich reaction, the following stepwise mechanism is proposed to account for this reaction. As shown in **Scheme S1**, the enamine **I** *in situ* generated from 1,4-ketoaldehyde **4** and proline **1**, reacts with imine **II** *in situ* prepared from aromatic aldehyde **2** and aromatic amines **3** *via* a direct Mannich reaction to produce **III**. The intermediate **III** undergoes intramolecular cyclization to dihydropyrrole **IV**, with the simultaneous release of catalyst **1**, and subsequently underwent aerobic oxidative aromatization to afford the heavily substituted pyrrole 3-carboxaldehyde **5**.

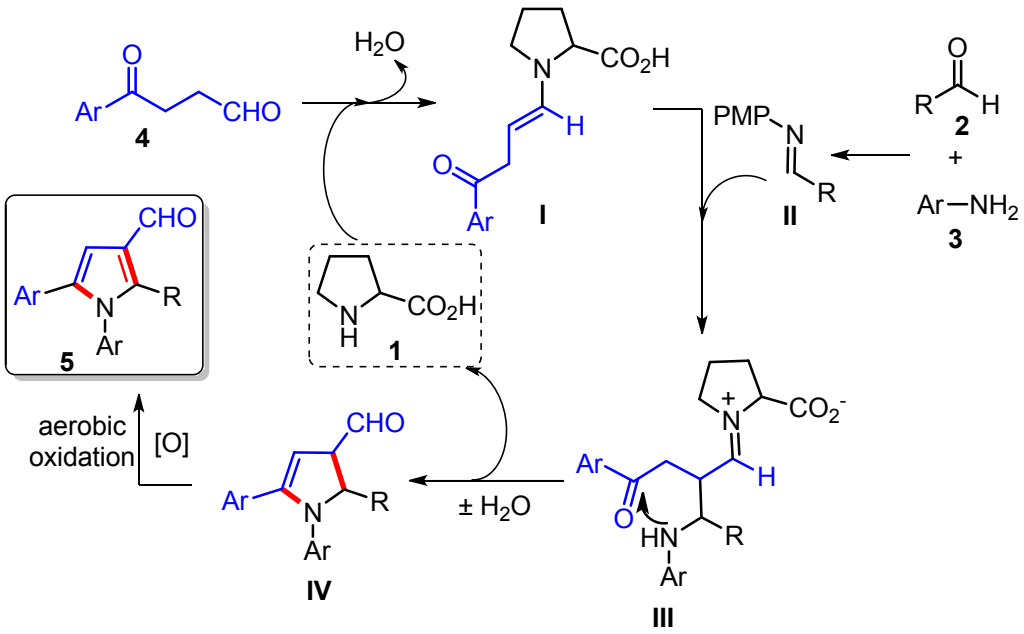

Scheme S1. Plausible mechanism of the proline catalyzed pyrrole synthesis

1.1 Supporting data for the biological studies

1.1.1 Bacterial culture

The pathogenic Gram negative bacterial strain *Escherichia coli* (MTCC 1652), *Pseudomonas putida* (MTCC 102) and gram positive bacteria *Bacillus subtilis* (MTCC 121) and *Staphylococcus aureus* (MTCC 96) were procured from Microbial Type Culture Collection and Gene Bank (MTCC), Chandigarh, India.

1.1.2 Antibacterial assay

The antibacterial assay (ZICs) was performed as per the well diffusion method. All compounds were dissolved in dimethylsulfoxide (DMSO) and serial dilution of each compound was prepared in the concentrations of 512, 256, 128, 64, 32, 16, 8, 4, 2, 1, 0.5 µg/ml. For the experimental work, autoclaved Muller-Hilton (Himedia, India) agar medium was prepared and poured into sterile glass petri-dishes under aseptic conditions using laminar airflow chamber. After solidification of medium, the suspension of the pathogenic microorganism (10^6 CFU/ml) was spread onto the individual media plates using a sterile glass spreader. After adsorption of bacterial suspension, well size of 6mm diameter was made by the sterile metallic borer and the solution of working compound of different concentration was poured into the wells. The plates were incubated at 37 °C for 18-24 h under dark conditions. The determination as to whether the organism is susceptible, intermediate, or resistant was made by measuring the size of zone of inhibition in comparison with standard antibiotic. DMSO was used as negative control while Chloramphenicol was used as a positive control. Similarly, antibacterial assay (MICs) was performed in vitro by the modified microbroth dilution method as per defined by the National Committee for Clinical Laboratory Standards (1993). Serial diluted test samples of each compound (90µl) were prepared in 96 well micro-trays. The same amount of test

microorganism was added to micro-trays well under aseptic condition to obtain a final volume of 180 µl and incubated at 37 °C for 24 h. MICs value is defined as the lowest concentration of compound that inhibit the visible growth of bacteria. All assays were performed in duplicate sets. The bactericidal activity of synthesized compounds was evaluated in terms of zone of inhibition (ZICs) and minimum inhibitory concentration (MICs).

Table S1: Antibacterial and antifungal test of the synthesized compound

Code of compound	*E. C*	*P. P*	*B. S*	*S. A*	*F.O*	*F.G*	*A.F*
5d	+	+	+	+	+	+	+
5e	+	+	+	+	-	-	-
5f	+	+	+	+	-	-	-
5g	+	+	+	+	+	+	+
5i	+	+	+	+	-	-	-
5m	+	+	+	+	-	-	-
9	+	+	+	+	-	-	-

EC: *Escherichia coli, PP*: *Pseudomonas putida*, *BS*: *Bacillus subtilis*, *SA*: *Staphylococcus auresus*, *FO*: *Fusarium oxysporum, FG: Fusarium graminearum*, *AF*: *Aspergillus flavus*.

1.2Antifungal assay

1.2.1 Fungal culture

The fungal strains namely *Fusarium oxysporum* (MTCC 284), *Fusarium graminearum* (1893) and *Aspergillus flavus* (MTCC 2798) procured from MTCC, were maintained on potato dextrose agar (PDA, Himedia, India) plate and used for antifungal assay.

1.2.2 Antifungal screening

Antifungal activities of chemically synthesized compounds were evaluated by agar well diffusion method at a varying concentration for all the compounds. For the experimental work, Potato dextrose broth (PDB, Himedia, India) was freshly prepared and autoclaved at 121°C at 15 psi for 15 min. After cooling to room temperature, a loopful of fungal mycelium was inoculated into freshly prepared PDB broth for 4-5 days at 28°C. After the proper growth, 100 µl of this inoculum was uniformly spread on the Potato dextrose agar plate. Following the adsorption of inoculum, well size of 6 mm diameter was prepared by the sterile metallic borer and compound solution was added in respective wells. Plates were incubated at 28°C for 4 days under dark conditions. Mean diameter of inhibition zone was measured to determine the antifungal activity. The experiment was performed in triplicates. MIC assay of all the compounds was performed at above mentioned concentrations. Tubes containing 10 mL of sterilized czapeks dox broth medium was inoculated with freshly grown culture. Appropriate amount of compound was added to achieve the desired concentrations. The tubes were incubated at 28 °C for 4 days under dark conditions and carefully observed for the presence of turbidity. Amphotericin B was used as positive control.

1.3 Supporting details for the docking studies:

Materials and methods:

The docking studies were carried out using Schrodinger software[2] (Version 2019-1, Schrodinger) installed on Intel Xenon W 3565 processor and Ubuntu enterprise version 14.04 as the operating system. Targeted ligands were drawn in ChemDraw 18.0. The result of the docking study was analyzed with the help of XP Visualiser (Version 2019-1, Schrodinger). Toxicity prediction studies were performed by using ProTox-II an online-based web server.

Ligand preparation:

The ligands used as input for docking study was sketched using ChemDraw software and cleaned up the structures for bond alignment, ligands were incorporated into the workstation, the energy was minimized using OPLS3e force field in Ligprep[2] (Version 2019-1, Schrodinger). This minimization helps to assign bond orders, addition of hydrogens to the ligands and conversion of 2D to 3D structure for the docking studies. The generated output file (the best conformations of the ligands) was further used for docking studies.

Receptor grid generation:

A receptor grid was generated around the protein by picking the inhibitory ligand (X-ray pose of the ligand in the protein). The centroid of the ligand is selected to create a grid box around it and the Vander Waal radius of receptor atoms was scaled to 1.00 Å with a partial atomic charge of 0.25.

Protein preparation:

Protein was prepared by using protein preparation wizar[3] (Version 2019-1, Schrodinger). Hydrogen atom was added to the proteins and charges were assigned. Generated Het states using Epik at pH 7.0 ±2.0. Pre-process the protein and refine, modify the protein by analyzing the workspace, water molecules and other heteroatoms were examined and the non-significant atoms were excluded from the crystal structure of the protein. Finally, the protein was minimized by using OPLS3e force filed. A grid was created by considering the co-crystallized ligand which was included in the active site of the selected target Bacterial DNA gyrase B (PDB-4DUH).

Docking studies:

Docking studies of the significantly active molecule (**5e**) was performed by using Glide modul[4] in Schrodinger. All docking calculations were performed by using Extra Precision (XP) mode. A scaling factor of 0.8 and a partial atomic charge of less than 0.15 was applied to the atoms of the protein. Glide docking score was used to determine the best-docked structure from the output. The interactions of these docked complexes were investigated further using XP visualizer.

***In-silico* prediction of Physicochemical parameters:**

The physicochemical parameters of the designed compounds were *in-silico* predicted by using Qik-prop Module in Schrödinger. The different parameters predicted were; molecular weight (M. Wt.), total solvent-accessible volume (TSAV), number of hydrogen bond donor (HBD), number of hydrogen bond acceptor (HBA), Van der walls polar surface area (PSA) of nitrogen and oxygen atoms, octanol/water partition coefficient (log P), aqueous solubility (Log S), predicted apparent Caco-2 cell permeability in nm/sec (PCaco), apparent Madin Darby Canine Kidney (MDCK) permeability and Percentage of human oral absorption.

Table S2: Principal descriptors predicted by QikProp

S. No	Code	M. Wt.[a]	Donor HB[b]	Accept HB[c]	Volume[d]	PSA[e]
1	[5d]	367.45	0	2.75	1204.69	46.88
2	[5e]	354.41	0	4.25	1133.41	59.84
3	[5f]	354.41	0	4.25	1133.61	59.85
4	[5g]	359.44	0	2.75	1118.24	47.16
5	[5i]	392.46	0	4.25	1271.03	72.67
6	[5m]	410.52	0	4.25	1345.94	59.79
7	[9]	578.54	1	6.25	1660.42	164.97

[a] *Molecular weight, in Da (range for 95% of drugs: 130–725 Da)*

[b] *No: of Hydrogen bonds donated by the molecule (range for 95% of drugs: 0-6).*

[c] *No: of Hydrogen bonds accepted by the molecule (range for 95% of drugs: 2-20)*

[d] *Total solvent-accessible volume in cubic angstroms using a probe with a 1.4 Å radius. (500– 2000)*

[e] *Van der Waals surface area of polar nitrogen and oxygen atoms. (7– 200)*

Table S3: Physicochemical descriptors predicted by Qikprop

S. No	CODE	logPo/w[f]	logS[g]	PCaco[h]	MDCK[i]	Percent Human Oral Absorption[j]
1	[5d]	5.79	-7.10	2034.32	1065.90	100
2	[5e]	4.42	-5.61	1099.95	548.36	100
3	[5f]	4.42	-5.61	1098.44	547.55	100
4	[5g]	5.35	-6.40	1985.46	1559.44	100
5	[5i]	4.95	-7.89	422.36	194.88	100
6	[5m]	5.72	-7.21	1166.82	584.49	100
7	[9]	5.62	-9.14	14.59	5.13	41.82

[f]*Predicted octanol / water partition co-efficient log P (acceptable range: –2.0 to 6.5)*

[g]*Predicted aqueous solubility; S in mol/L (acceptable range: –6.5 to 0.5).*

[h]*Apparent Caco-2 permeability (nm/s) (<25 poor, >500 great).*

[i]*Apparent MDCK permeability (nm/s) (<25 poor, >500 great).*

[J]*Percentage of human oral absorption (<25% poor and >80% is high)*

In-silico prediction of Physicochemical and ADME properties:

Pharmacokinetic properties of a compound play a vital role in the drug distribution and metabolism studies. The prediction studies of the above-discussed parameters are crucial for the new compound to develop as a lead molecule. The newly synthesized targeted compounds were obeyed all the studied parameters. The critical descriptors like molecular weight, volume, hydrogen bond acceptors and donors, and polar surface area of the titled compounds (Table-S2), predicted values were within the acceptable range only.

The physicochemical descriptors of the titled compounds were predicted. Most of the titled compounds were following the parameters that were followed by majority of the approved drugs. Partition coefficient predicted values were within the acceptable range only (Table-S3). The aqueous solubility of the compounds was less when compared with the standard values. The compounds **5d**, **5i**, **5m** and **9** showed the less aqueous solubility and the compound 9 only showed less Caco-2 permeability. All the compounds exhibited 100% human oral absorption except **9**, but these are in

acceptable range only, the compound **9** was deviating all the predicted parameters. The maximum of the titled compounds obeyed the rules which were followed by the approved drugs. So, based on these predictions, the titled compounds may not face any problem in further screening in the mere future.

In-silico toxicity prediction studies

Toxicity prediction studies were carried out by using ProTox-II[5] online server and various toxicity endpoints, such as hepatotoxicity, carcinogenicity, immunotoxicity, mutagenicity and cytotoxicity has been predicted. The structures were converted into Smiles format as input for the prediction and the results were analyzed.

Table S4: Results of In-silico toxicity prediction

S. No	Code	Hepatotoxicity	Carcinogenicity	Immunotoxicity	Mutagenicity	Cytotoxicity
1	[5d]	Active	Active	Inactive	Inactive	Inactive
2	[5e]	Inactive	Active	Inactive	Inactive	Inactive
3	[5f]	Inactive	Active	Inactive	Inactive	Inactive
4	[5g]	Active	Active	Inactive	Inactive	Inactive
5	[5i]	Inactive	Active	Inactive	Inactive	Inactive
6	[5m]	Inactive	Active	Inactive	Inactive	Inactive
7	[9]	Active	Active	Active	Active	Inactive

Results and discussion for the toxicity studies

The result of the toxicity prediction studies of the titled compounds revealed that all the compounds were inactive in cytotoxicity, mutagenicity and immunotoxicity. Carcinogenicity was revealed by all the compounds, but the probability is less (average probability 0.5). Some of the compounds (**5d**, **5g**, **5ao**, **5i** and **9**) showed hepatotoxicity. However, overall the study revealed that the compounds are weakly toxic (except compound **9**) and some of the parameters were displayed extremely non-toxic (Table S4)

Molecular docking studies

The crystal structure of Bacterial DNA gyrase-B (PDB-4DUH)[6] was retrieved from Protein data bank[7] (https://www.rcsb.org/structure/4DUH) with a resolution of 1.5 A°. The protein consist of 2 chains A and B (homodimer). After importing the crystal structure into the work station of Schrodinger, the protein was prepared by protein reparation wizard and the A chain was selected. A grid was generated by using the co-crystallized ligand. The co-crystal ligand was extracted from the protein and re-docked into the generated grid and checked for superimposition for the validation of the protocol. The Root meansquare deviation (RMSD) was found to be 0.61A° indicated that the docking protocol could be reliable for the docking study (Figure-S1).

Table S5: Docking relations between aminoacid residues, water molecules with the co-crystal ligand and significantly active compound in the targeted protein

S. No.	Code	Hydrogen-bond	Aromatic bond	π-cationic interactions	Salt bridge	Glide score (Kcal/mol)	Glide energy (Kcal/mol)
1	**Co-crystal ligand (PDB - 4DUH)**	GLY-101 ASP-73 HOH-614 HOH-702 ARG-136 (2)	GLY-101	LYS-103	ARG-136 ARG-76	-9.5	-66.12
2	**Significantly active compound-5ak**	ARG-76	GLY-101 (2)	ARG-76	-	-2.4	-28.09

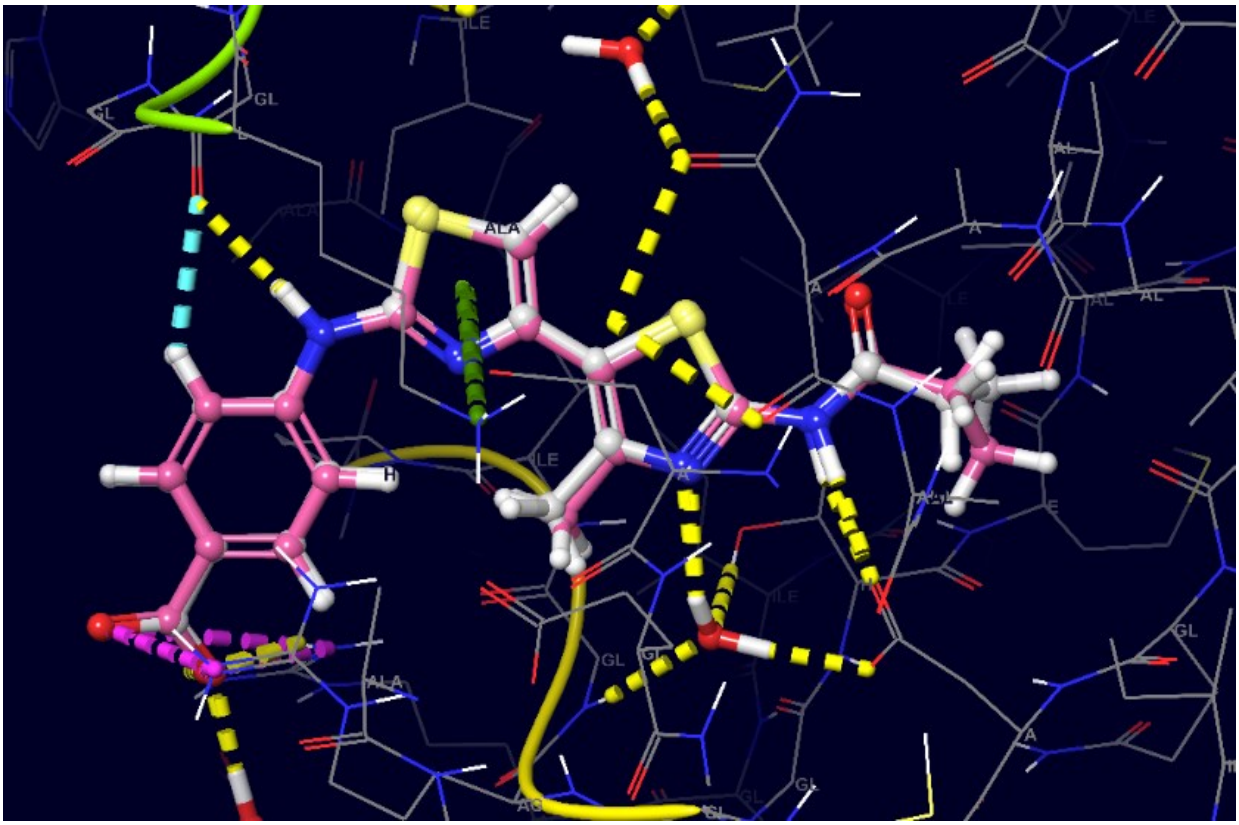

Figure S1. Superimposed view of the native pose of ligand (X-ray crystallized pose) and docked pose of the same ligand in the active site of the protein (4DUH) (Root mean square deviation 0.61A^{O})

(Color interpretation - Pink color- Binding pose after docking, White color- X-ray native pose of ligand)

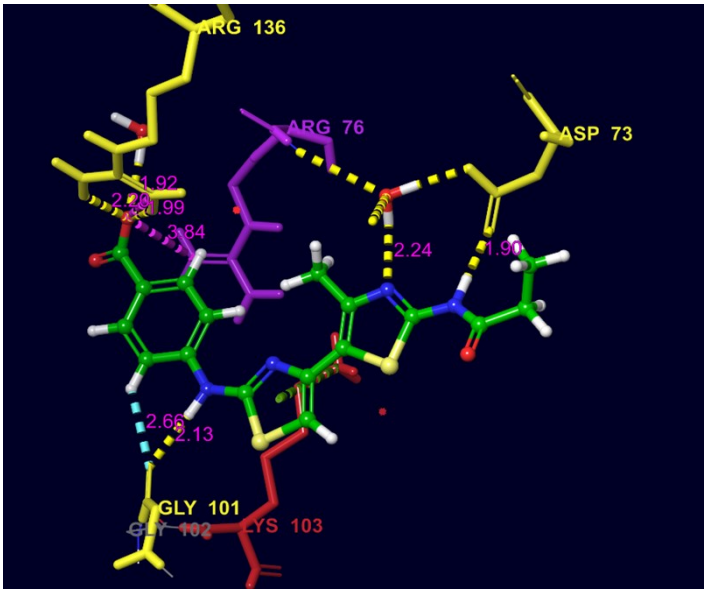

Figure S2. Docked pose of Co-crystallized ligand (green color) and its interactions in the active site of the protein-4DUH (rest of the protein was suppressed for the clarity)

[Color interpretation Yellow- Hydrogen bond, Blue- Aromatic bond, Red- Pi cationic interaction and Magenta- salt bridge]

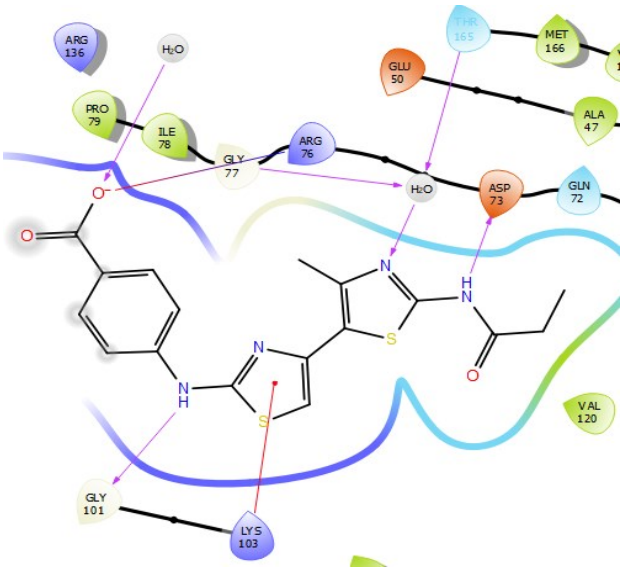

Figure S3. 2D representation of the docked pose of the co-crystallized ligand

[Color interpretation Magenta- Hydrogen bond, Red – Pi cationic interaction]

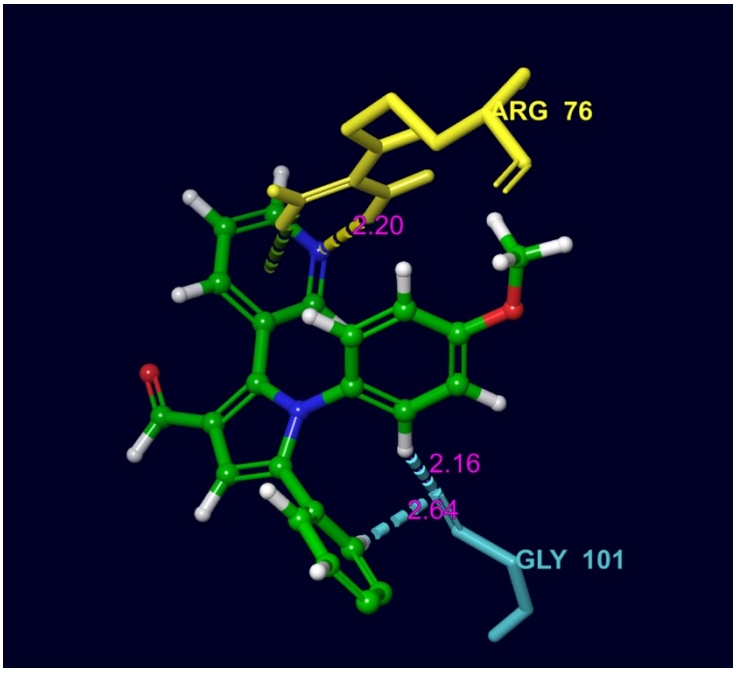

Figure S4. Docked pose of the significantly active compound **5e** (green color) exhibited various interactions in the active site of the protein (4DUH) (rest of the protein was suppressed for the clarity)

[Color interpretation Yellow- Hydrogen bond, Blue- Aromatic bond]

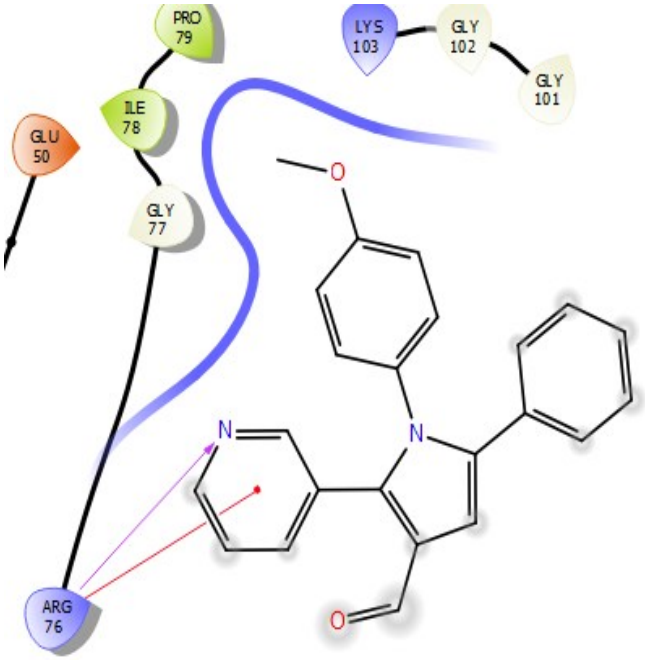

Figure S5. 2D representation of the docked pose of the significantly active compound **5e**

[Color interpretation Magenta- Hydrogen bond, Red – Pi-cationic interaction]

Results and discussion for docking studies

The docking study of the native pose of the ligand (co-crystal ligand, 3D pose) showed good interactions with the surrounded amino-acid residues and water molecules (Figure-S2). The 2D docked pose revealed six hydrogen bond interactions were displayed by the co-crystal ligand (Figure-S3), which plays an essential role in the stable conformation of the co-crystal ligand with a docking score of -9.5 kcal/mol and energy of -66.12 kcal/mol (Table-S5). GLY-101 and ASP-73 amino acid residues contributed their role in the hydrogen bond formation. Amino acid residue ARG-136 displayed two hydrogen bond interactions. Apart from hydrogen bond, the amino-acid residue GLY-101 is also exhibited one aromatic bond interaction. With one π-cationic interaction with LYS-103 and two salt bridges with ARG-136, ARG-76 played their part in the significant bond formation with the co-crystal ligand.

Similar, docking studies was performed to find the putative binding mode of compound **5e** in the active site of the target. The close observation of the 3D docked pose of compound **5e** exhibited lesser bond interaction with the surrounded amino-acid residues and water molecules (Figure-S4). The pyridine nitrogen of **5e** was actively participated in the hydrogen bond formation (2D pose of the compound) with the amino-acid residue AGR-76 (Figure-S5). The docking score (-2.4 kcal/mol) is less when compared with the co-crystal ligand and docking energy is -28.09 kcal/mol. Again, the same pyridine ring was involved in the π-cationic interaction with the amino-acid residue ARG-76. Apart from the hydrogen and π-cationic interactions, methoxyphenyl and phenyl rings attached to the pyrrole moiety, contributed to the aromatic bond interaction with the amino-acid residue-GLY-101. *In-vitro* antibacterial and antifungal studies of the significantly active compound was also revealed the same in the study. The *in-silico* and *in-vitro* studies were well correlated. The measured zone of inhibition of the compound displayed the maximum inhibition of 19, 18, 18 and 18 mm at 16 µg/mL against the gram-positive and gram-negative bacterial strains (*E. coli, E. putida, B. subtilis,* and *S.auresus*), which is comparable to standard drug Chloramphenicol.

References:

(1) Yang, S.-B.; Gan, F.-F.; Chen, G.-J.; Xu, P.-F. *SynLett*. **2008**, *16*, 2532.
(2) Schrödinger Release 2019-1: Maestro, Schrödinger, LLC, New York, NY, **2019.**
(3) Schrödinger Release 2019-1: Schrödinger Suite 2019-1 Protein Preparation Wizard; Epik, Schrödinger, LLC, New York, NY, 2019.
(4) R. A. Friesner, J. L. Banks, R. B. Murphy, T. A. Halgren, J. J. Klicic, D. T. Mainz, M. P. Repasky, E. H. Knoll, M. Shelley, J. K. Perry, *J. Med. Chem.,* 2004, **47,** 1739–1749.
(5) P. Banerjee, A. O. Eckert, A. K. Schrey, R. Preissner, *Nucleic Acids Res.*, 2018, **46**, W257–W263.
(6) M. Brvar, A. Perdih, M. Renko, G. Anderluh, D. Turk, T. Solmajer, *J. Med. Chem.*, 2012, **55**, 6413–6426.
(7) S. K. Burley, H. M. Berman, C. Bhikadiya, C. Bi, L. Chen, L. Di Costanzo, C. Christie, K. Dalenberg, J. M. Duarte, S. Dutta, *Nucleic Acids Res.*, 2019, **47**, D464–D474.

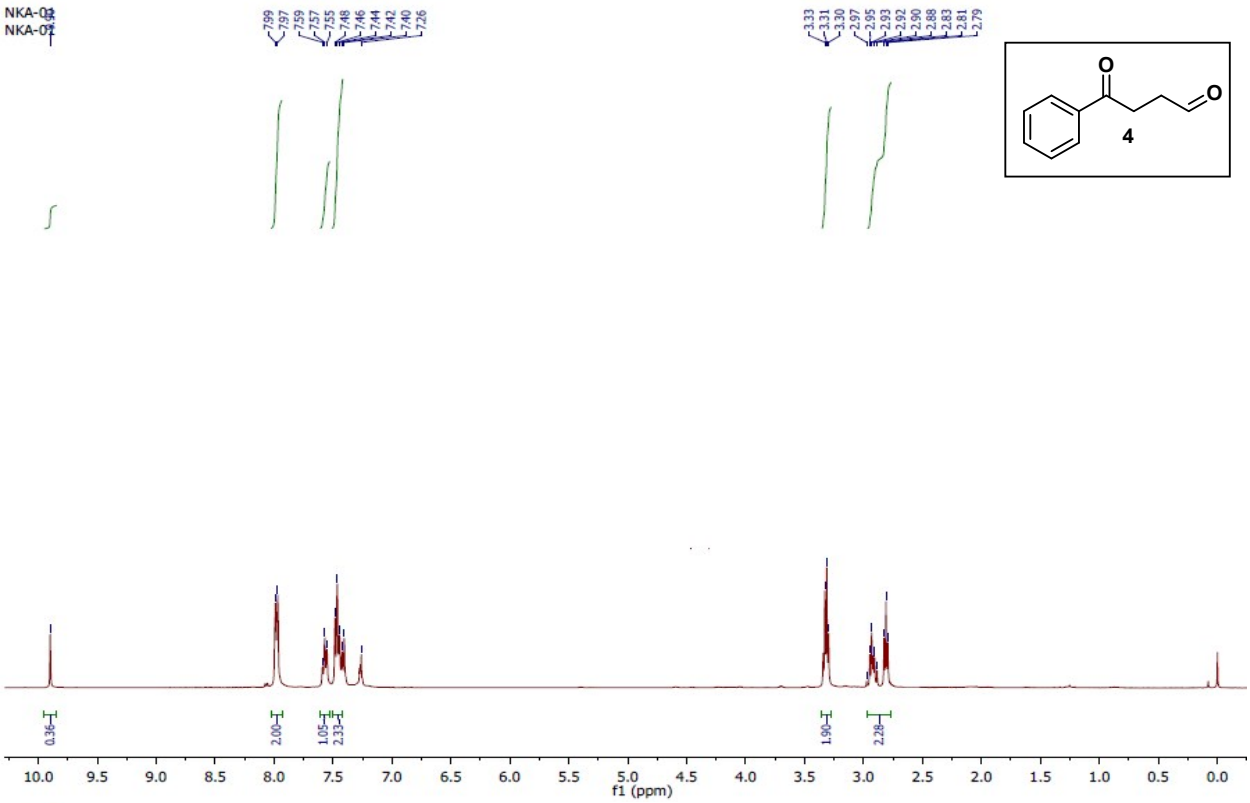
NKA-01
NKA-01
7.99
7.97
7.59
7.57
7.55
7.48
7.46
7.44
7.42
7.40
7.26
3.33
3.31
3.30
2.97
2.95
2.93
2.92
2.90
2.88
2.83
2.81
2.79
O
O
4
0.36
2.00
1.05
2.33
1.90
2.28
10.0
9.5
9.0
8.5
8.0
7.5
7.0
6.5
6.0
5.5
5.0
4.5
4.0
3.5
3.0
2.5
2.0
1.5
1.0
0.5
0.0
f1 (ppm)

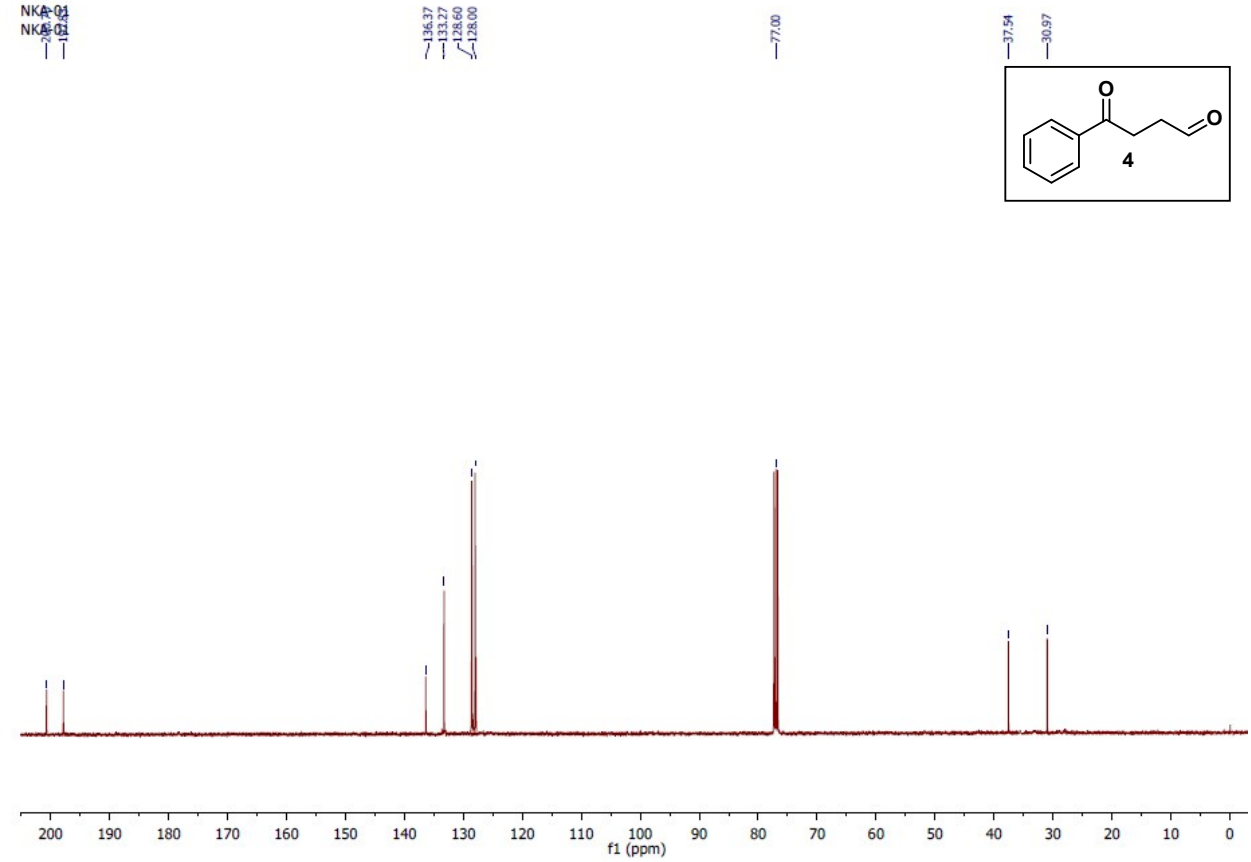
NKA-01
NKA-01
136.37
133.27
128.60
128.00
77.00
37.54
30.97
O
O
4
200
190
180
170
160
150
140
130
120
110
100
90
80
70
60
50
40
30
20
10
0
f1 (ppm)

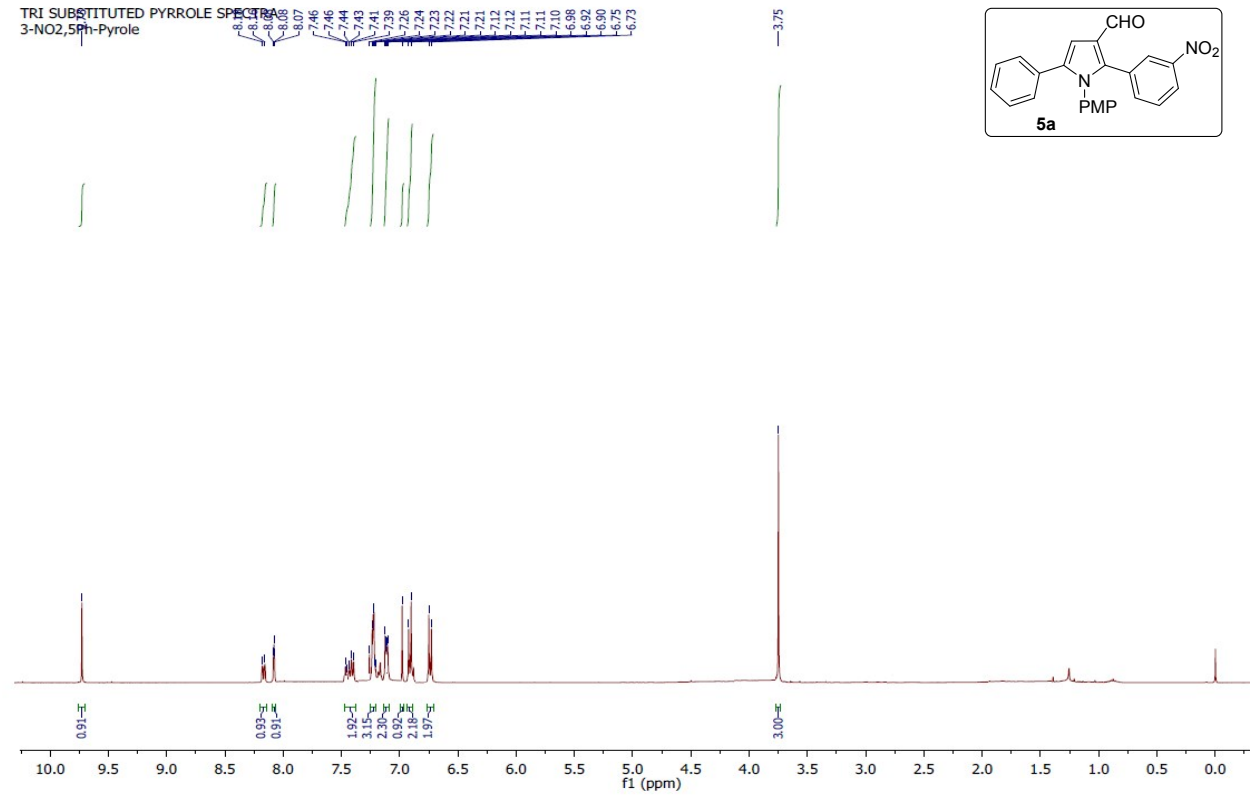
TRI SUBSTITUTED PYRROLE SPECTRA
3-NO2,5Ph-Pyrole
CHO
NO2
N
PMP
5a
f1 (ppm)

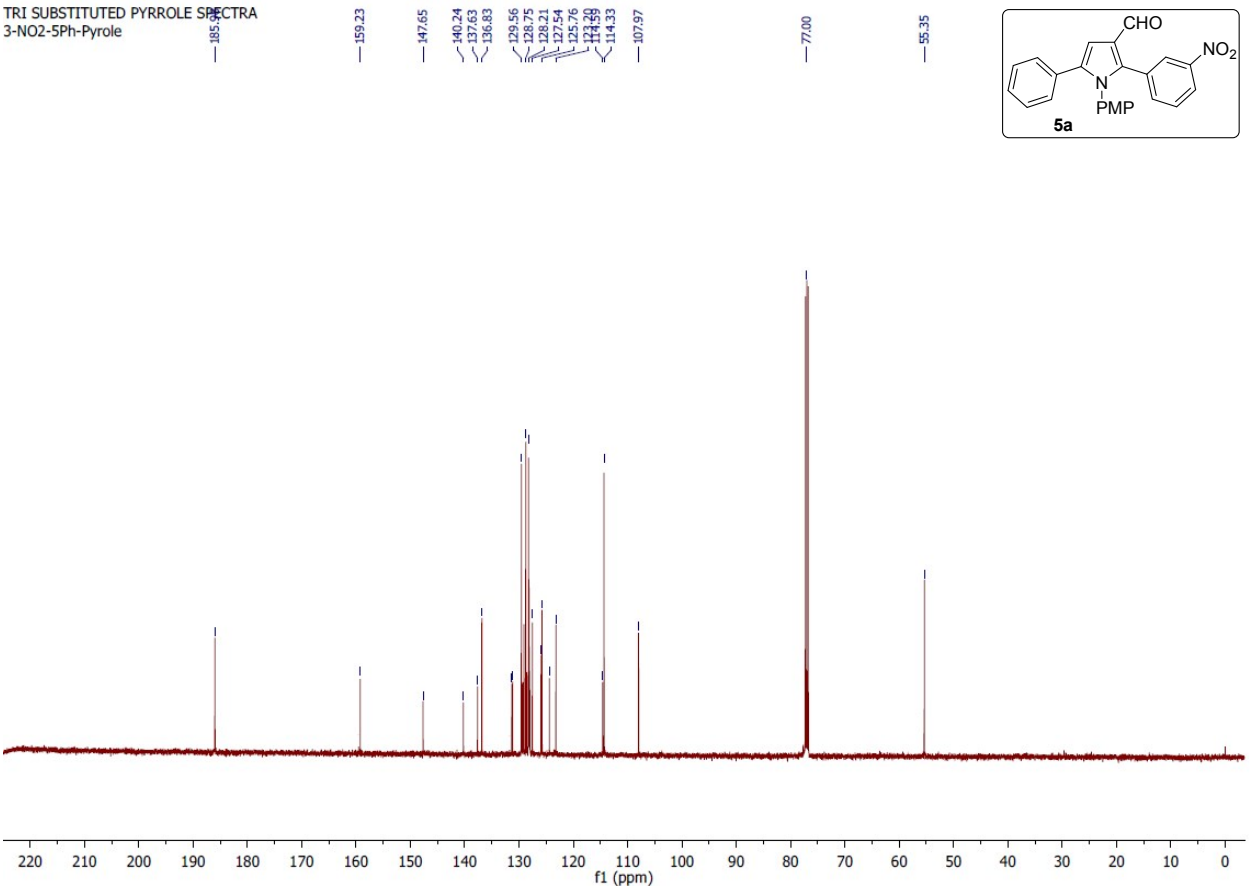
TRI SUBSTITUTED PYRROLE SPECTRA
3-NO2-5Ph-Pyrole
CHO
NO2
N
PMP
5a
f1 (ppm)

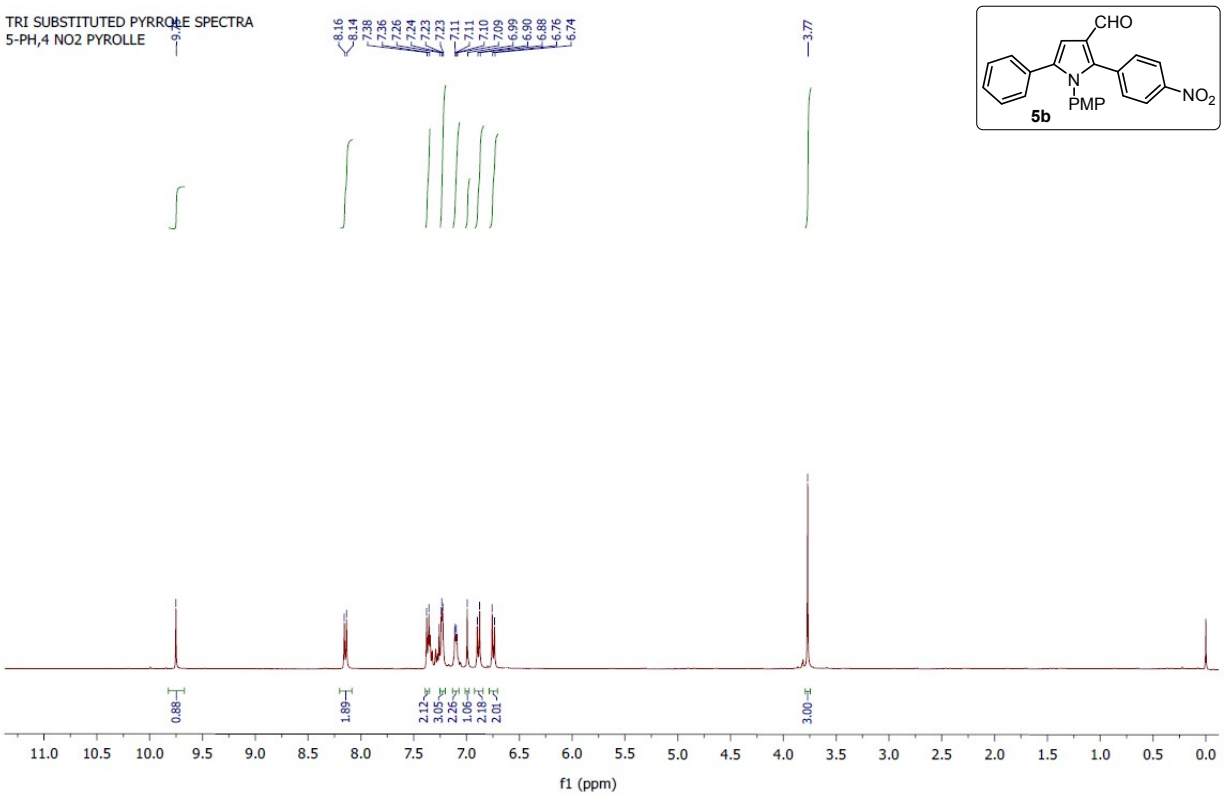
TRI SUBSTITUTED PYRROLE SPECTRA
5-PH,4 NO2 PYROLLE
9.75
8.16
8.14
7.38
7.36
7.26
7.24
7.23
7.23
7.11
7.11
7.10
7.09
6.99
6.90
6.88
6.76
6.74
3.77
CHO
N
PMP
NO2
5b
0.88
1.89
2.12
3.05
2.26
1.06
2.18
2.01
3.00
11.0 10.5 10.0 9.5 9.0 8.5 8.0 7.5 7.0 6.5 6.0 5.5 5.0 4.5 4.0 3.5 3.0 2.5 2.0 1.5 1.0 0.5 0.0
f1 (ppm)

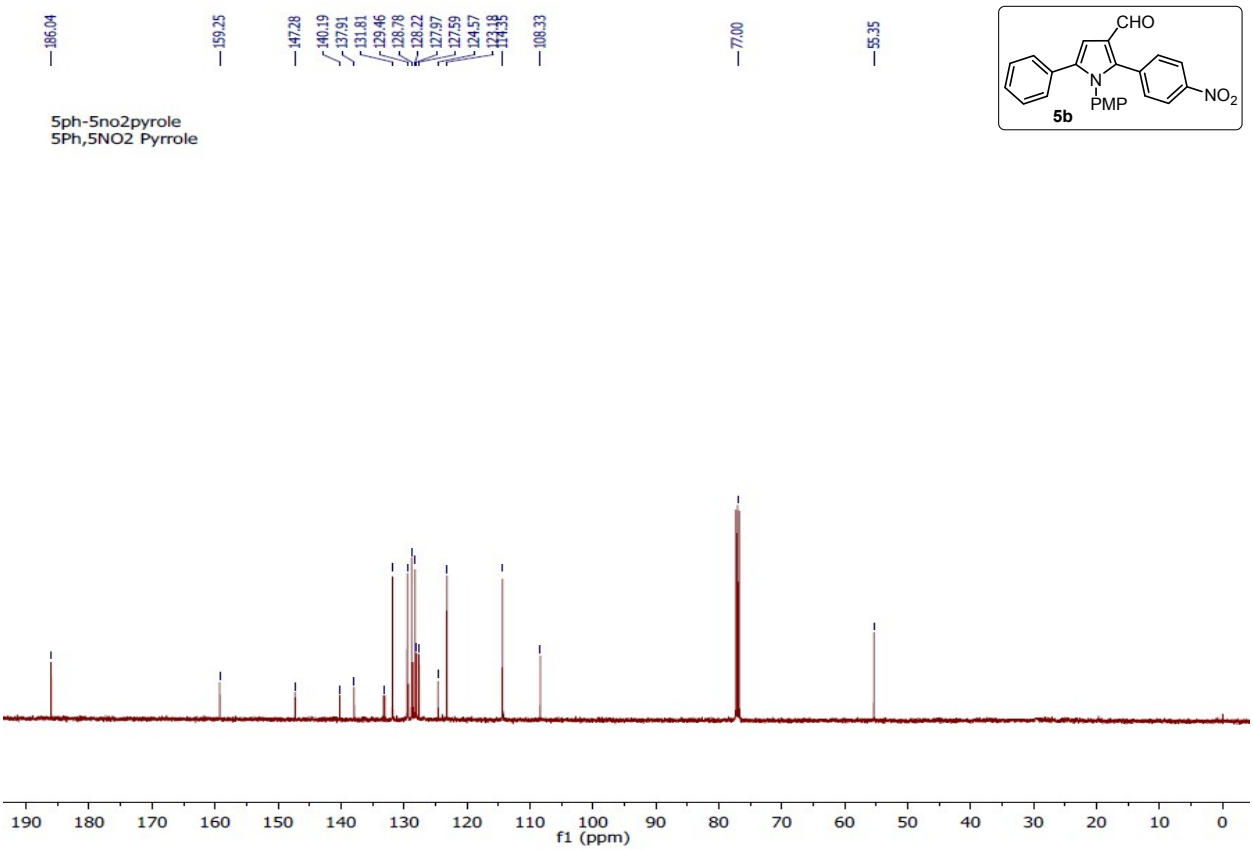
186.04
159.25
147.28
140.19
137.91
131.81
129.46
128.78
128.22
127.97
127.59
124.57
123.18
114.35
108.33
77.00
55.35
CHO
N
PMP
NO2
5b
5ph-5no2pyrole
5Ph,5NO2 Pyrrole
190 180 170 160 150 140 130 120 110 100 90 80 70 60 50 40 30 20 10 0
f1 (ppm)

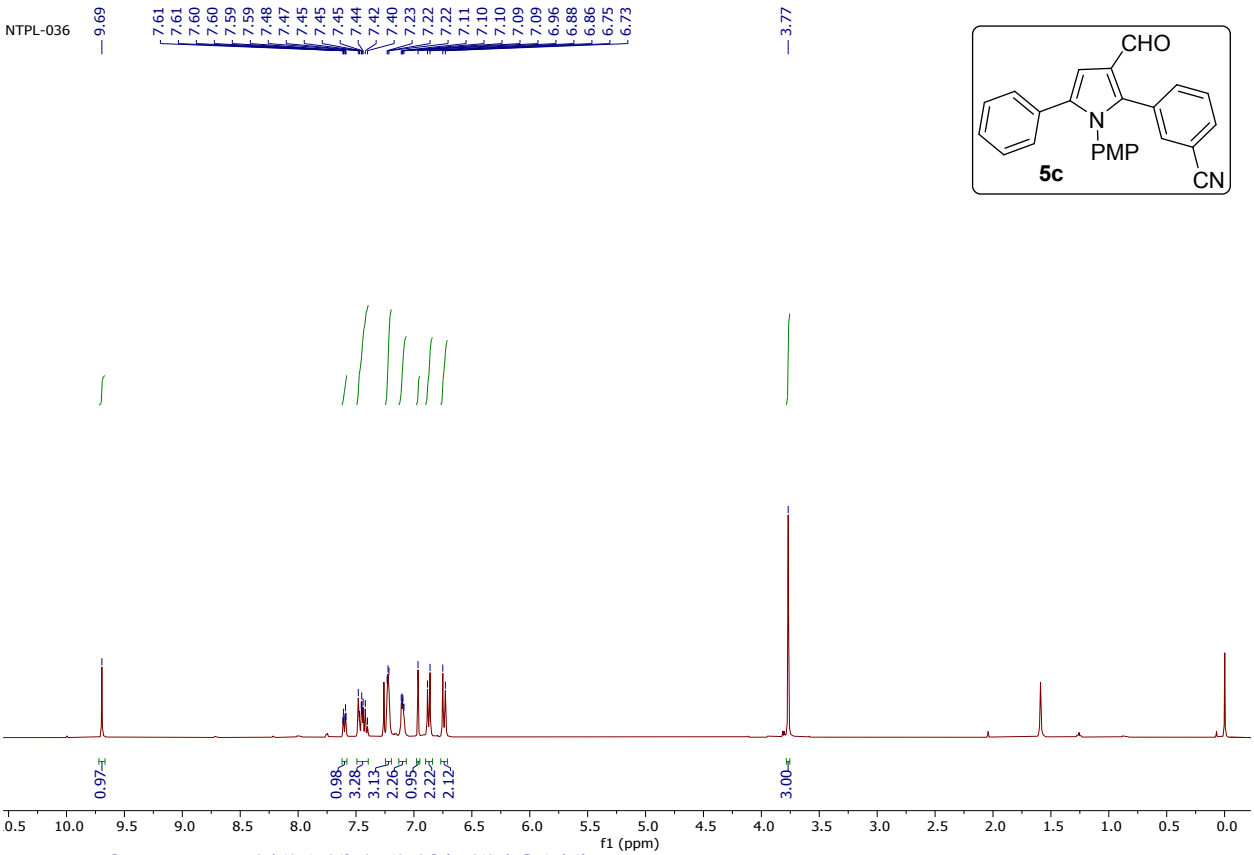
NTPL-036
9.69
7.61
7.61
7.60
7.60
7.59
7.59
7.48
7.47
7.45
7.45
7.45
7.44
7.42
7.40
7.23
7.22
7.22
7.11
7.10
7.10
7.09
7.09
6.96
6.88
6.86
6.75
6.73
3.77
CHO
N
PMP
CN
5c
0.97
0.98
3.28
3.13
2.26
0.95
2.22
2.12
3.00
f1 (ppm)

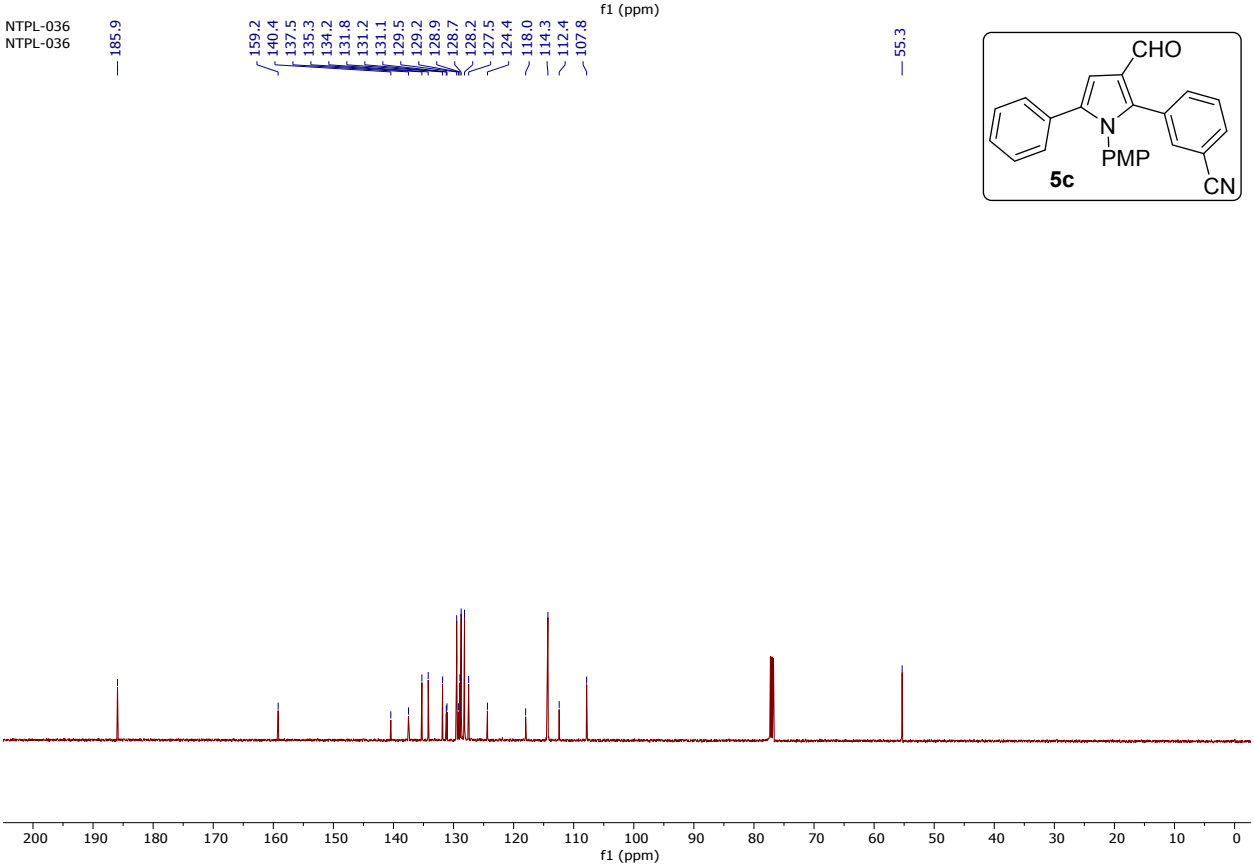
NTPL-036
NTPL-036
185.9
159.2
140.4
137.5
135.3
134.2
131.8
131.2
131.1
129.5
129.2
128.9
128.7
128.2
127.5
124.4
118.0
114.3
112.4
107.8
55.3
CHO
N
PMP
CN
5c
f1 (ppm)

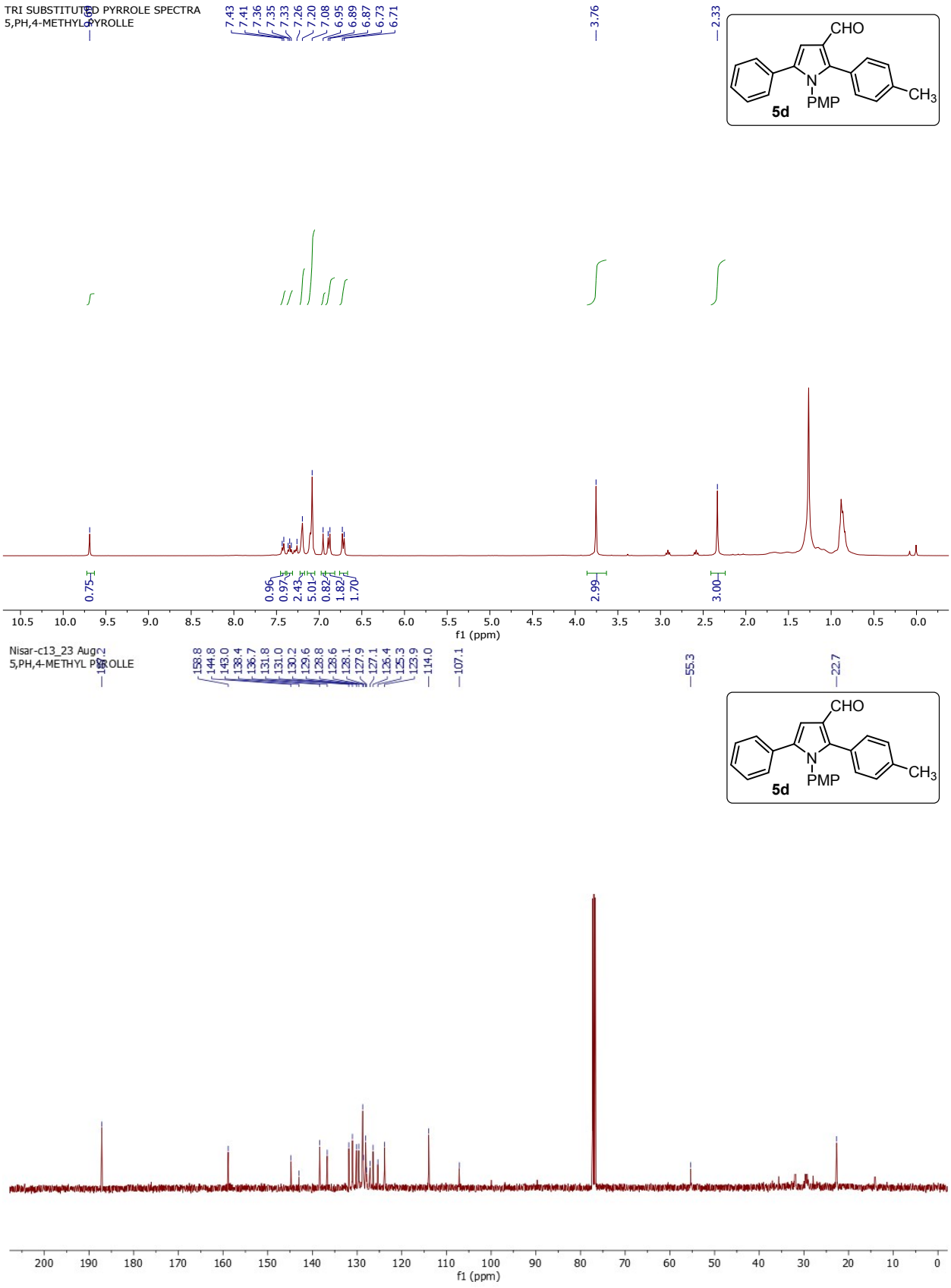
TRI SUBSTITUTED PYRROLE SPECTRA
5,PH,4-METHYL PYRROLLE
7.43
7.41
7.36
7.35
7.33
7.26
7.20
7.08
6.95
6.89
6.87
6.73
6.71
3.76
2.33
CHO
N
PMP
CH3
5d
0.75
0.96
0.97
2.43
5.01
0.82
1.82
1.70
2.99
3.00
f1 (ppm)
Nisar-c13_23 Aug
5,PH,4-METHYL PYRROLLE
158.8
144.8
143.0
138.4
136.7
131.8
131.0
130.2
129.6
128.8
128.6
128.1
127.9
127.1
126.4
125.3
123.9
114.0
107.1
55.3
22.7
CHO
N
PMP
CH3
5d
f1 (ppm)

TRI SUBSTITUTED PYRROLE SPECTRA
5-Ph-3-Pyridine-Pyrole

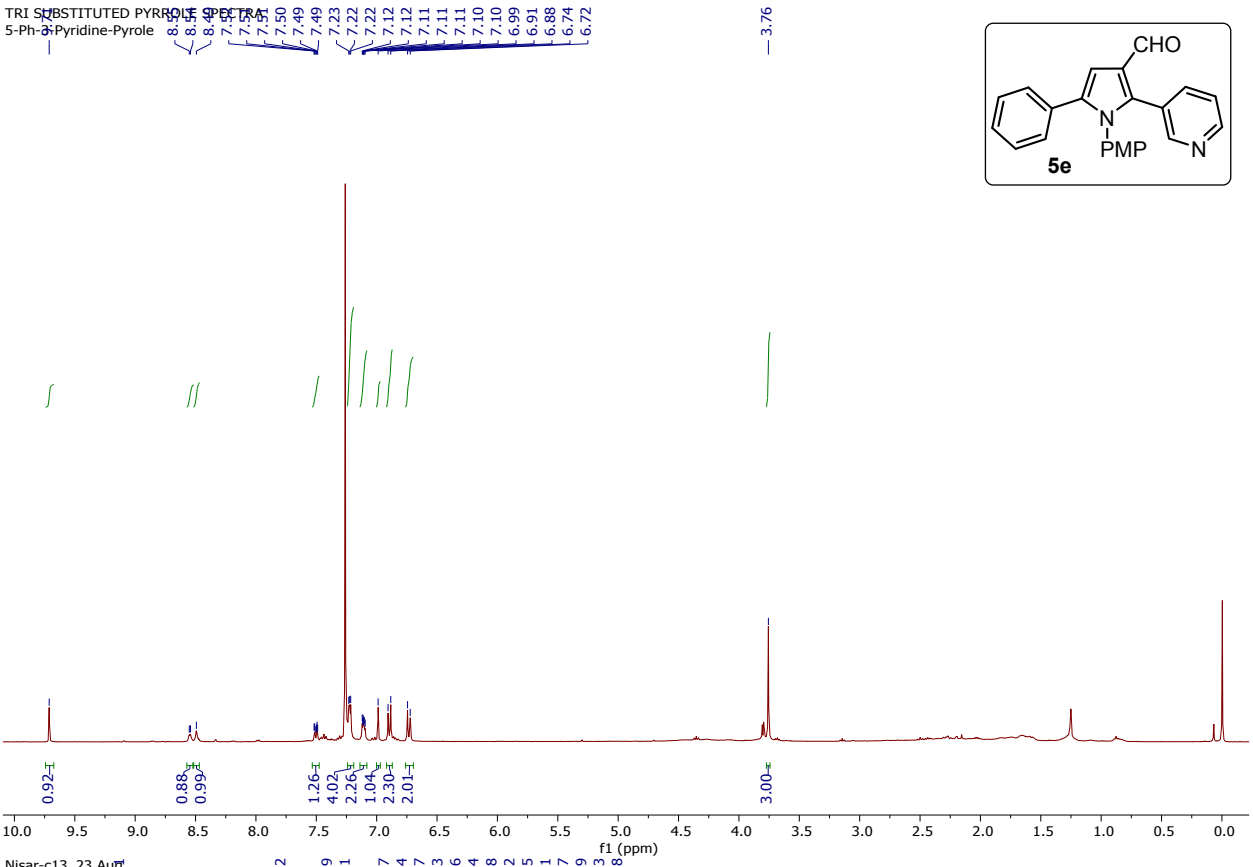

Nisar-c13_23 Aud
5-PH-PYRIDINE-3-PYROLLE

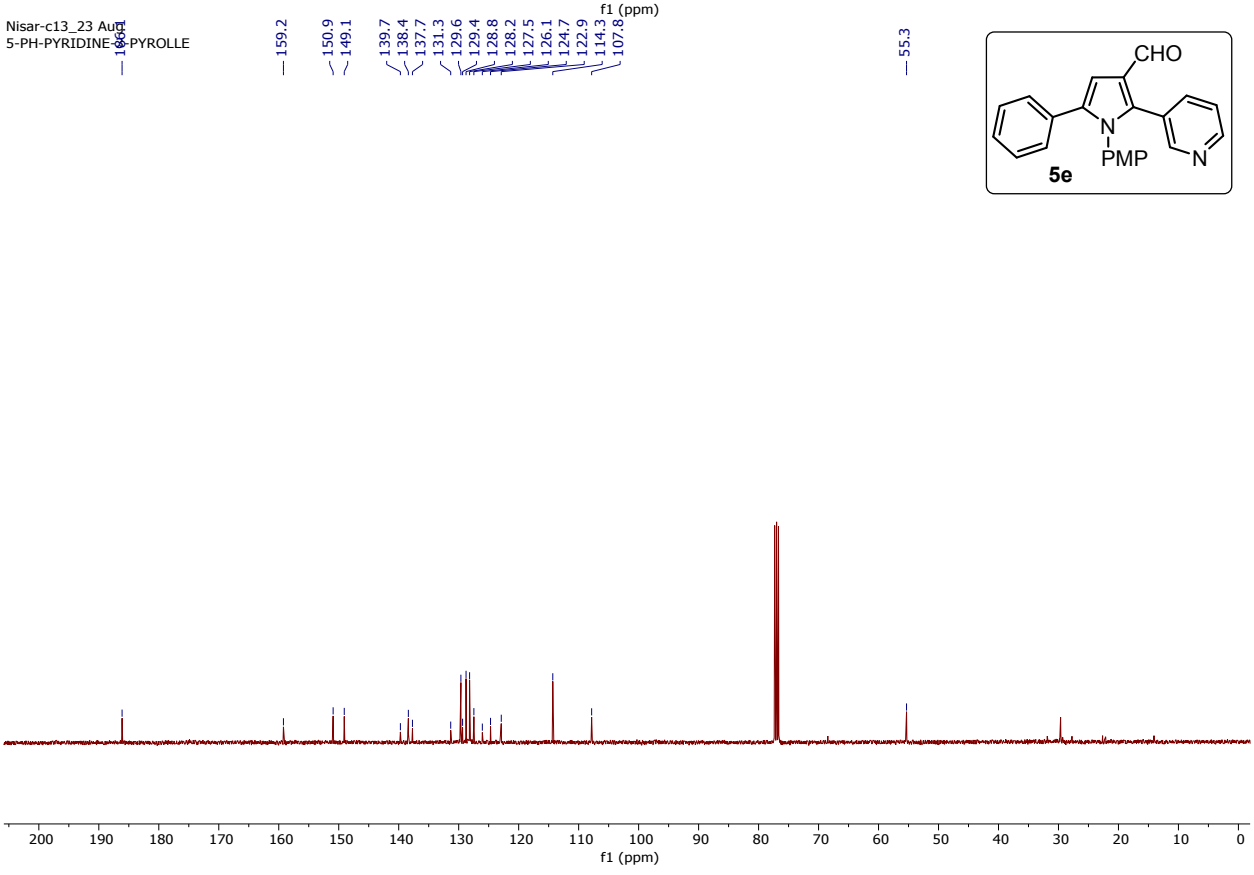

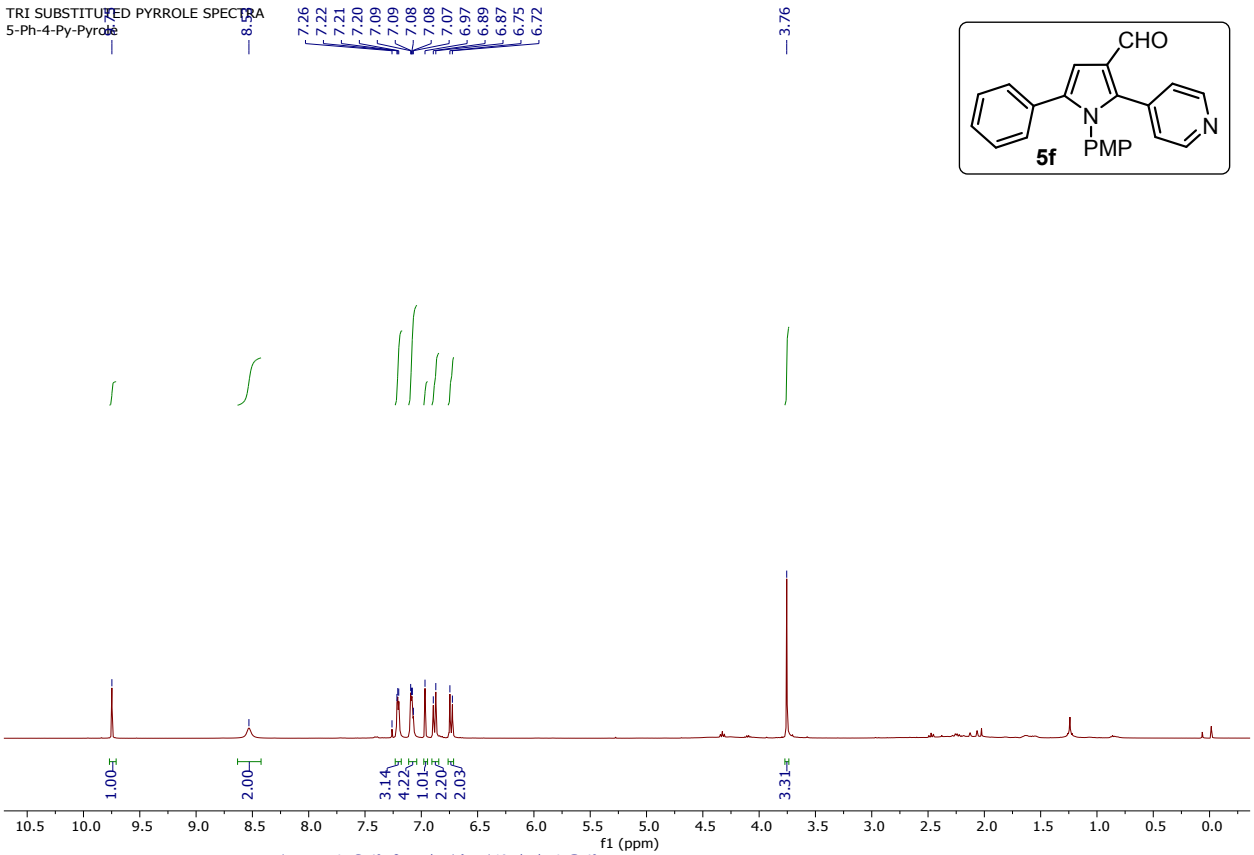
TRI SUBSTITUTED PYRROLE SPECTRA
5-Ph-4-Py-Pyrole
10.06
8.59
7.26
7.22
7.21
7.20
7.09
7.09
7.08
7.08
7.07
6.97
6.89
6.87
6.75
6.72
3.76
CHO
N
PMP
5f
N
1.00
2.00
3.14
4.22
1.01
2.20
2.03
3.31
10.5 10.0 9.5 9.0 8.5 8.0 7.5 7.0 6.5 6.0 5.5 5.0 4.5 4.0 3.5 3.0 2.5 2.0 1.5 1.0 0.5 0.0
f1 (ppm)

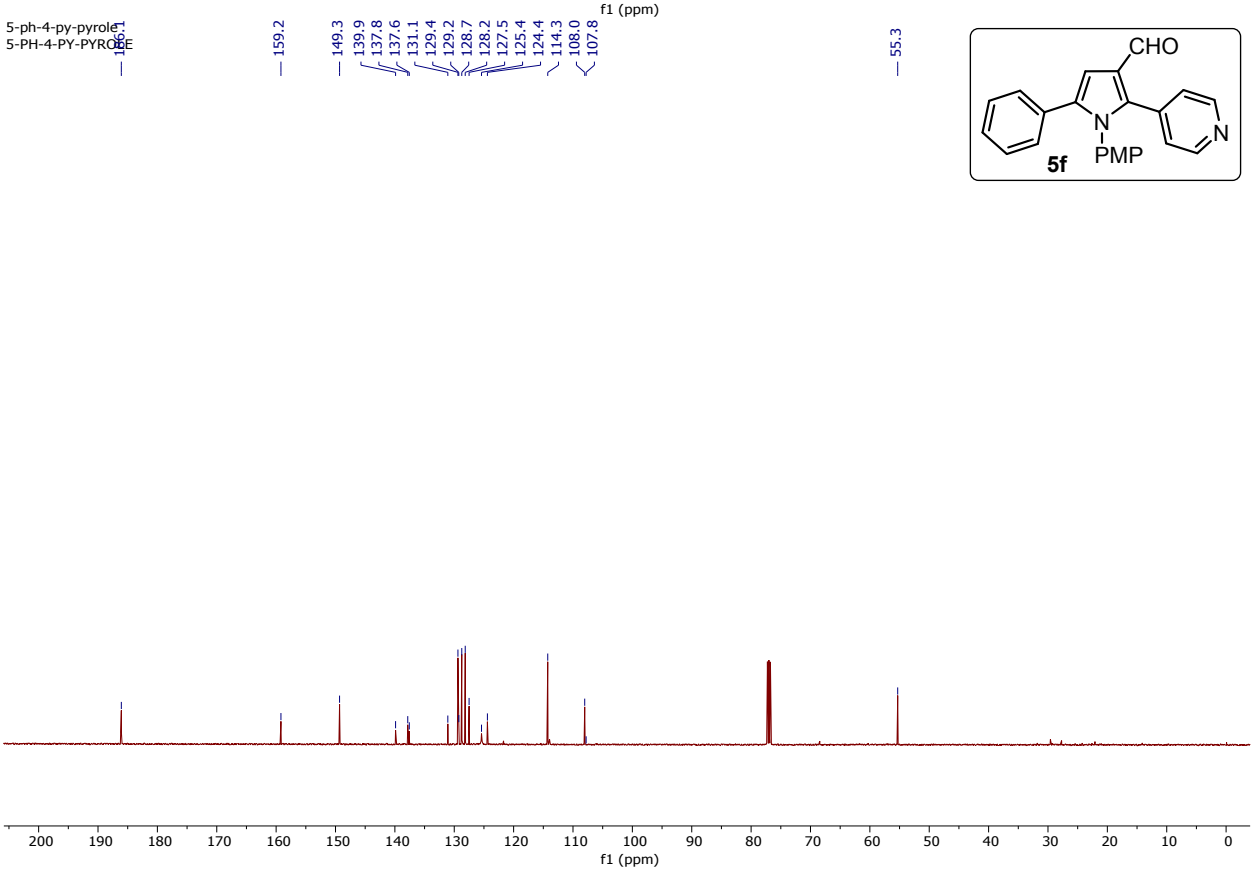
5-ph-4-py-pyrole
5-PH-4-PY-PYROLE
196.1
159.2
149.3
139.9
137.8
137.6
131.1
129.4
129.2
128.7
128.2
127.5
125.4
124.4
114.3
108.0
107.8
55.3
CHO
N
PMP
5f
N
200 190 180 170 160 150 140 130 120 110 100 90 80 70 60 50 40 30 20 10 0
f1 (ppm)

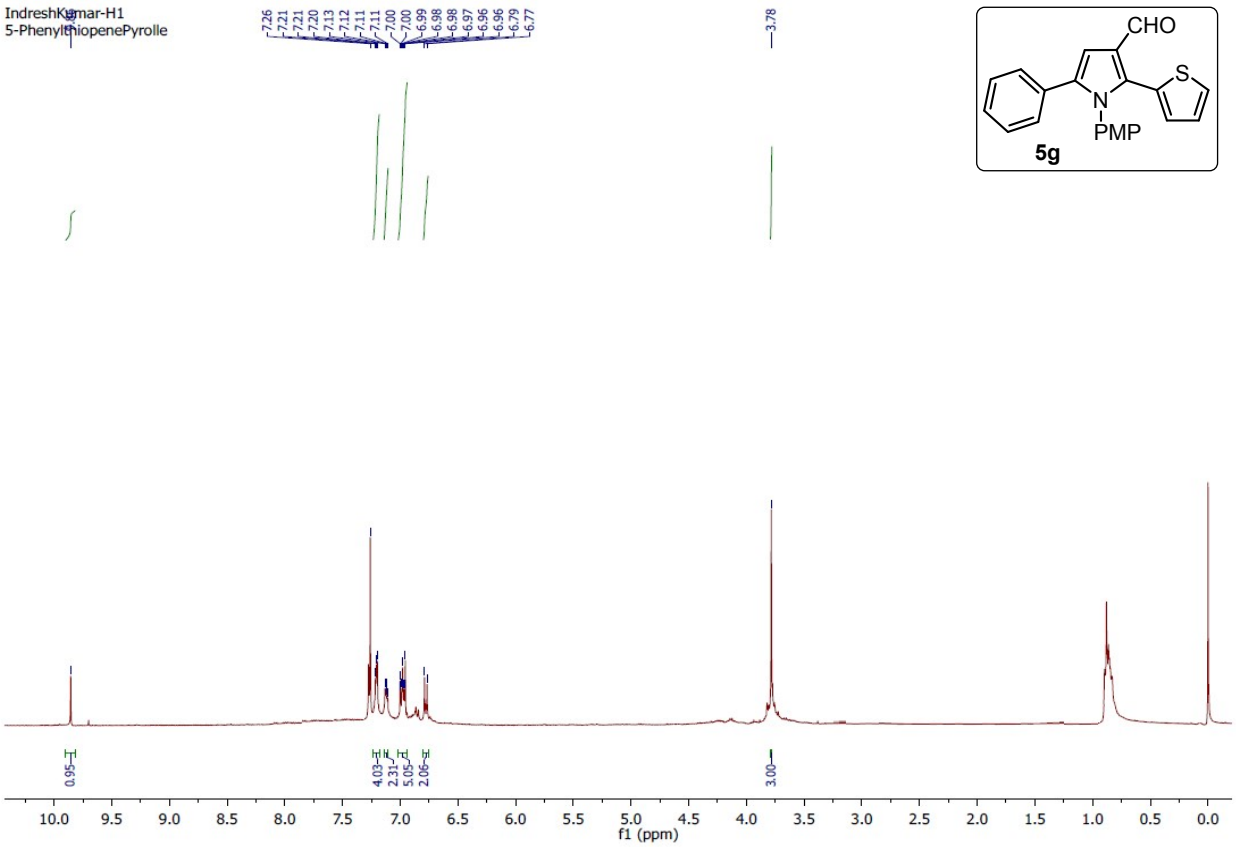
IndreshKumar-H1
5-PhenylthiopenePyrolle
7.26
7.21
7.21
7.20
7.13
7.12
7.11
7.11
7.00
7.00
6.99
6.98
6.98
6.97
6.96
6.96
6.79
6.77
3.78
CHO
S
N
PMP
5g
0.95
4.03
2.31
5.05
2.06
3.00
10.0 9.5 9.0 8.5 8.0 7.5 7.0 6.5 6.0 5.5 5.0 4.5 4.0 3.5 3.0 2.5 2.0 1.5 1.0 0.5 0.0
f1 (ppm)

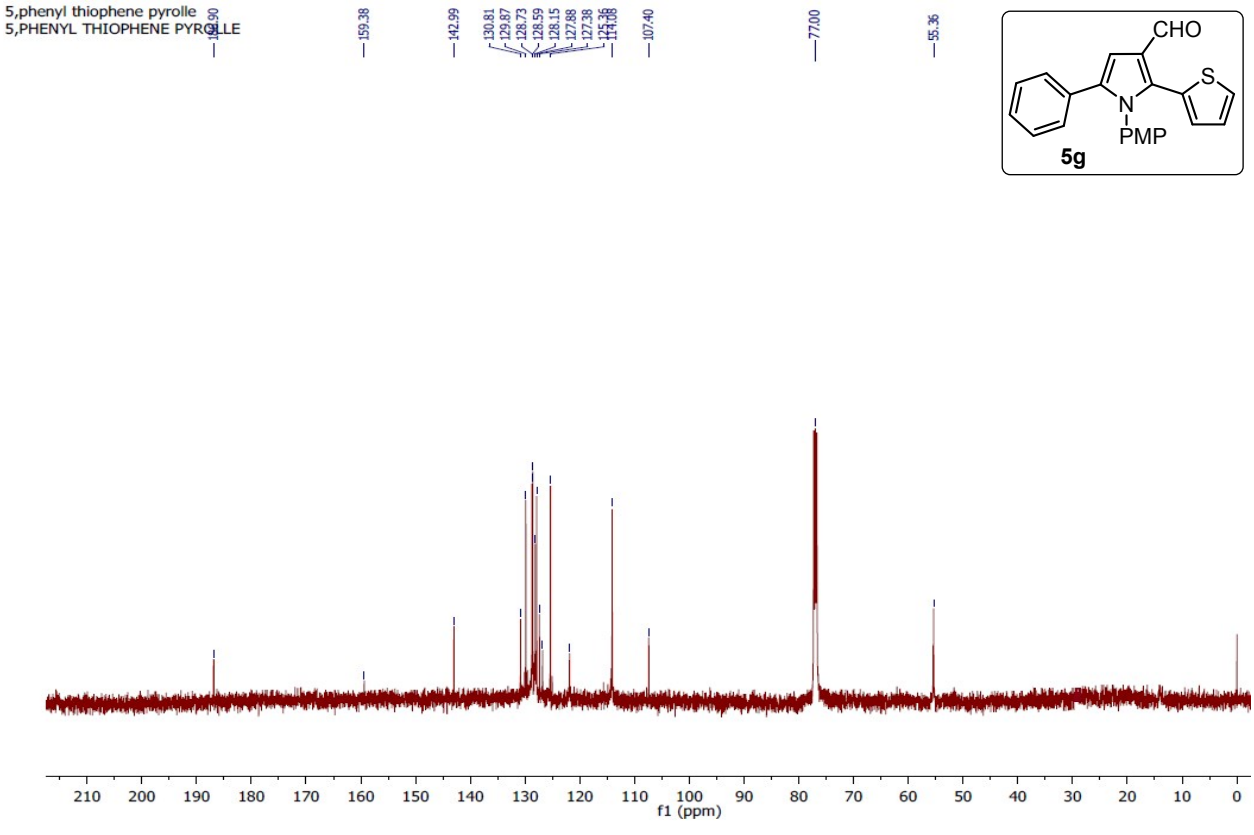
5,phenyl thiophene pyrolle
5,PHENYL THIOPHENE PYROLLE
159.38
142.99
130.81
129.87
128.73
128.59
128.15
127.88
127.38
107.40
77.00
55.36
CHO
S
N
PMP
5g
210 200 190 180 170 160 150 140 130 120 110 100 90 80 70 60 50 40 30 20 10 0
f1 (ppm)

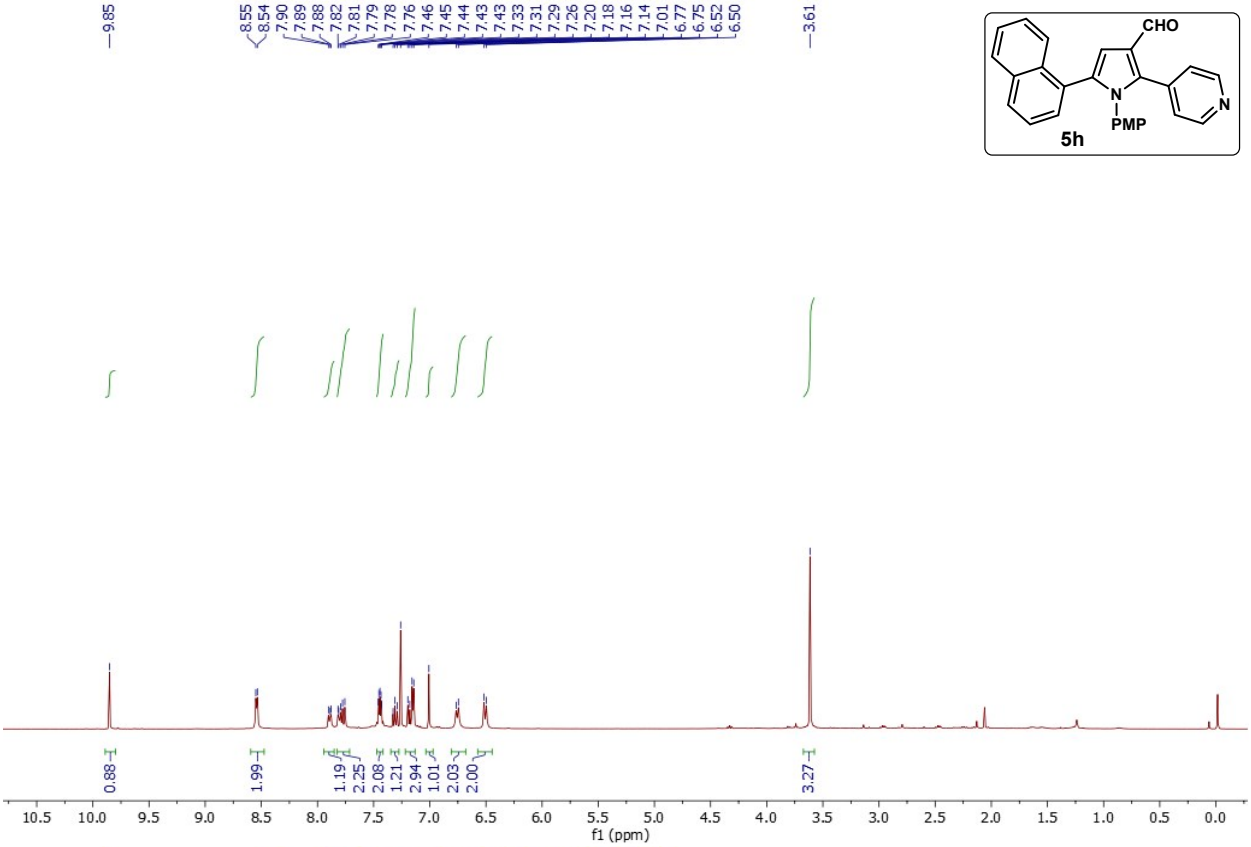
9.85
8.55
8.54
7.90
7.89
7.88
7.82
7.81
7.79
7.78
7.76
7.46
7.45
7.44
7.43
7.43
7.33
7.31
7.29
7.26
7.20
7.18
7.16
7.14
7.01
6.77
6.75
6.52
6.50
3.61
CHO
N
PMP
5h
0.88
1.99
1.19
2.25
2.08
1.21
2.94
1.01
2.03
2.00
3.27
f1 (ppm)

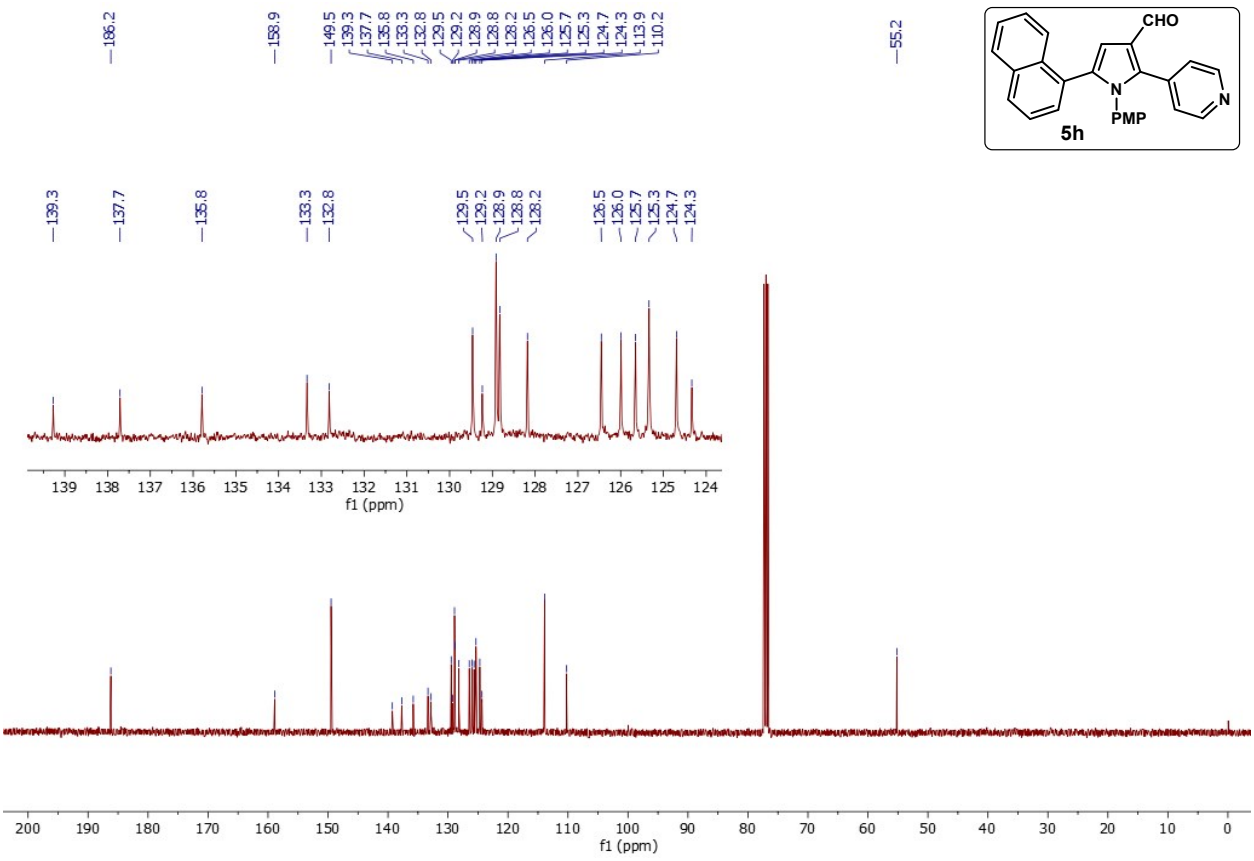
186.2
158.9
149.5
139.3
137.7
135.8
133.3
132.8
129.5
129.2
128.9
128.8
128.2
126.5
126.0
125.7
125.3
124.7
124.3
113.9
110.2
55.2
CHO
N
PMP
5h
139.3
137.7
135.8
133.3
132.8
129.5
129.2
128.9
128.8
128.2
126.5
126.0
125.7
125.3
124.7
124.3
f1 (ppm)

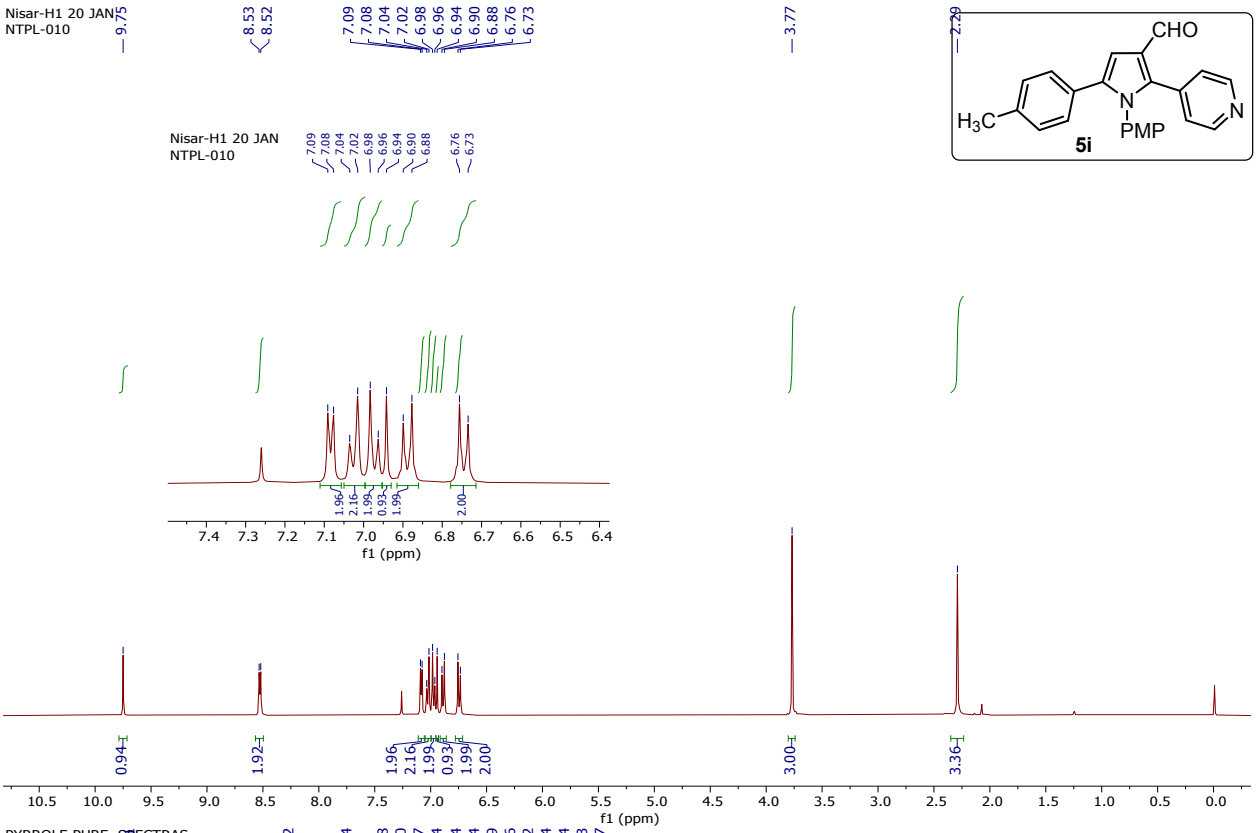
Nisar-H1 20 JAN
NTPL-010
9.75
8.53
8.52
7.09
7.08
7.04
7.02
6.98
6.96
6.94
6.90
6.88
6.76
6.73
3.77
2.29
CHO
H3C
N
PMP
N
5i
f1 (ppm)
0.94
1.92
1.96
2.16
1.99
0.93
1.99
2.00
3.00
3.36

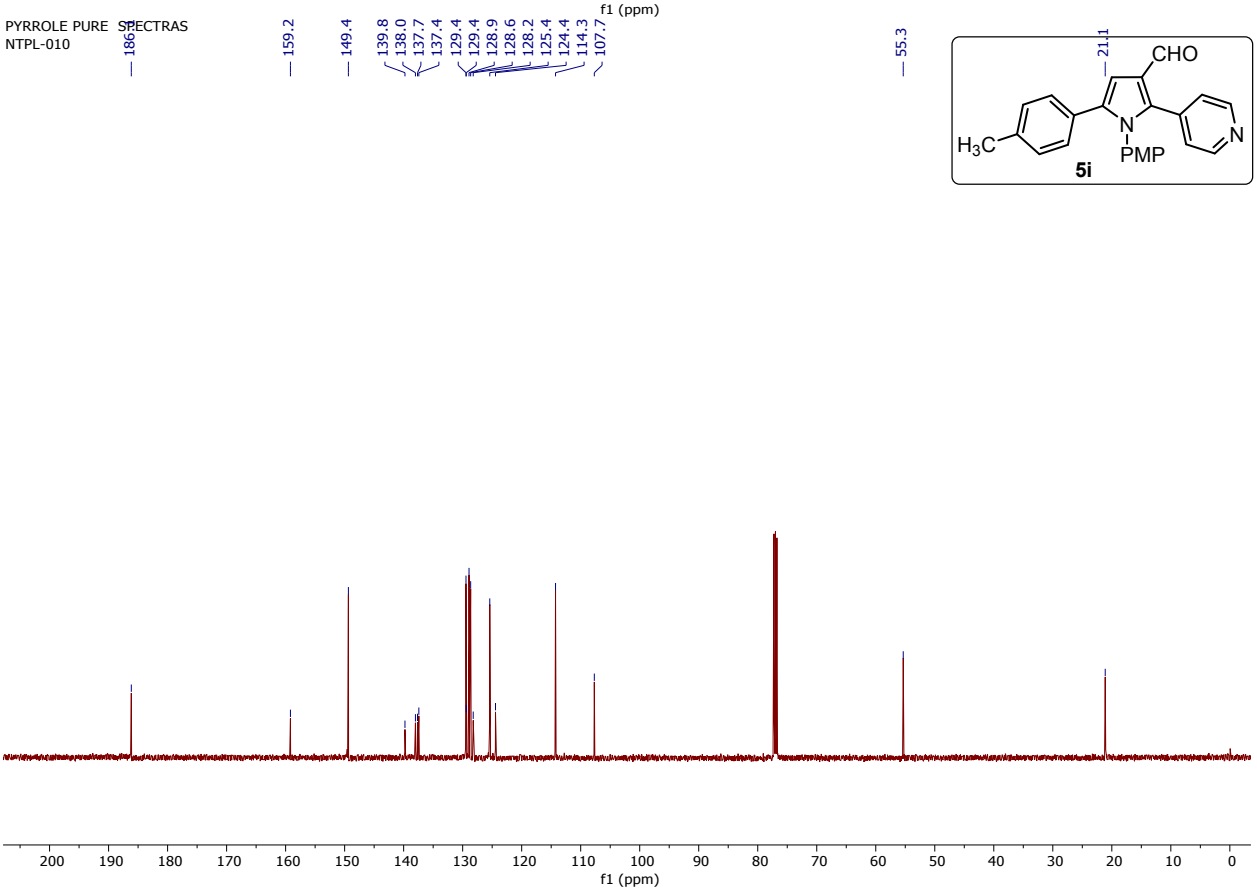
PYRROLE PURE SPECTRAS
NTPL-010
186.4
159.2
149.4
139.8
138.0
137.7
137.4
129.4
129.4
128.9
128.6
128.2
125.4
124.4
114.3
107.7
55.3
21.1
CHO
H3C
N
PMP
N
5i
f1 (ppm)

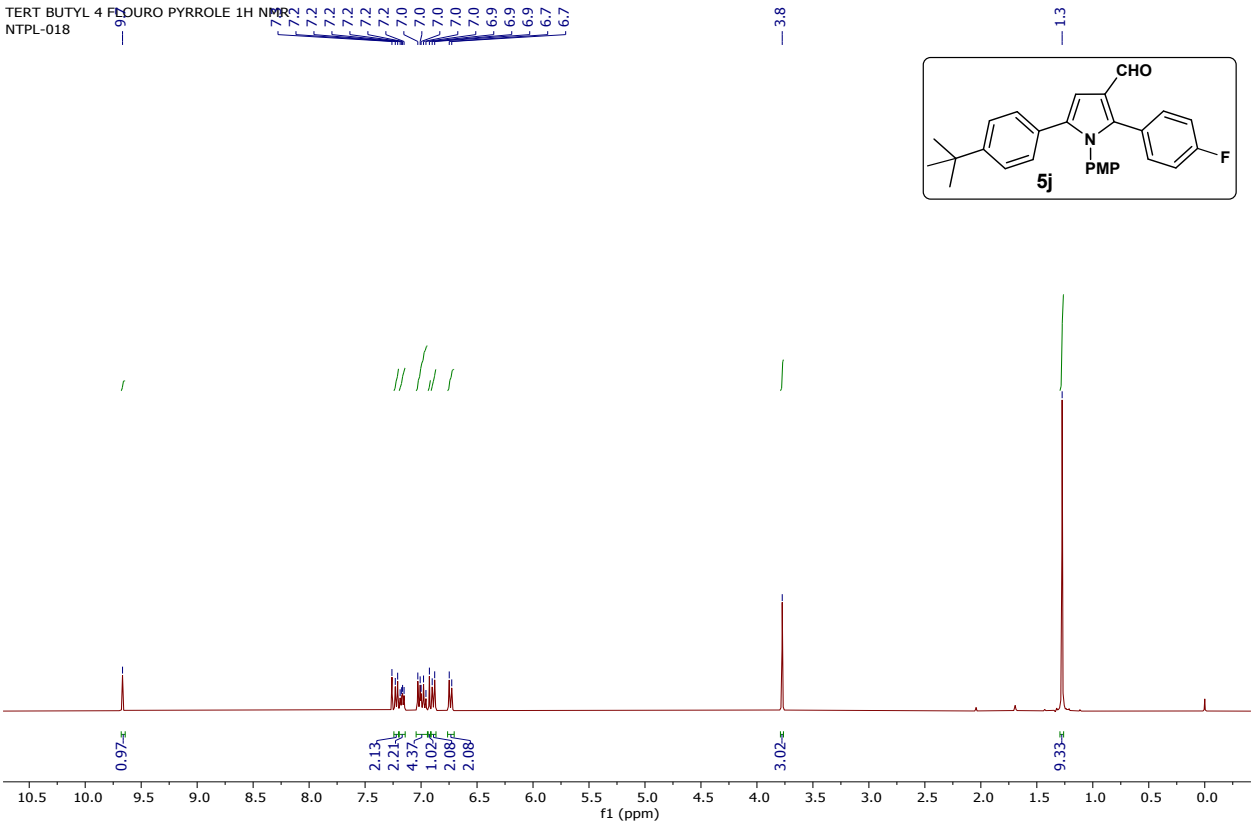
TERT BUTYL 4 FLOURO PYRROLE 1H NMR
NTPL-018
9.7
7.2
7.0
6.9
6.7
3.8
1.3
CHO
N
PMP
F
5j
0.97
2.13
2.21
4.37
1.02
2.08
2.08
3.02
9.33
f1 (ppm)

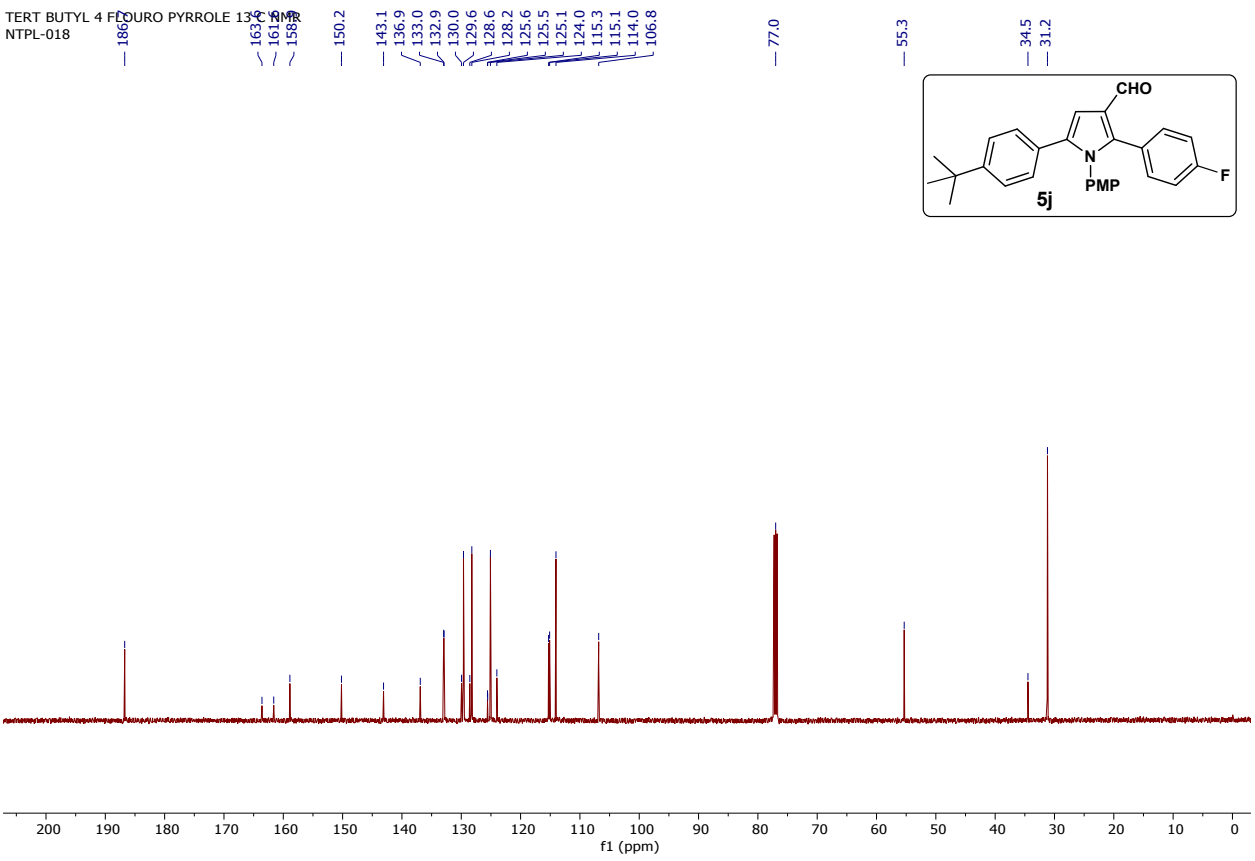
TERT BUTYL 4 FLOURO PYRROLE 13C NMR
NTPL-018
186
163.4
161.0
158.8
150.2
143.1
136.9
133.0
132.9
130.0
129.6
128.6
128.2
125.6
125.5
125.1
124.0
115.3
115.1
114.0
106.8
77.0
55.3
34.5
31.2
CHO
N
PMP
F
5j
f1 (ppm)

TERT BUTYL 4 CHLORO PYRROLE 1H NMR
NTPL-019

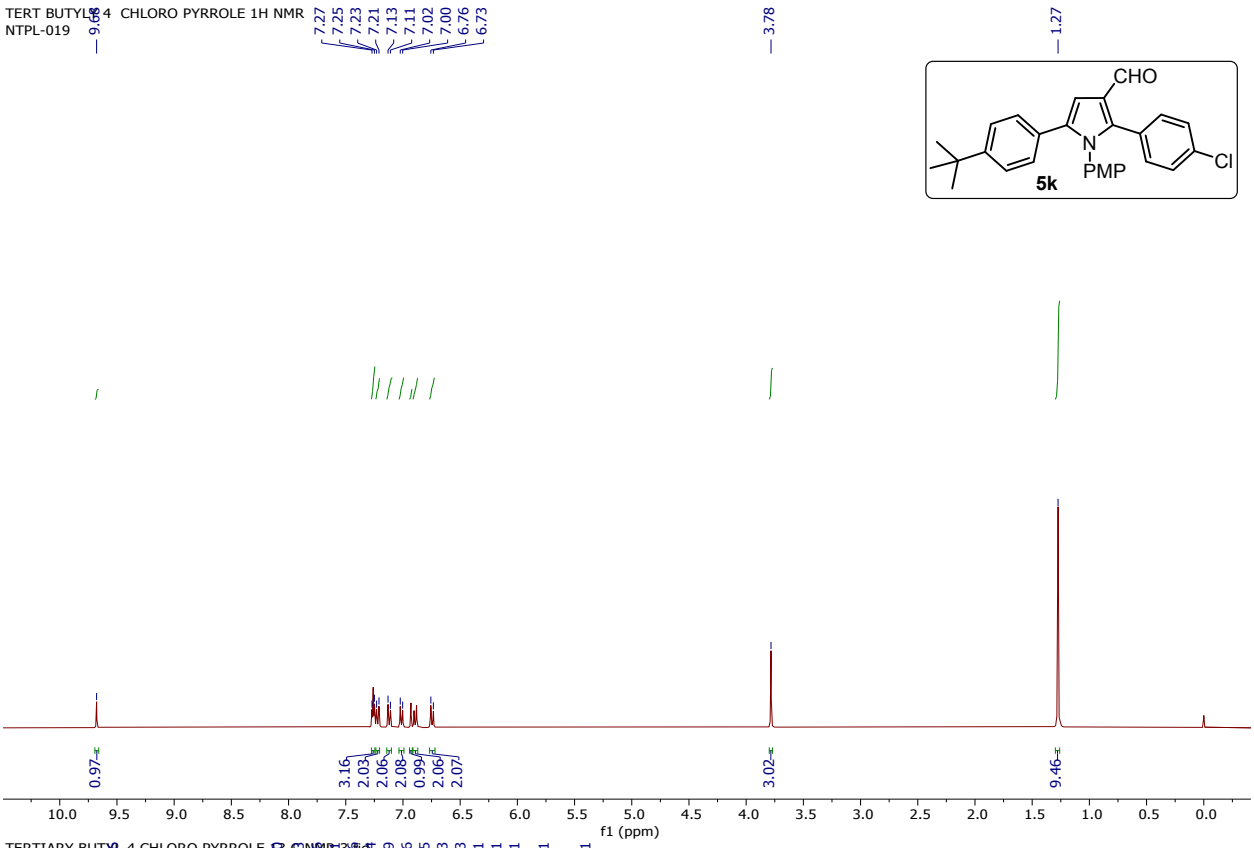

TERTIARY BUTYL 4 CHLORO PYRROLE 13C NMR 125MHz
NTPL-019

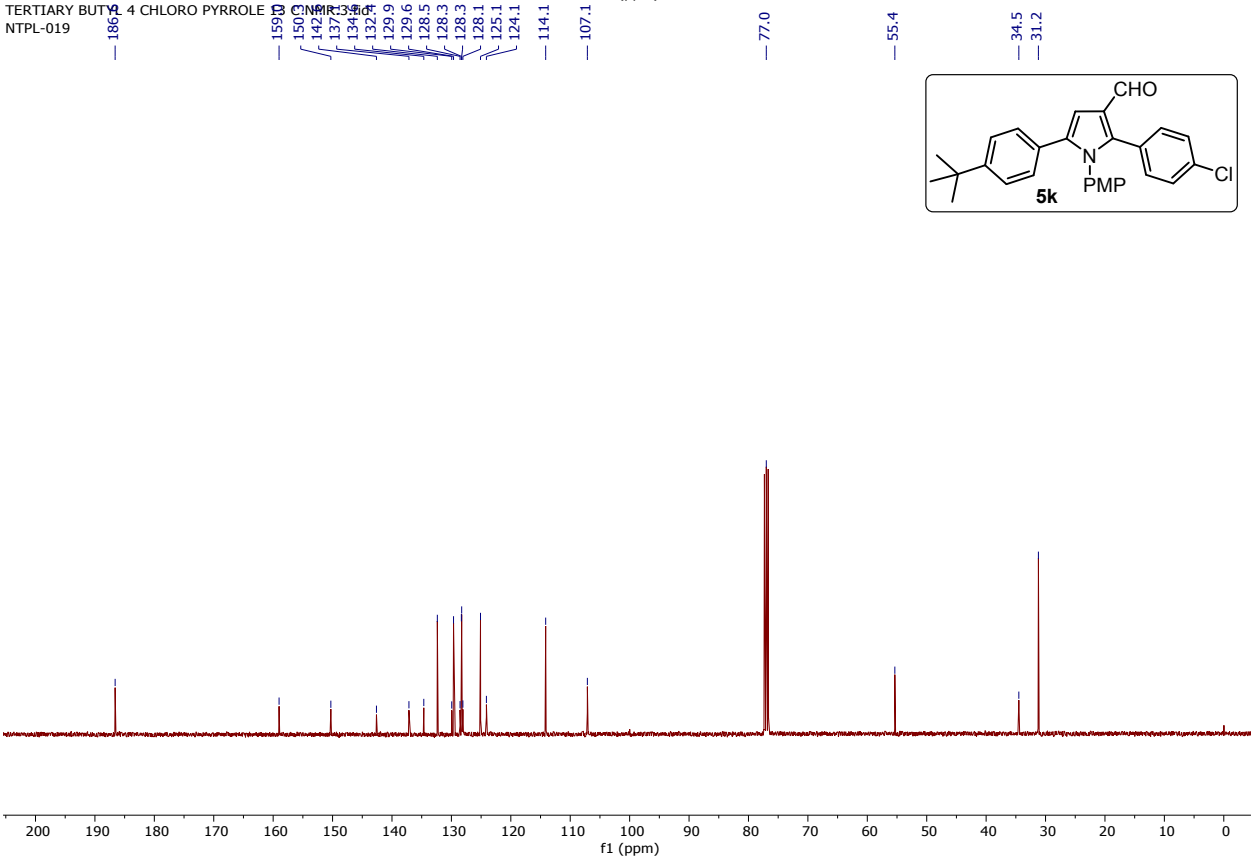

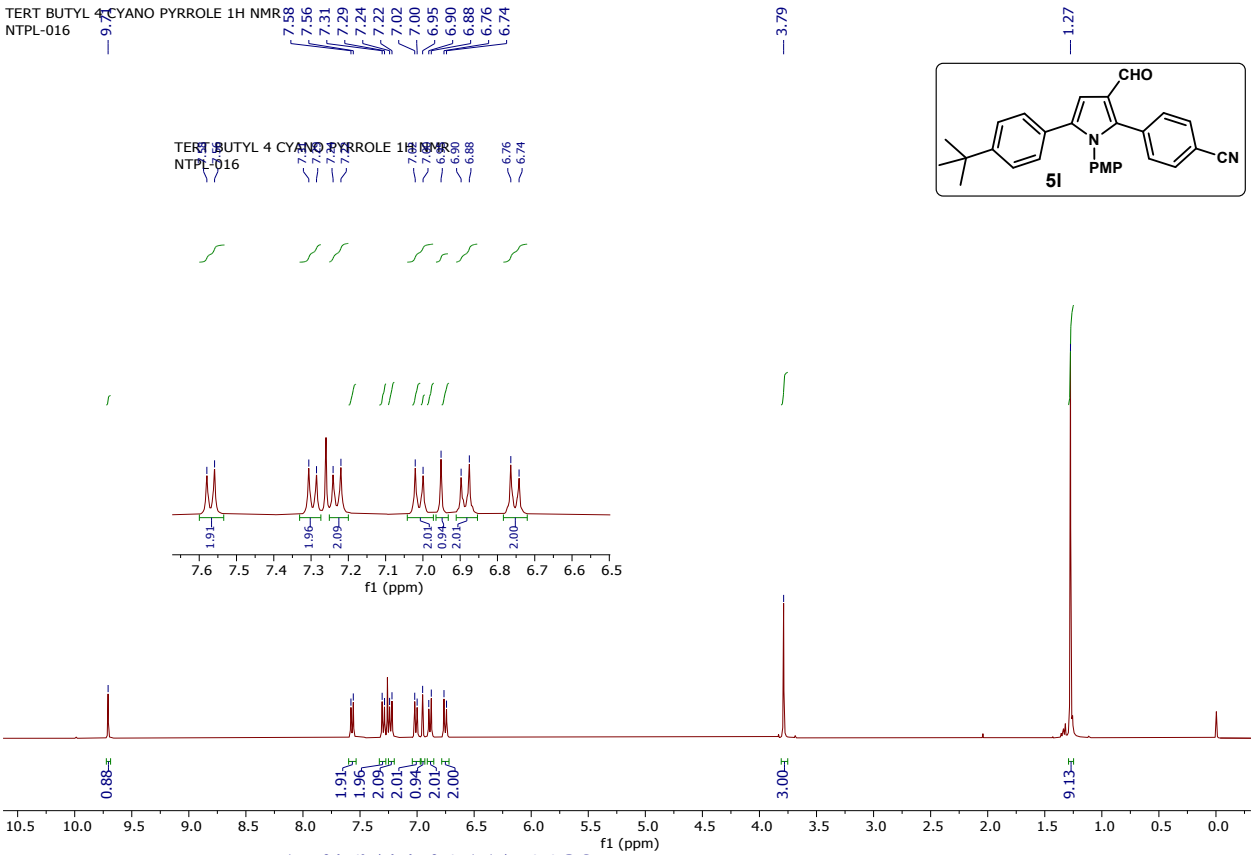
TERT BUTYL 4 CYANO PYRROLE 1H NMR
NTPL-016
9.77
7.58
7.56
7.31
7.29
7.24
7.22
7.02
7.00
6.95
6.90
6.88
6.76
6.74
3.79
1.27
CHO
N
PMP
CN
5l
1.91
1.96
2.09
2.01
0.94
2.01
2.00
0.88
3.00
9.13
f1 (ppm)

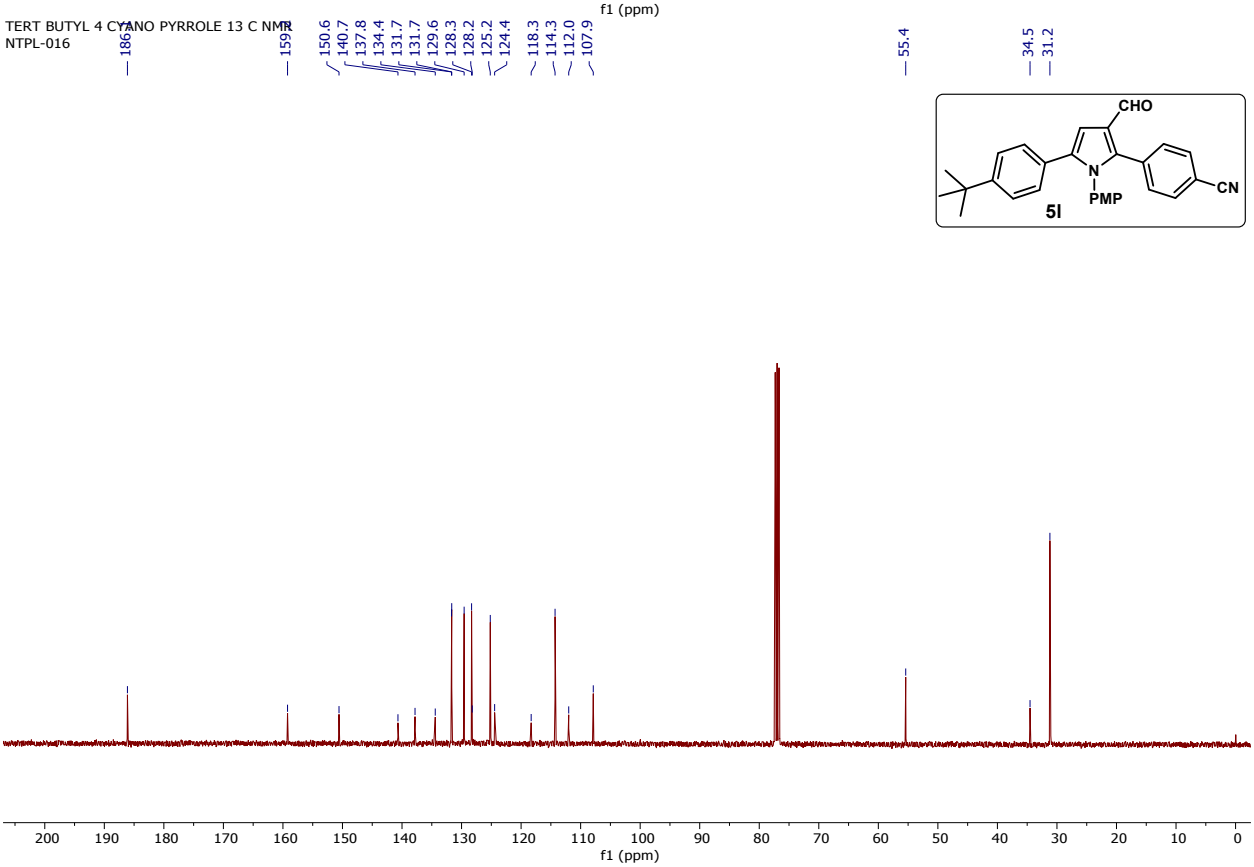
TERT BUTYL 4 CYANO PYRROLE 13 C NMR
NTPL-016
186.3
159.8
150.6
140.7
137.8
134.4
131.7
131.7
129.6
128.3
128.2
125.2
124.4
118.3
114.3
112.0
107.9
55.4
34.5
31.2
CHO
N
PMP
CN
5l
f1 (ppm)

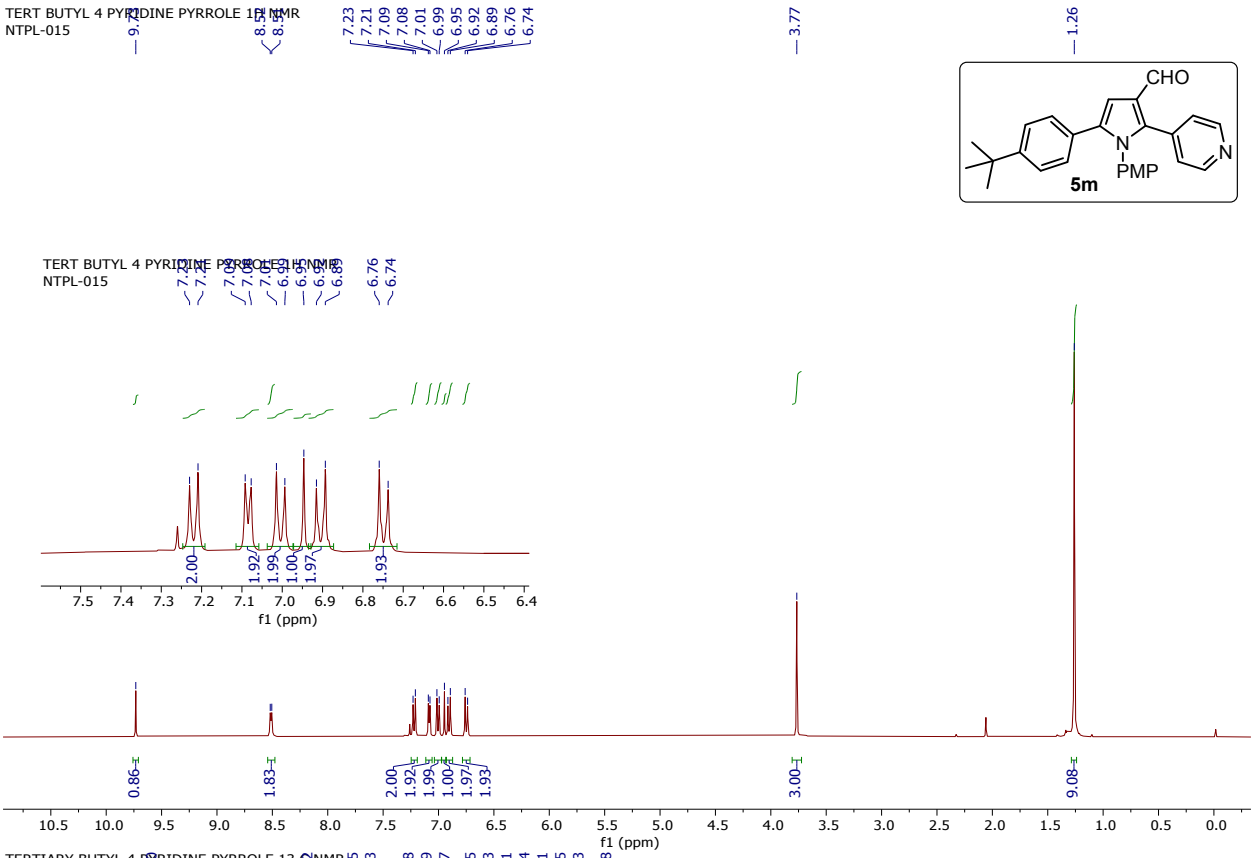
TERT BUTYL 4 PYRIDINE PYRROLE 1H NMR
NTPL-015
9.21
8.51
8.50
7.23
7.21
7.09
7.08
7.01
6.99
6.95
6.92
6.89
6.76
6.74
3.77
1.26
CHO
N
PMP
N
5m
TERT BUTYL 4 PYRIDINE PYRROLE 1H NMR
NTPL-015
7.24
7.23
7.09
7.08
7.05
7.03
6.99
6.97
6.95
6.92
6.89
6.76
6.74
2.00
1.92
1.99
1.00
1.97
1.93
7.5 7.4 7.3 7.2 7.1 7.0 6.9 6.8 6.7 6.6 6.5 6.4
f1 (ppm)
0.86
1.83
2.00
1.92
1.99
1.00
1.97
1.93
3.00
9.08
10.5 10.0 9.5 9.0 8.5 8.0 7.5 7.0 6.5 6.0 5.5 5.0 4.5 4.0 3.5 3.0 2.5 2.0 1.5 1.0 0.5 0.0
f1 (ppm)

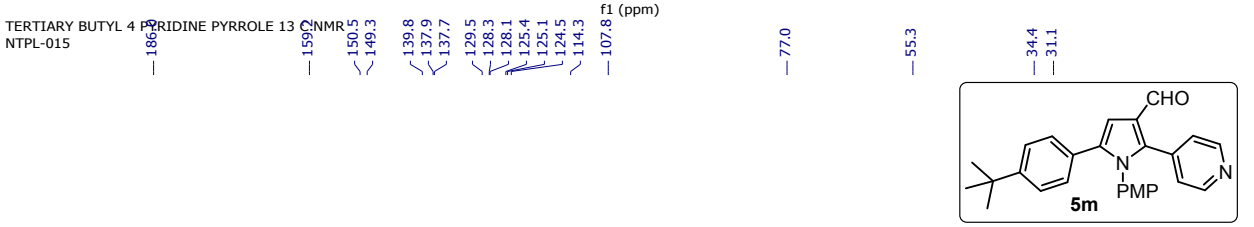
TERTIARY BUTYL 4 PYRIDINE PYRROLE 13 CNMR
NTPL-015
186.2
159.2
150.5
149.3
139.8
137.9
137.7
129.5
128.3
128.1
125.4
125.1
124.5
114.3
107.8
77.0
55.3
34.4
31.1
CHO
N
PMP
N
5m

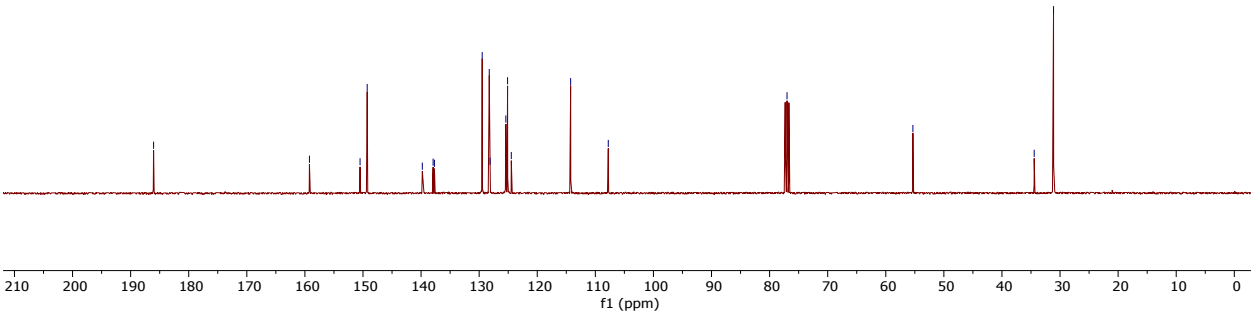
210 200 190 180 170 160 150 140 130 120 110 100 90 80 70 60 50 40 30 20 10 0
f1 (ppm)

3 METHOXY 4 PYRIDINE PYRROLE 1H NMR.25.fid
NTPL-026

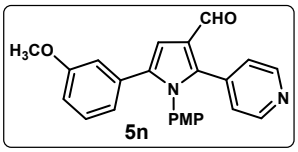

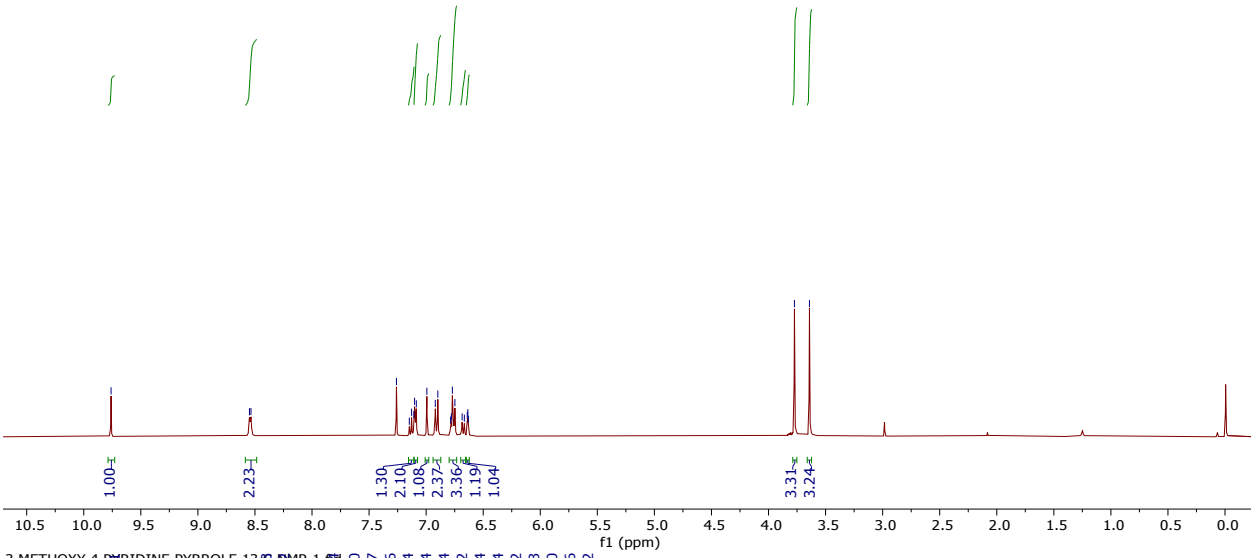

3 METHOXY 4 PYRIDINE PYRROLE 13C NMR.1.fid
NTPL-026

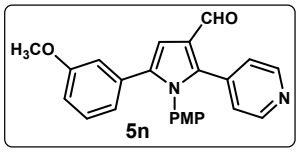

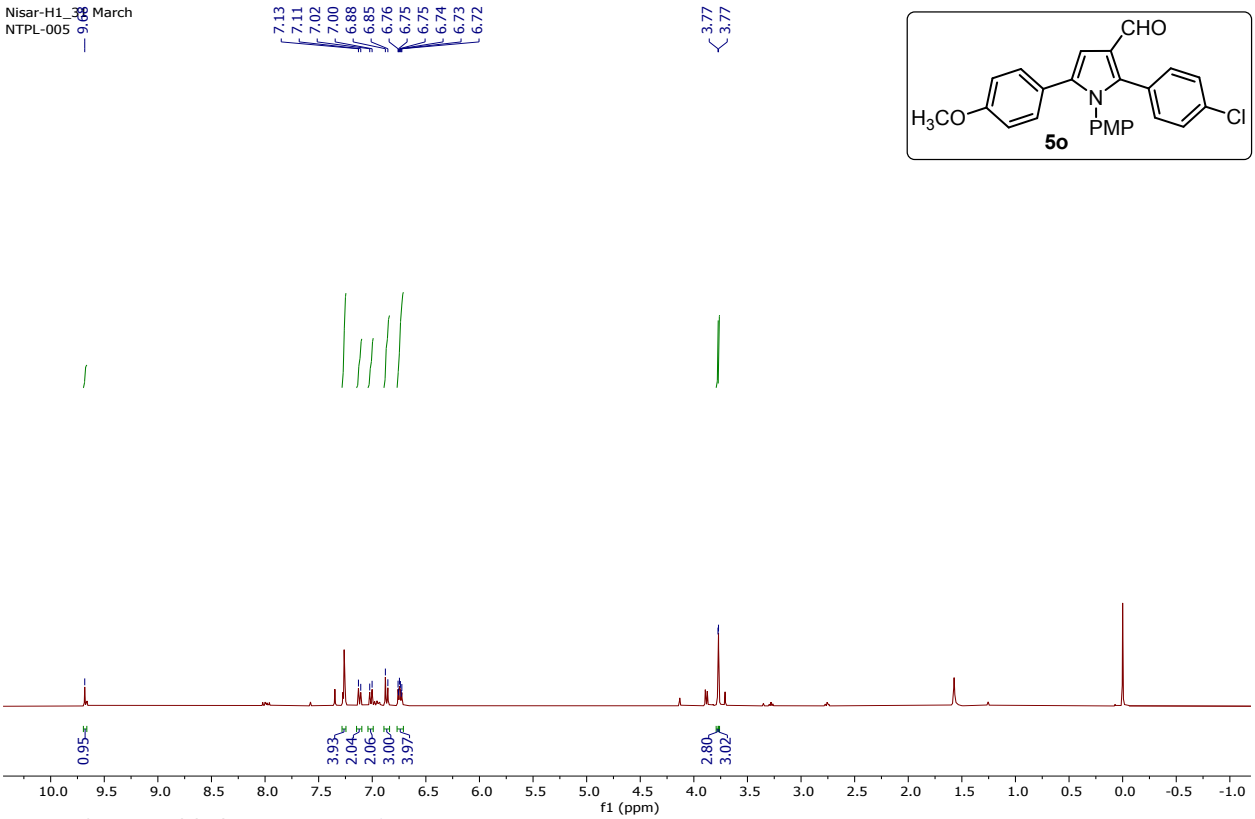
Nisar-H1_30 March
NTPL-005
9.68
7.13
7.11
7.02
7.00
6.88
6.85
6.76
6.75
6.75
6.74
6.73
6.72
3.77
3.77
CHO
N
PMP
H3CO
Cl
5o
0.95
3.93
2.04
2.06
3.00
3.97
2.80
3.02
f1 (ppm)

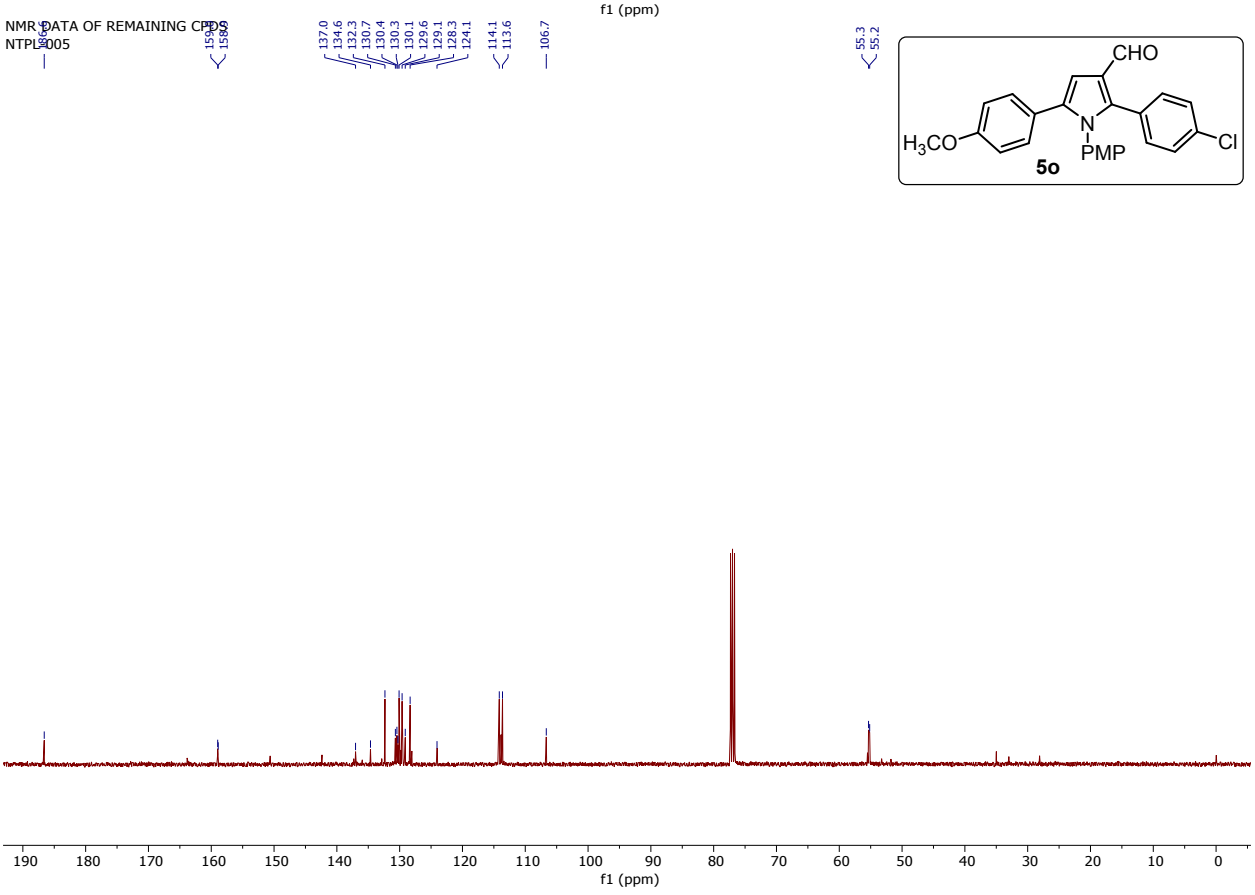
NMR DATA OF REMAINING CPDS
NTPL-005
159.6
159.0
158.0
137.0
134.6
132.3
130.7
130.4
130.3
130.1
129.6
129.1
128.3
124.1
114.1
113.6
106.7
55.3
55.2
CHO
N
PMP
H3CO
Cl
5o
f1 (ppm)

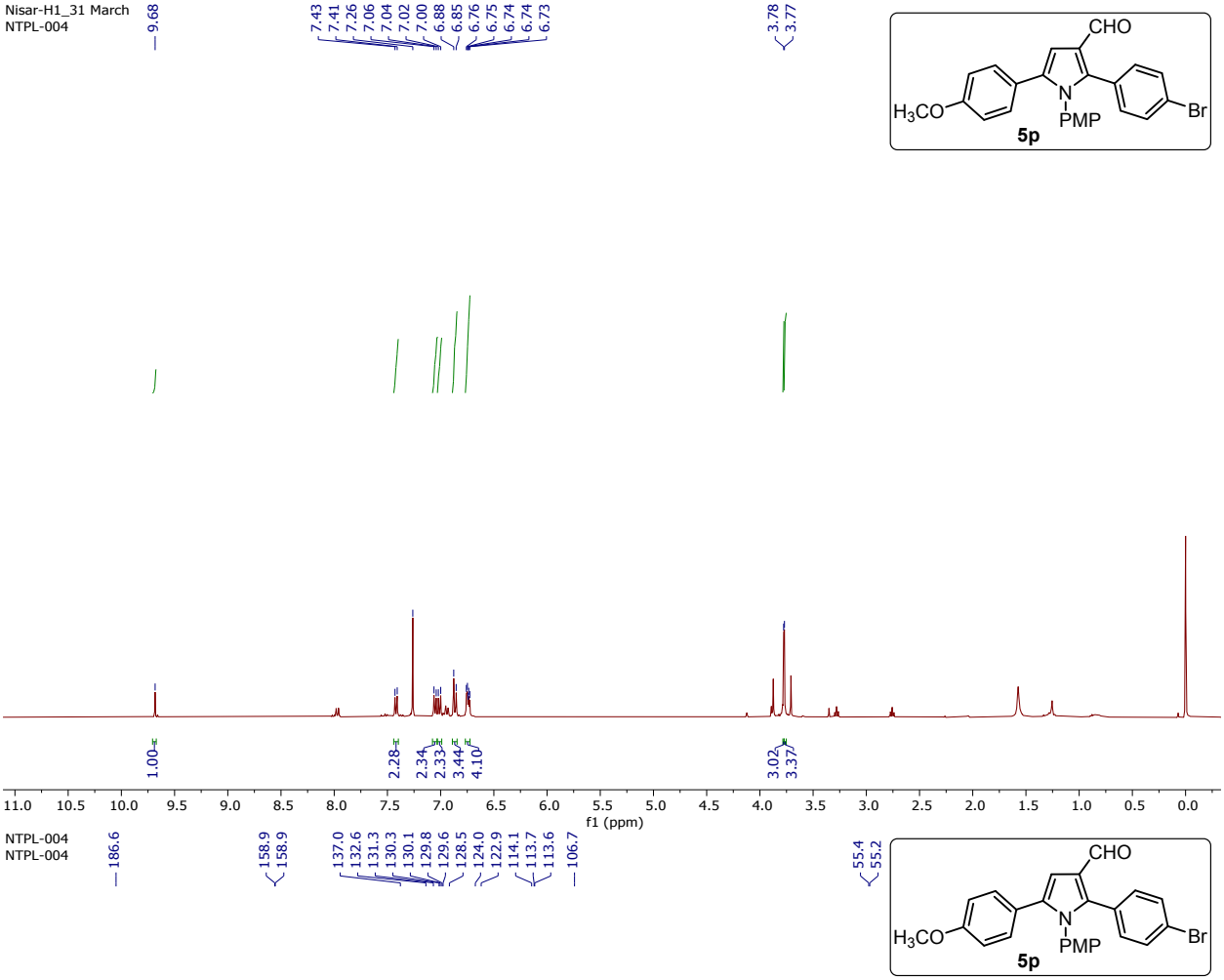
Nisar-H1_31 March
NTPL-004
9.68
7.43
7.41
7.26
7.06
7.04
7.02
7.00
6.88
6.85
6.76
6.75
6.74
6.73
3.78
3.77
CHO
H_3CO
N
PMP
Br
5p
1.00
2.28
2.34
2.33
3.44
4.10
3.02
3.37
f1 (ppm)

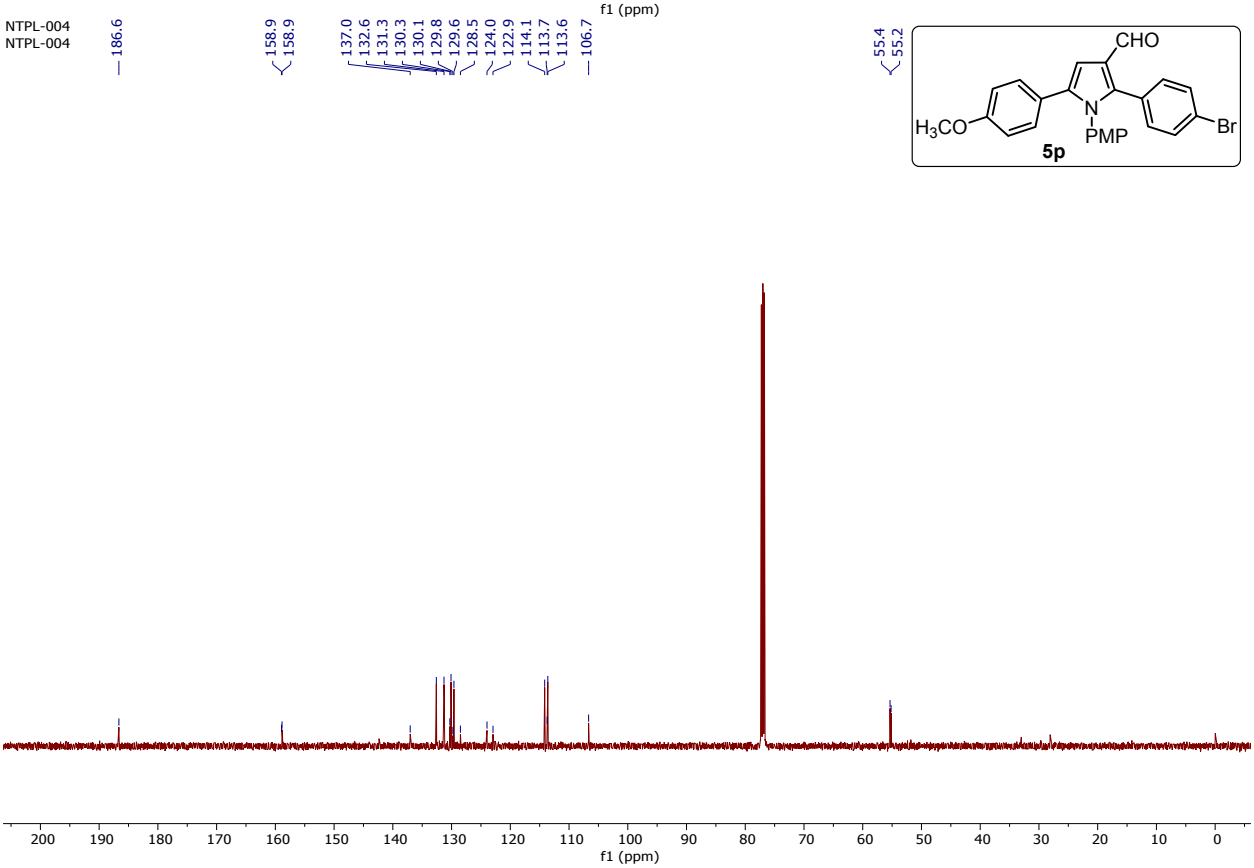
NTPL-004
NTPL-004
186.6
158.9
158.9
137.0
132.6
131.3
130.3
130.1
129.8
129.6
128.5
124.0
122.9
114.1
113.7
113.6
106.7
55.4
55.2
CHO
H_3CO
N
PMP
Br
5p
f1 (ppm)

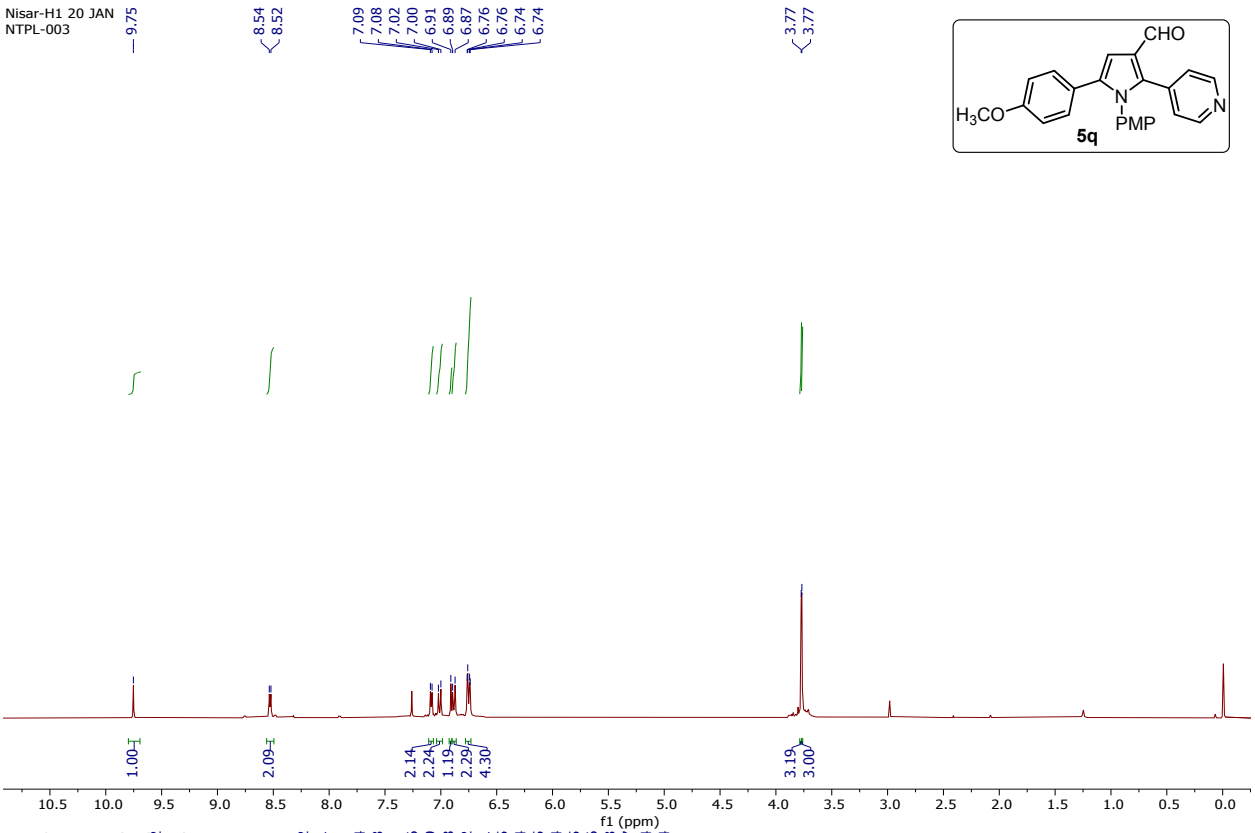
Nisar-H1 20 JAN
NTPL-003
9.75
8.54
8.52
7.09
7.08
7.02
7.00
6.91
6.89
6.87
6.76
6.76
6.74
6.74
3.77
3.77
CHO
H3CO
N
PMP
N
5q
1.00
2.09
2.14
2.24
1.19
2.29
4.30
3.19
3.00
f1 (ppm)

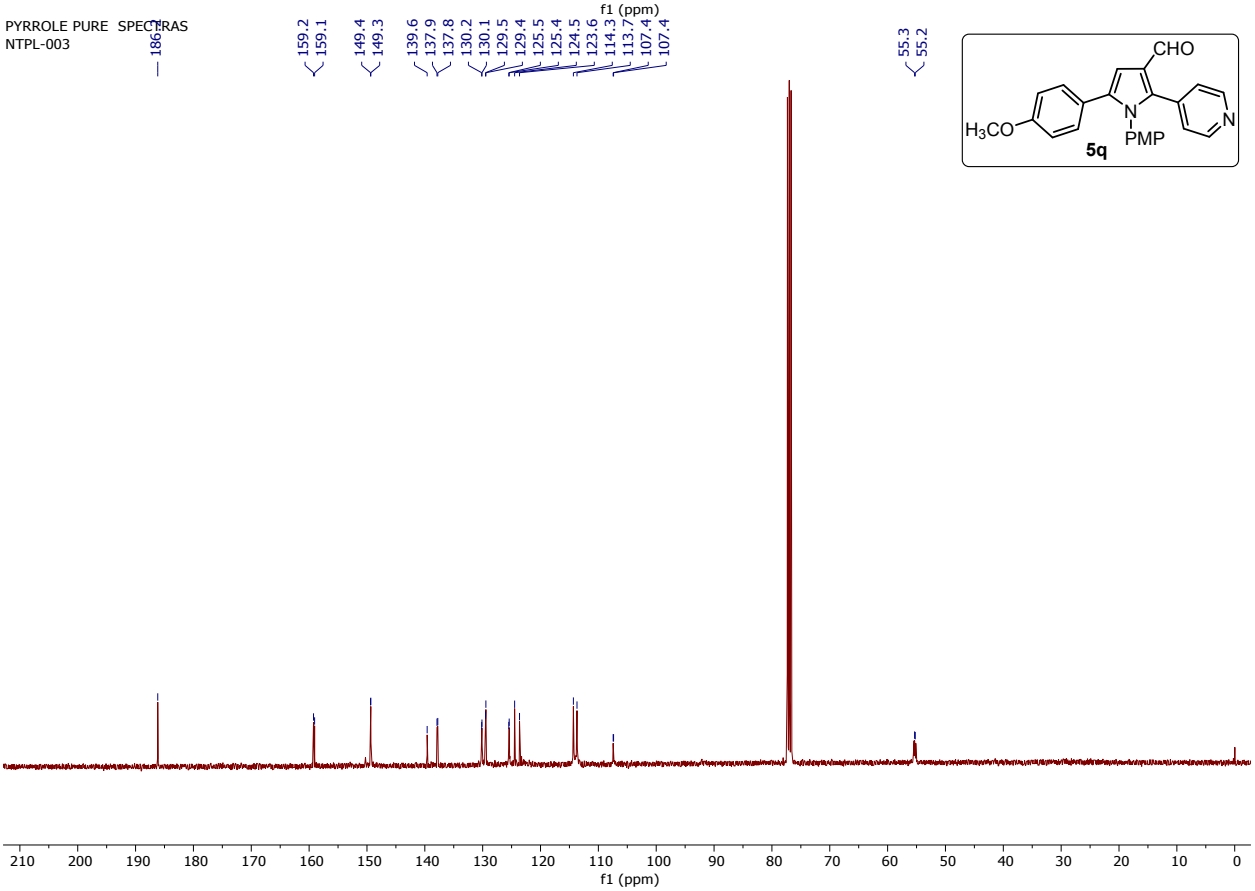
PYRROLE PURE SPECTRAS
NTPL-003
186.2
159.2
159.1
149.4
149.3
139.6
137.9
137.8
130.2
130.1
129.5
129.4
125.5
125.4
124.5
123.6
114.3
113.7
107.4
107.4
55.3
55.2
CHO
H3CO
N
PMP
N
5q
f1 (ppm)

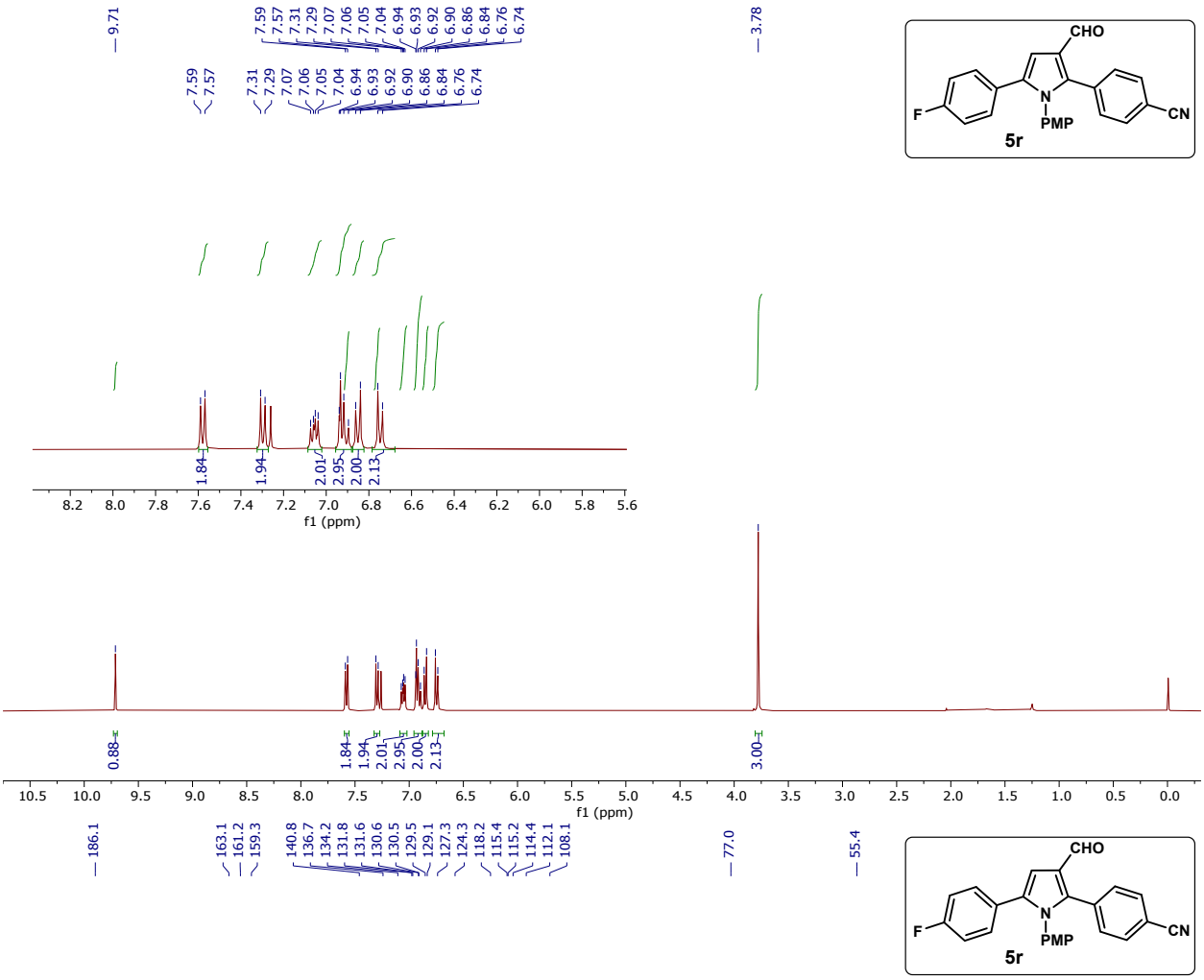
9.71
7.59
7.57
7.31
7.29
7.07
7.06
7.05
7.04
6.94
6.93
6.92
6.90
6.86
6.84
6.76
6.74
3.78
CHO
F
N
PMP
CN
5r
1.84
1.94
2.01
2.95
2.00
2.13
3.00
0.88
f1 (ppm)

186.1
163.1
161.2
159.3
140.8
136.7
134.2
131.8
131.6
130.6
130.5
129.5
129.1
127.3
124.3
118.2
115.4
115.2
114.4
112.1
108.1
77.0
55.4
CHO
F
N
PMP
CN
5r
f1 (ppm)

4 FLOURO 4 PYRIDINE PYRROLE 1H NMR
NTPL-031

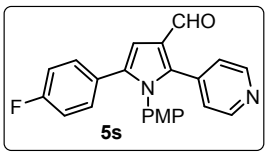

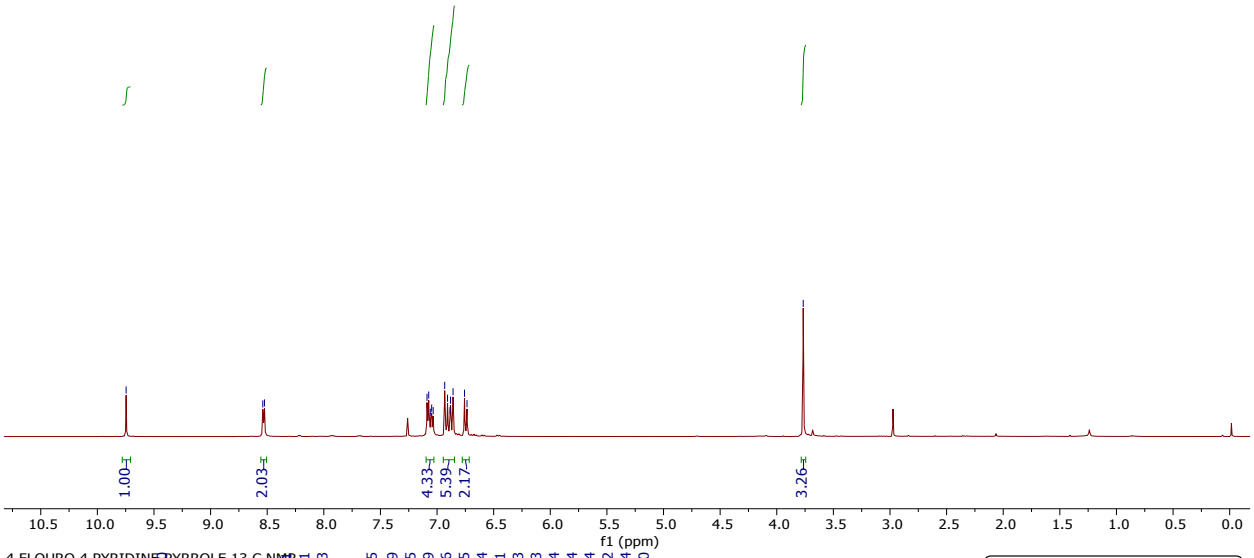

4 FLOURO 4 PYRIDINE PYRROLE 13 C NMR
NTPL-031

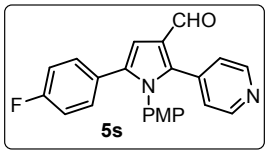

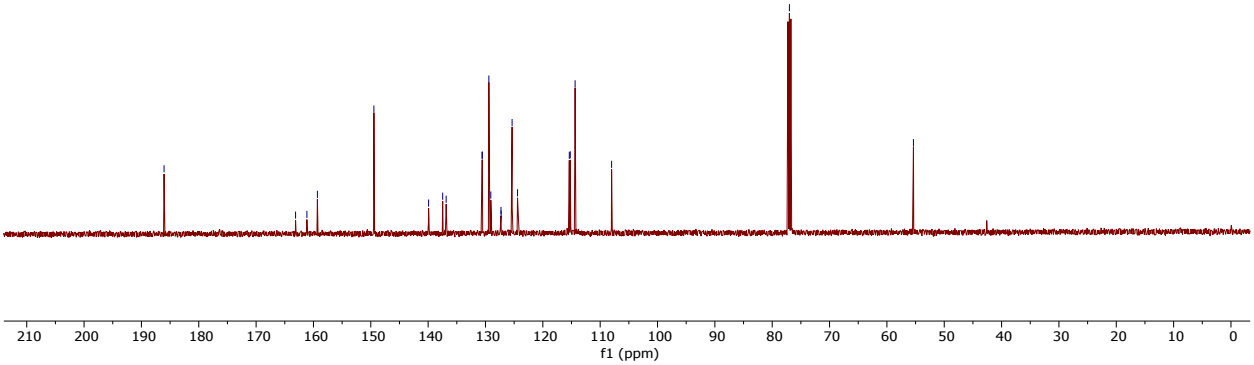

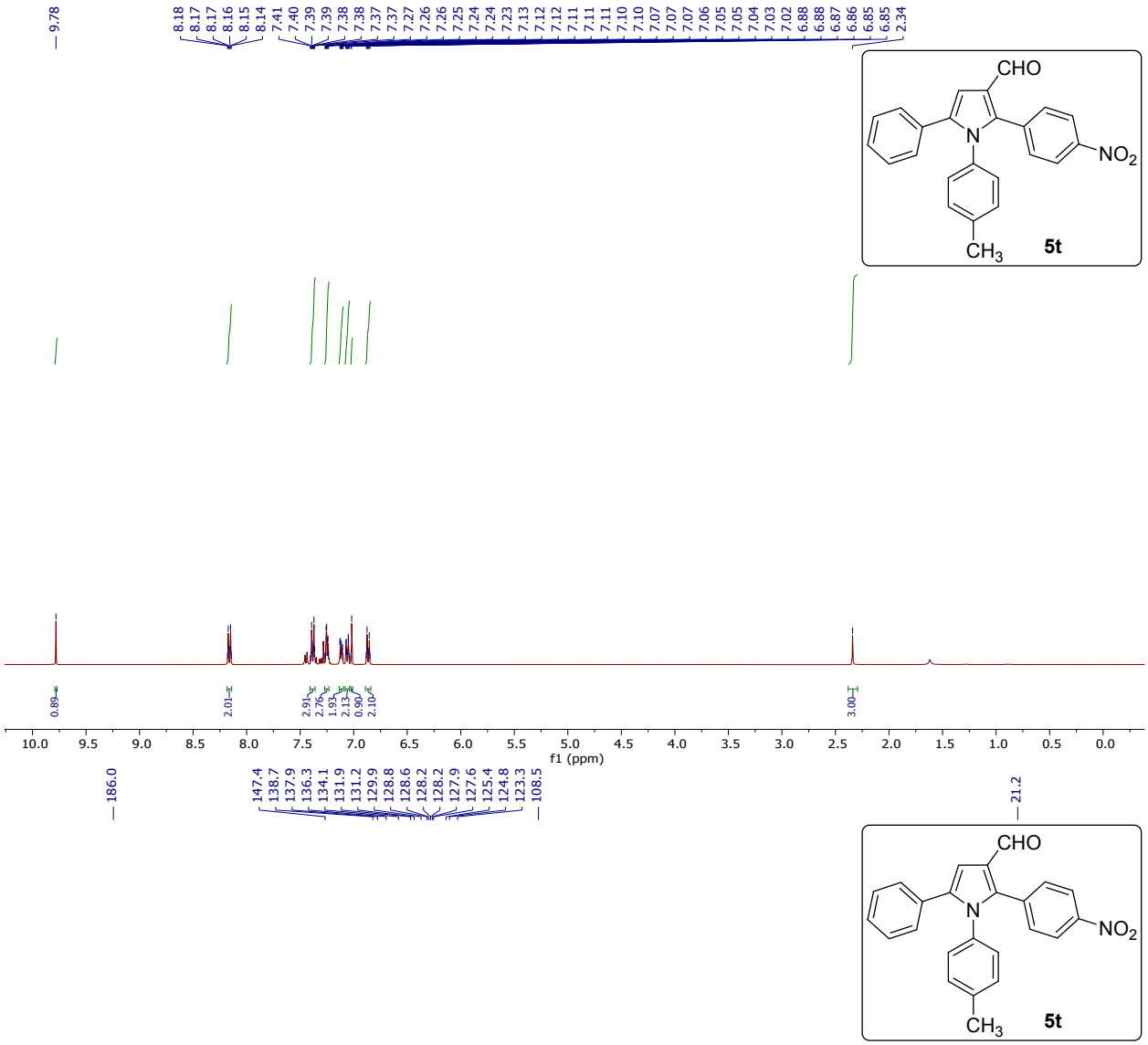
9.78
8.18
8.17
8.17
8.16
8.15
8.14
7.41
7.40
7.39
7.39
7.38
7.38
7.37
7.37
7.27
7.26
7.26
7.25
7.24
7.24
7.23
7.13
7.12
7.12
7.11
7.11
7.11
7.10
7.10
7.07
7.07
7.07
7.06
7.05
7.05
7.04
7.03
7.02
6.88
6.88
6.87
6.86
6.85
6.85
2.34
CHO
N
NO2
CH3
5t
0.89
2.01
2.91
2.76
1.93
2.13
0.90
2.10
3.00
f1 (ppm)
186.0
147.4
138.7
137.9
136.3
134.1
131.9
131.2
129.9
128.8
128.6
128.2
128.2
127.9
127.6
125.4
124.8
123.3
108.5
21.2
CHO
N
NO2
CH3
5t
f1 (ppm)

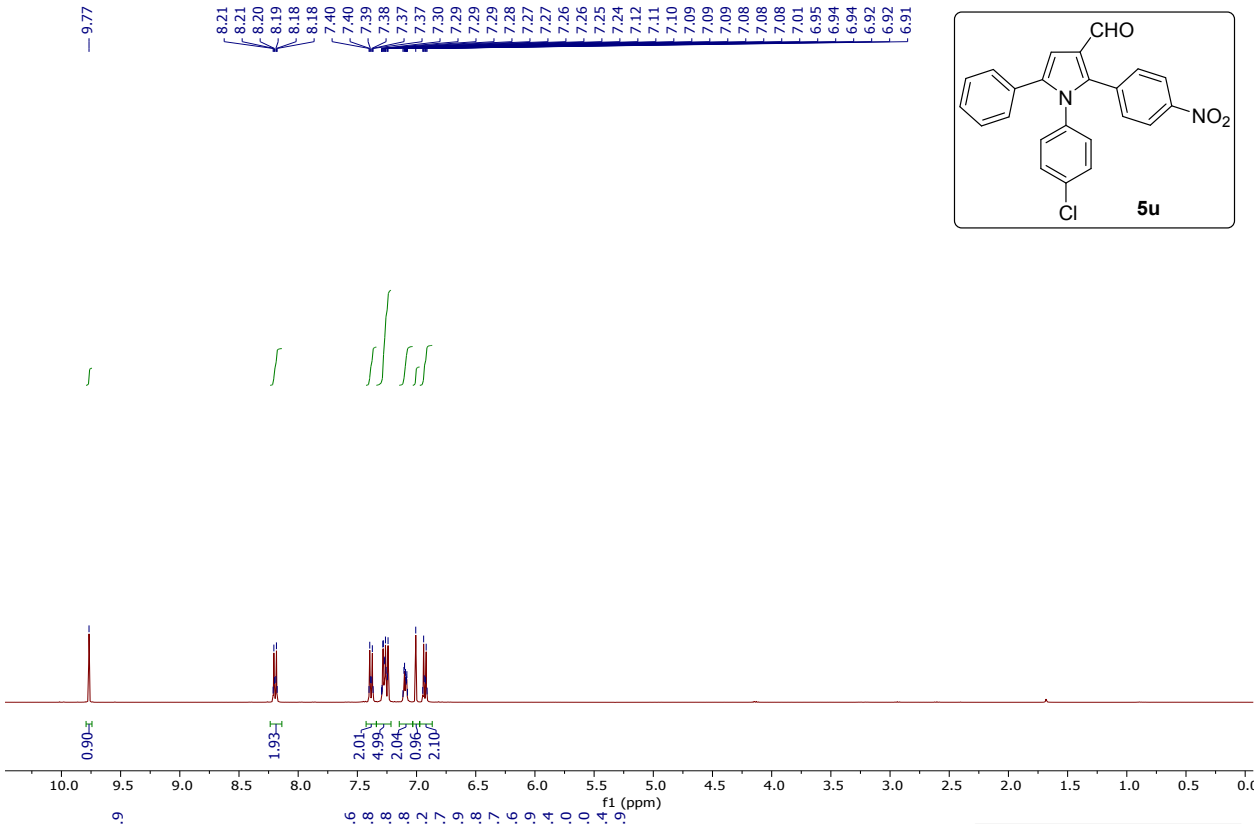
9.77
8.21
8.21
8.20
8.19
8.18
8.18
7.40
7.39
7.38
7.37
7.37
7.30
7.29
7.29
7.29
7.28
7.27
7.27
7.26
7.26
7.25
7.24
7.12
7.11
7.10
7.09
7.09
7.09
7.08
7.08
7.08
7.01
6.95
6.94
6.92
6.92
6.91
CHO
N
NO2
Cl
5u
0.90
1.93
2.01
4.99
2.04
0.96
2.10
10.0
9.5
9.0
8.5
8.0
7.5
7.0
6.5
6.0
5.5
5.0
4.5
4.0
3.5
3.0
2.5
2.0
1.5
1.0
0.5
f1 (ppm)

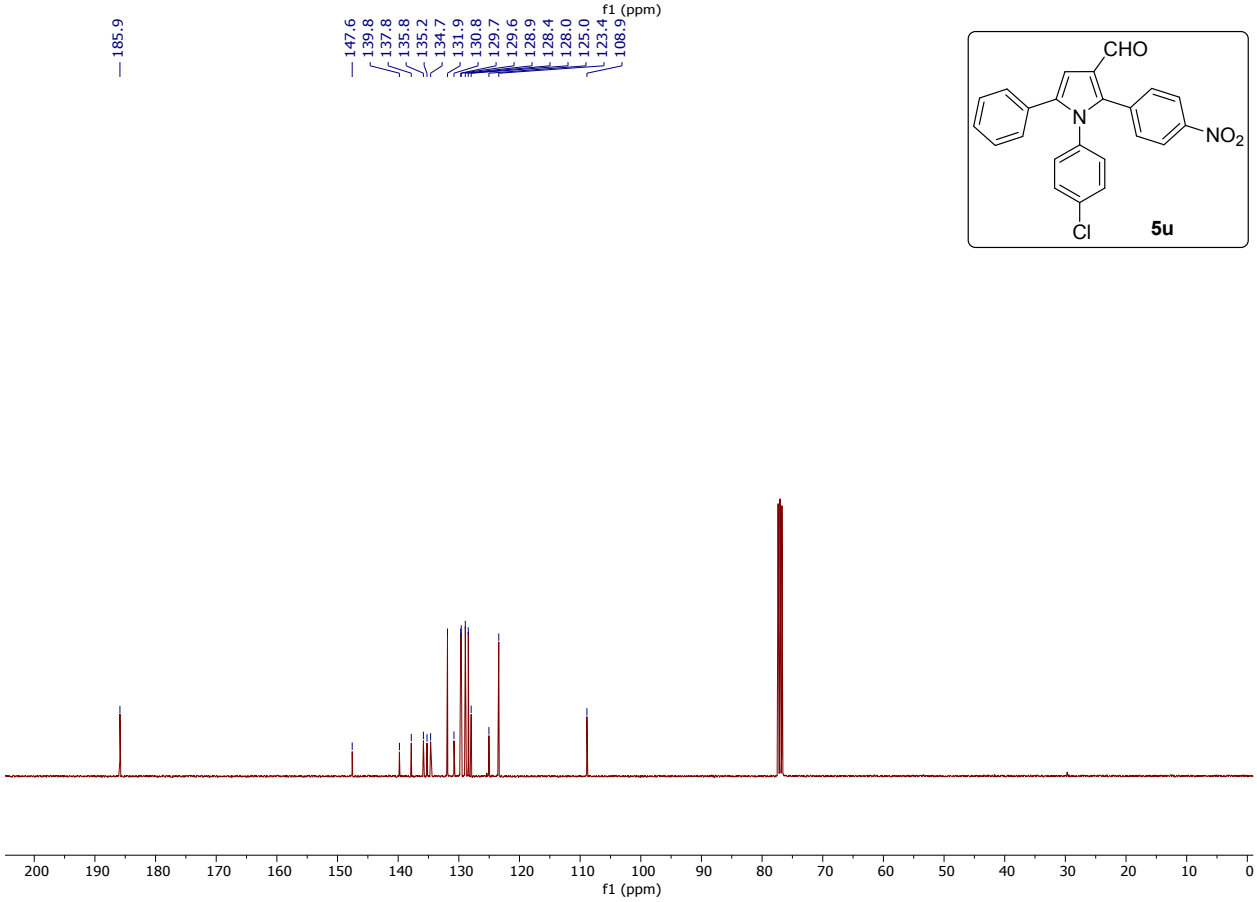
185.9
147.6
139.8
137.8
135.8
135.2
134.7
131.9
130.8
129.7
129.6
128.9
128.4
128.0
125.0
123.4
108.9
CHO
N
NO2
Cl
5u
200
190
180
170
160
150
140
130
120
110
100
90
80
70
60
50
40
30
20
10
0
f1 (ppm)

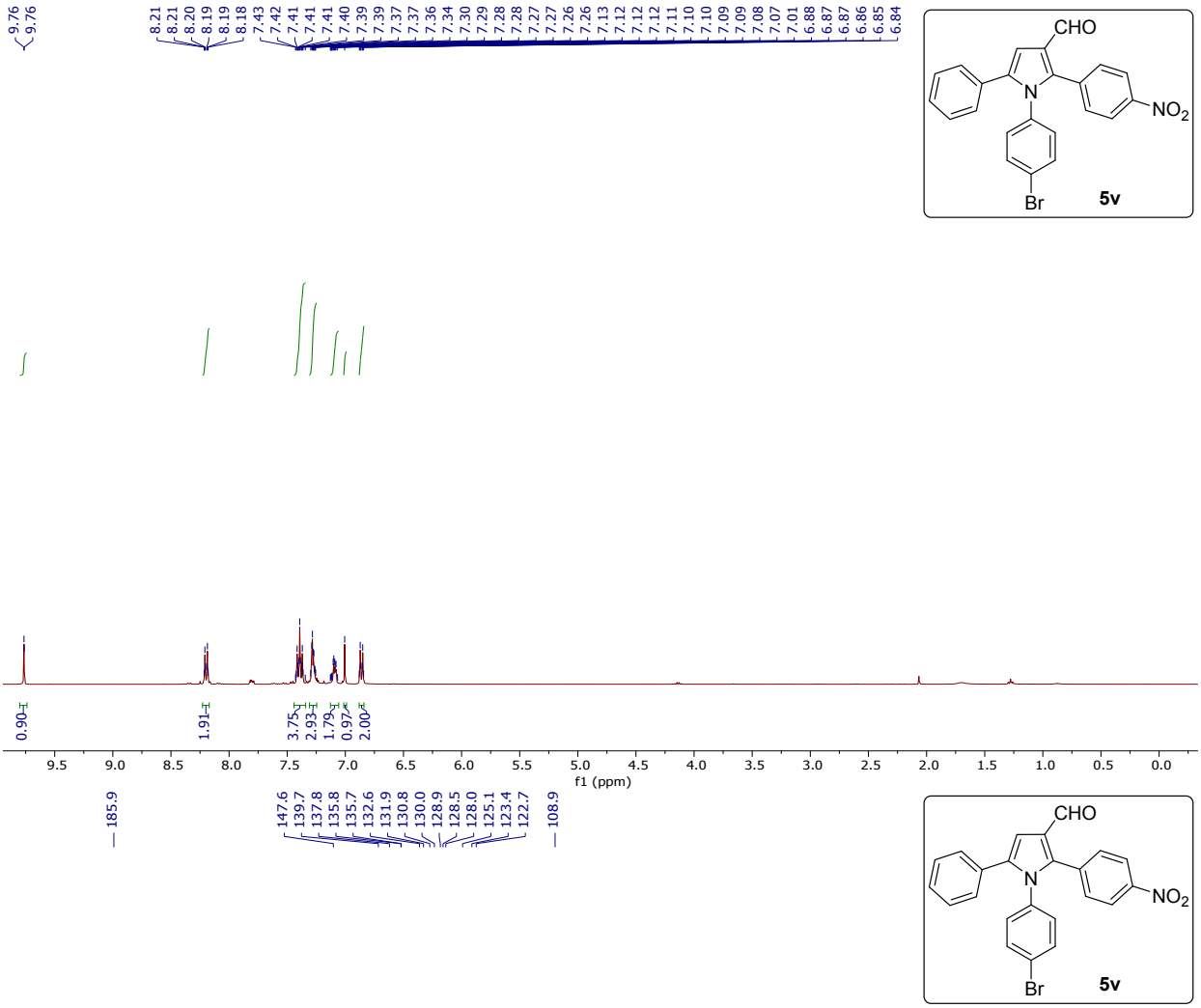
9.76
9.76
8.21
8.21
8.20
8.19
8.19
8.18
7.43
7.42
7.41
7.41
7.41
7.40
7.39
7.39
7.37
7.37
7.36
7.34
7.30
7.29
7.28
7.28
7.27
7.27
7.26
7.26
7.13
7.12
7.12
7.12
7.11
7.10
7.10
7.09
7.09
7.08
7.07
7.01
6.88
6.87
6.87
6.86
6.85
6.84
CHO
N
NO2
Br
5v
0.90
1.91
3.75
2.93
1.79
0.97
2.00
f1 (ppm)
185.9
147.6
139.7
137.8
135.8
135.7
132.6
131.9
130.8
130.0
128.9
128.5
128.0
125.1
123.4
122.7
108.9
CHO
N
NO2
Br
5v
f1 (ppm)

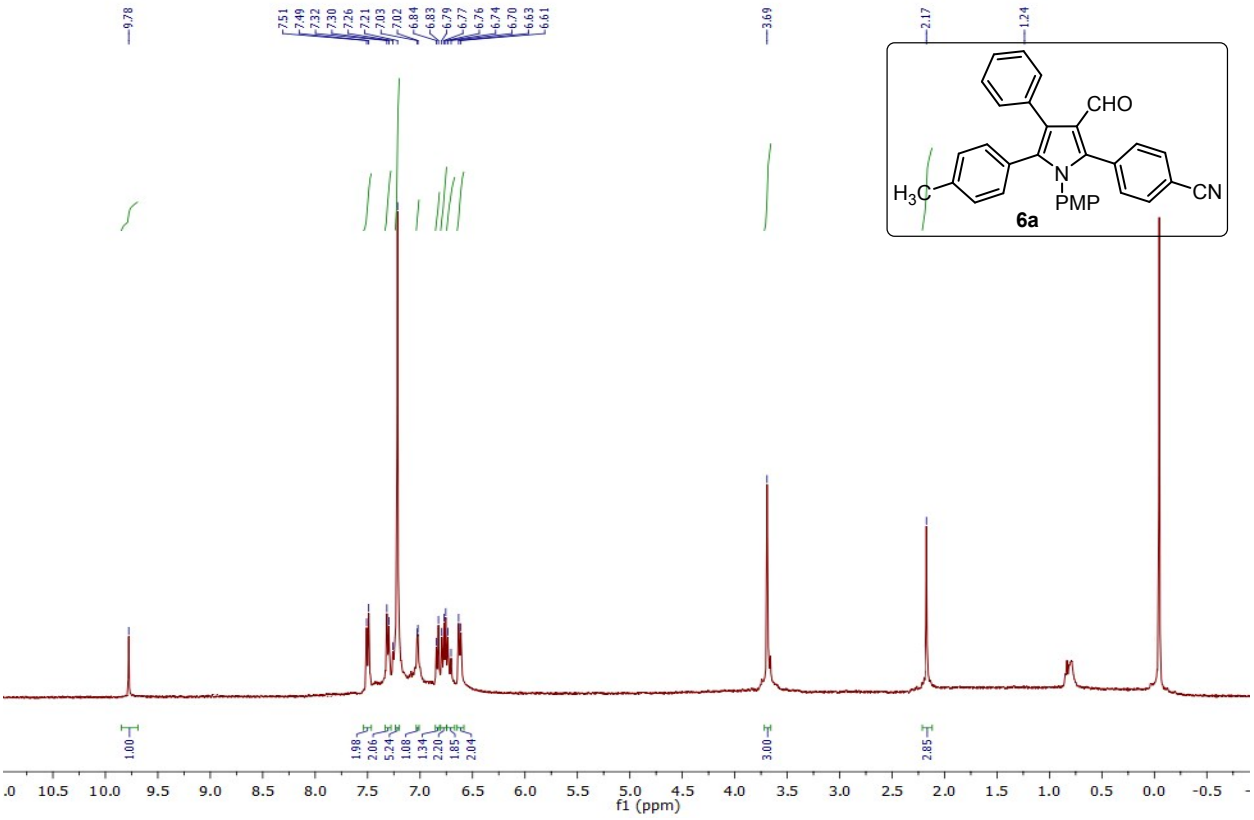
9.78
7.51
7.49
7.32
7.30
7.26
7.21
7.03
7.02
6.84
6.83
6.79
6.77
6.76
6.74
6.70
6.63
6.61
3.69
2.17
1.24
CHO
N
PMP
H_3C
CN
6a
1.00
1.98
2.06
5.24
1.08
1.34
2.20
1.85
2.04
3.00
2.85
f1 (ppm)

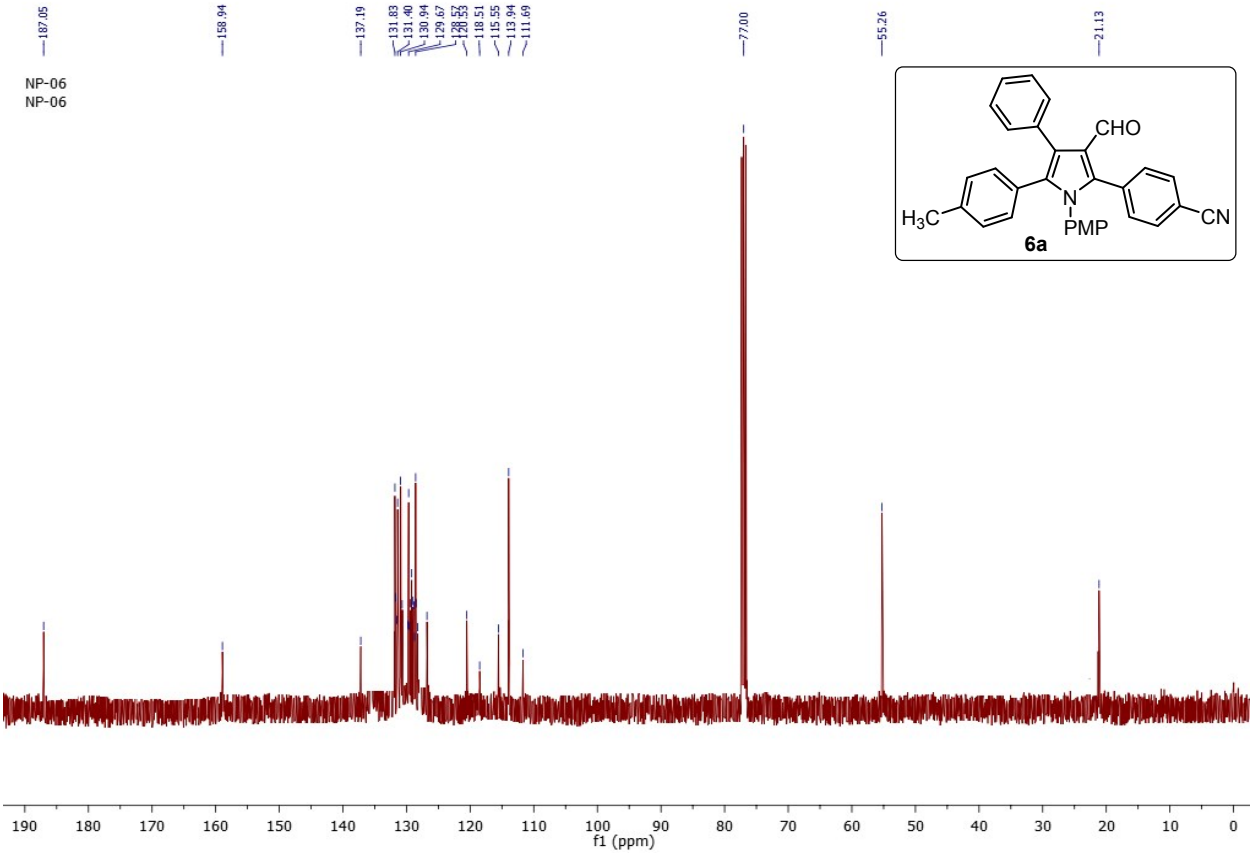
187.05
158.94
137.19
131.83
131.40
130.94
129.67
118.51
115.55
113.94
111.69
77.00
55.26
21.13
NP-06
NP-06
CHO
N
PMP
H_3C
CN
6a
f1 (ppm)

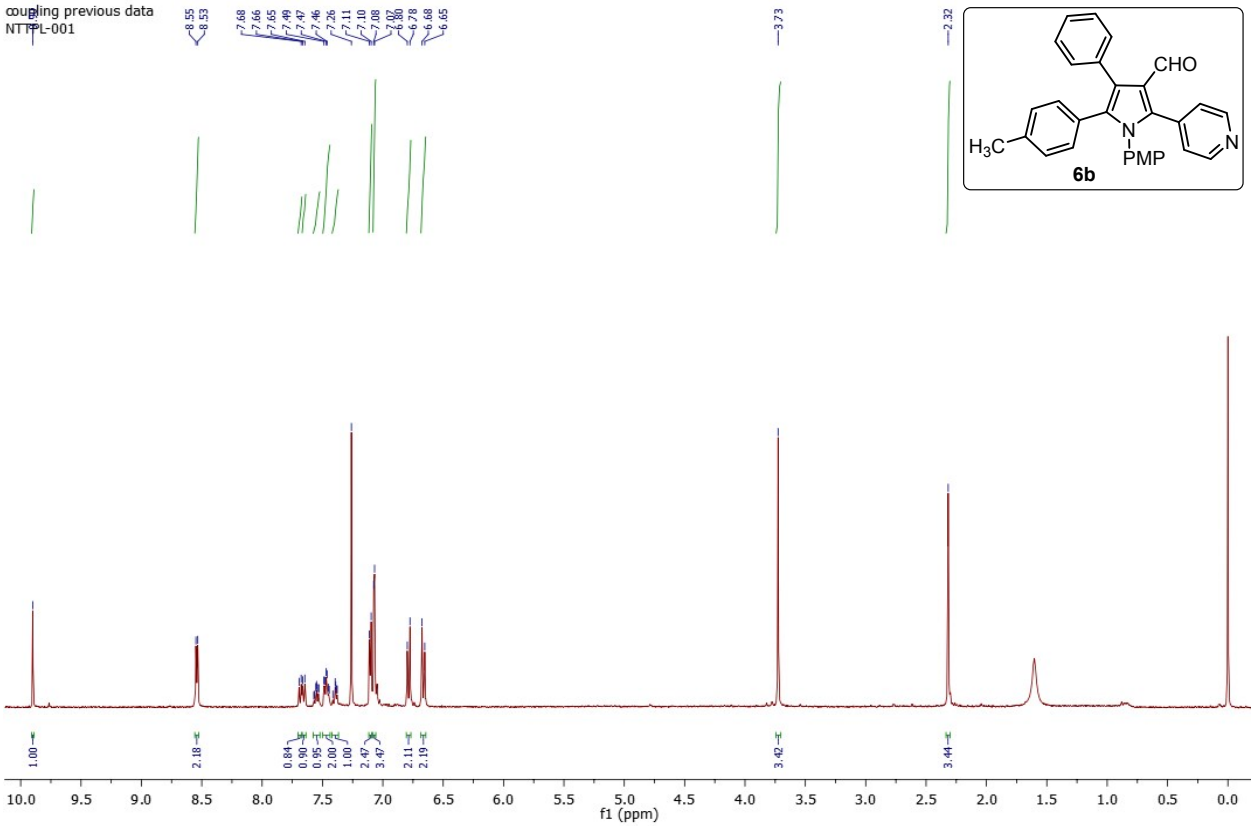
coupling previous data
NTTPL-001
8.55
8.53
7.68
7.66
7.65
7.49
7.47
7.46
7.26
7.11
7.10
7.08
6.78
6.68
6.65
3.73
2.32
CHO
H_3C
N
PMP
N
6b
1.00
2.18
0.84
0.90
0.95
2.00
1.00
2.47
3.47
2.11
2.19
3.42
3.44
10.0
9.5
9.0
8.5
8.0
7.5
7.0
6.5
6.0
5.5
5.0
4.5
4.0
3.5
3.0
2.5
2.0
1.5
1.0
0.5
0.0
f1 (ppm)

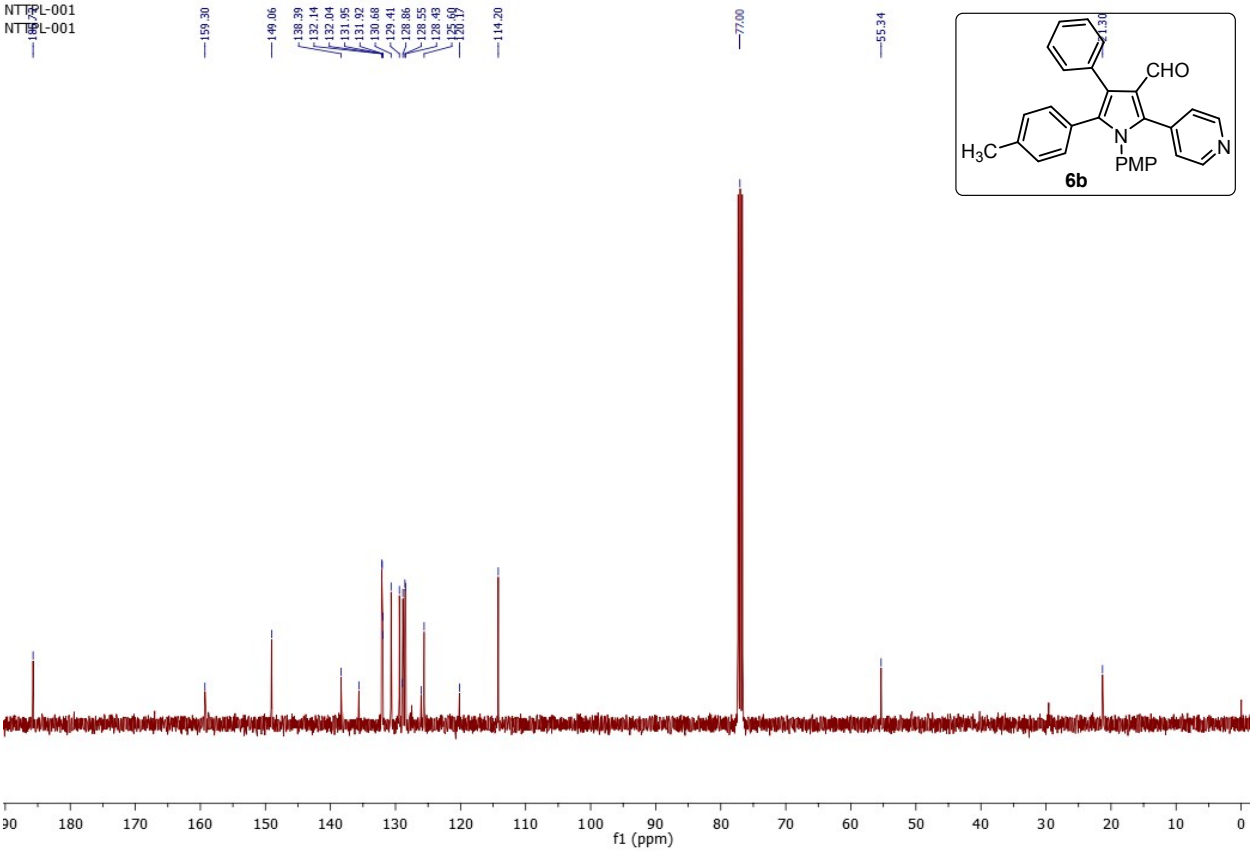
NTTPL-001
NTTPL-001
159.30
149.06
138.39
132.14
132.04
131.95
131.92
130.68
129.41
128.86
128.55
128.43
125.60
120.17
114.20
77.00
55.34
21.30
CHO
H_3C
N
PMP
N
6b
90
180
170
160
150
140
130
120
110
100
90
80
70
60
50
40
30
20
10
0
f1 (ppm)

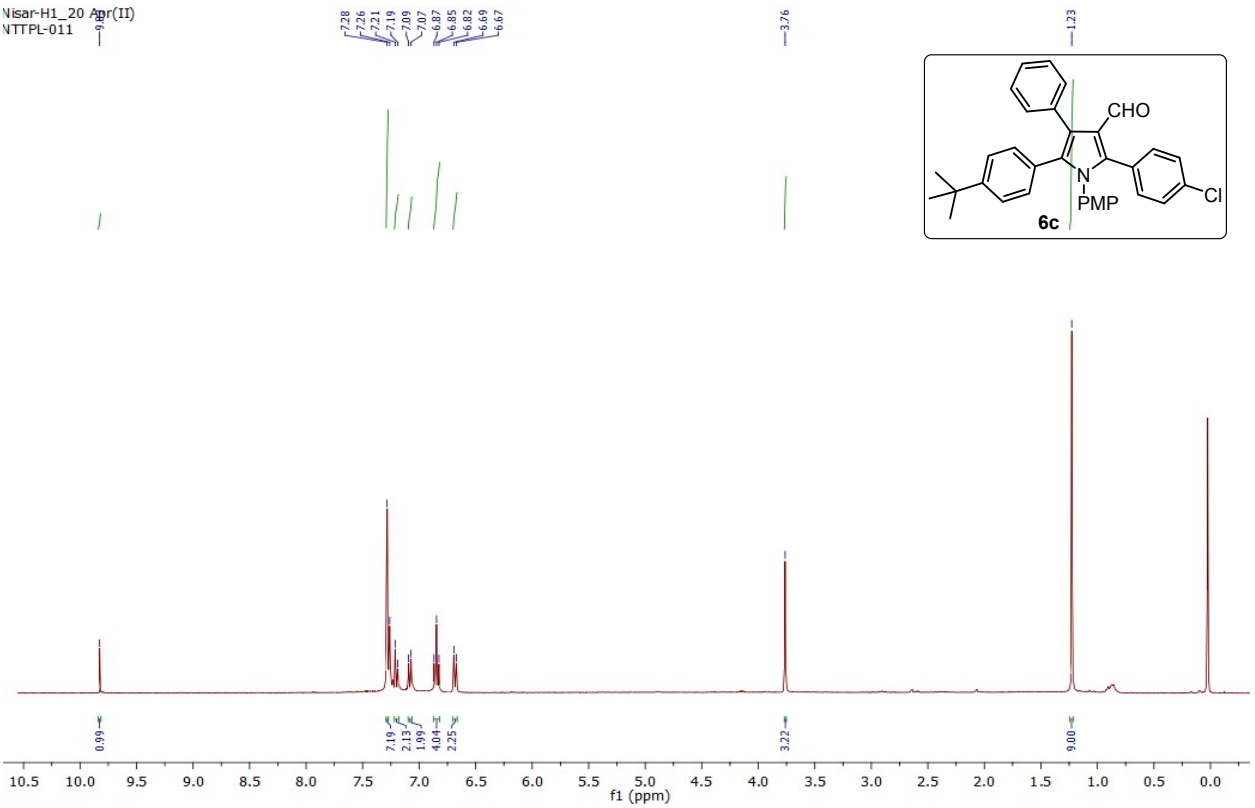
Nisar-H1_20 Apr(II)
NTTPL-011
9.88
7.28
7.26
7.21
7.19
7.09
7.07
6.87
6.85
6.82
6.69
6.67
3.76
1.23
CHO
N
PMP
Cl
6c
0.99
7.19
2.13
1.99
4.04
2.25
3.22
9.00
f1 (ppm)

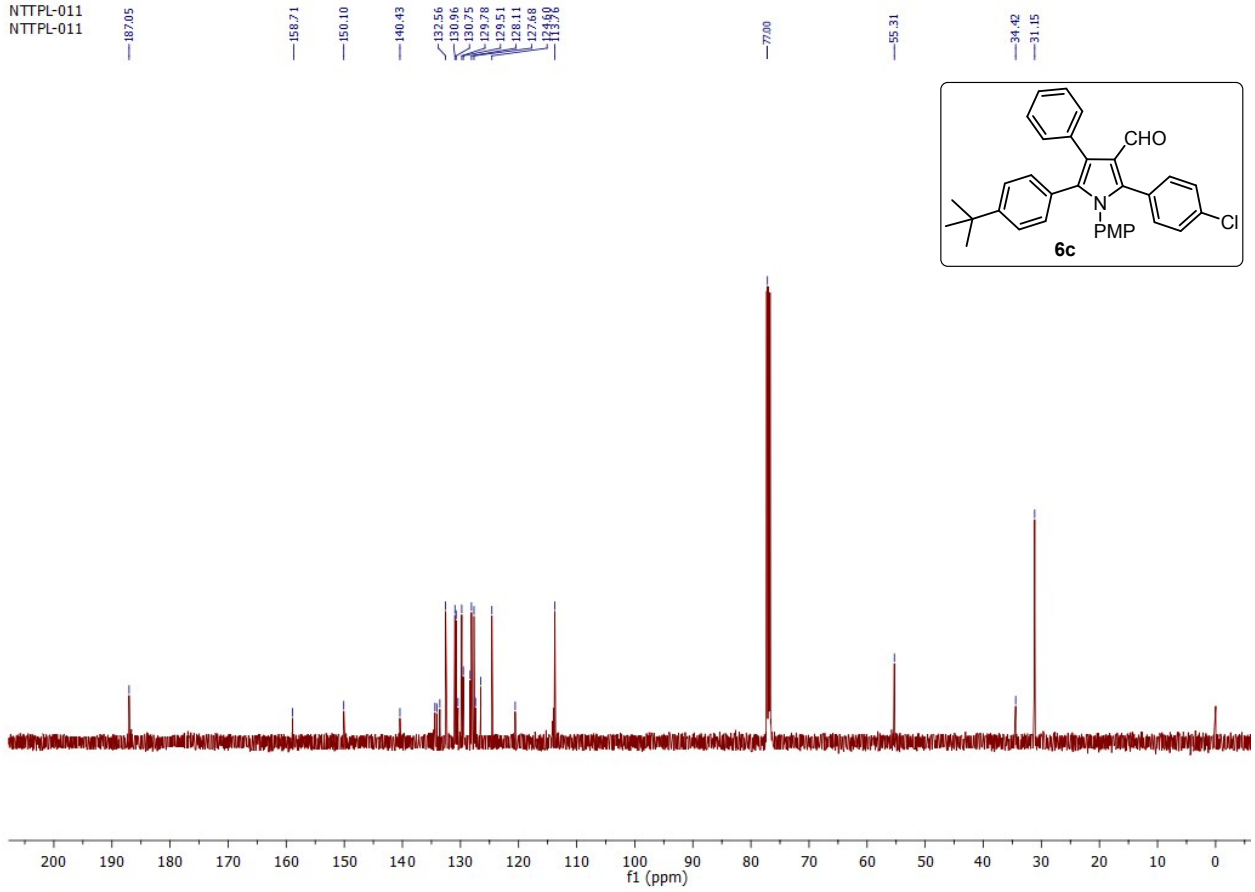
NTTPL-011
NTTPL-011
187.05
158.71
150.10
140.43
132.56
130.96
130.75
129.78
129.51
128.11
127.68
114.60
113.76
77.00
55.31
34.42
31.15
CHO
N
PMP
Cl
6c
f1 (ppm)

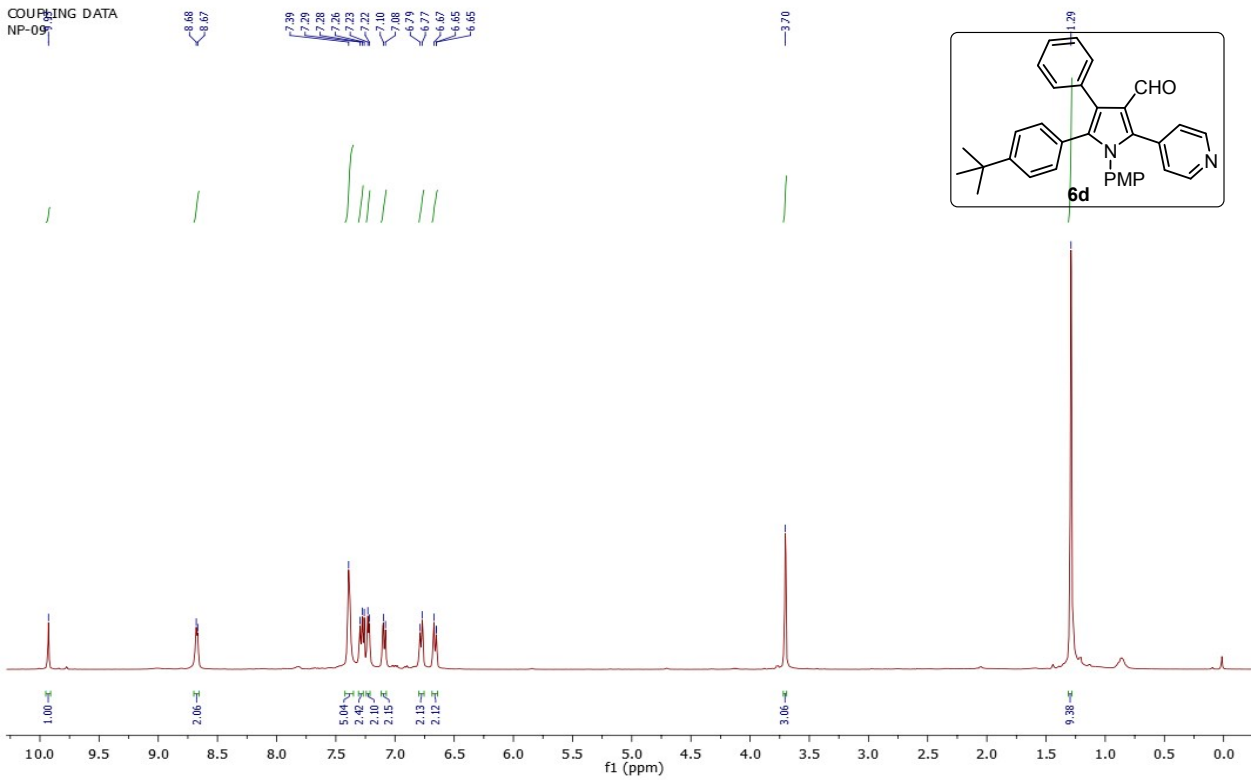
COUPLING DATA
NP-09
8.68
8.67
7.39
7.29
7.28
7.26
7.23
7.22
7.10
7.08
6.79
6.77
6.67
6.65
6.65
3.70
1.29
CHO
N
PMP
N
6d
1.00
2.06
5.04
2.42
2.10
2.15
2.13
2.12
3.06
9.38
f1 (ppm)

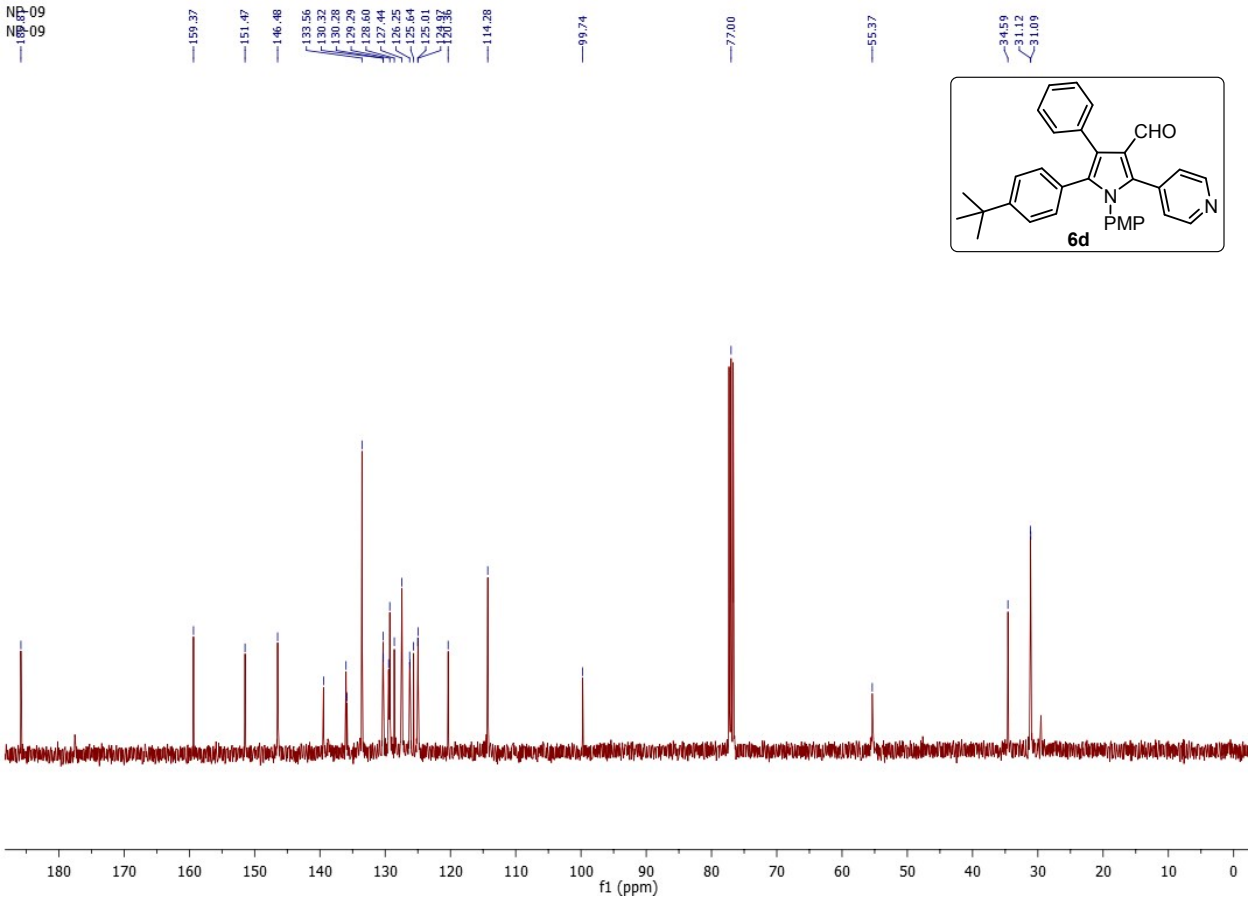
NP-09
NP-09
159.37
151.47
146.48
133.56
130.32
130.28
129.29
128.60
127.44
126.25
125.64
125.01
114.28
99.74
77.00
55.37
34.59
31.12
31.09
CHO
N
PMP
N
6d
f1 (ppm)

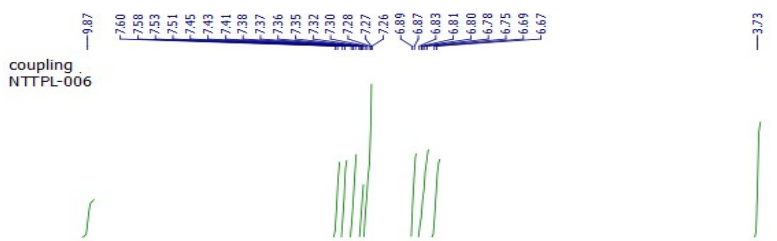
9.87
7.60
7.58
7.53
7.51
7.45
7.43
7.41
7.38
7.37
7.36
7.35
7.32
7.30
7.28
7.27
7.26
6.89
6.87
6.83
6.81
6.80
6.78
6.75
6.69
6.67
3.73
coupling
NTTPL-006

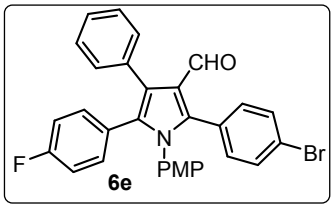
CHO
F
N
PMP
Br
6e

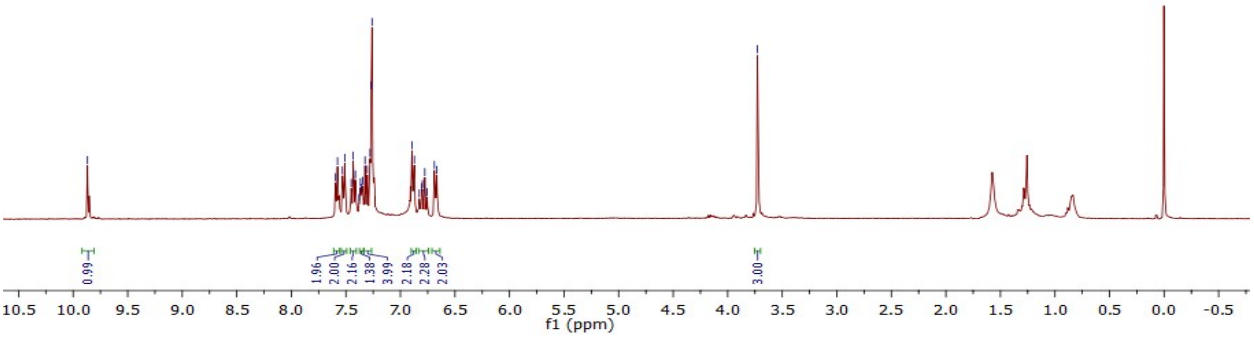
0.99
1.96
2.00
2.16
1.38
3.99
2.18
2.28
2.03
3.00
10.5
10.0
9.5
9.0
8.5
8.0
7.5
7.0
6.5
6.0
5.5
5.0
4.5
4.0
3.5
3.0
2.5
2.0
1.5
1.0
0.5
0.0
-0.5
f1 (ppm)

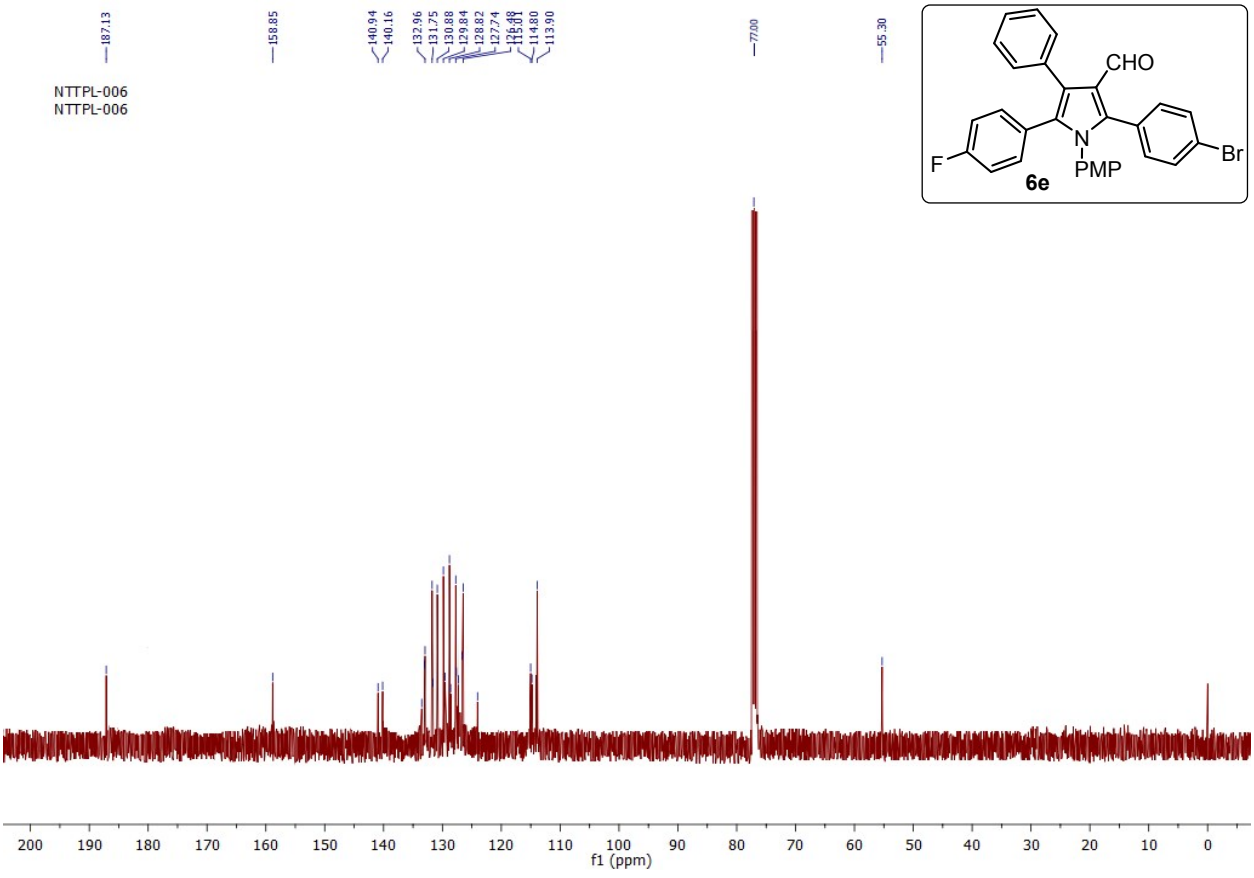
187.13
158.85
140.94
140.16
132.96
131.75
130.88
129.84
128.82
127.74
114.80
113.90
77.00
55.30
NTTPL-006
NTTPL-006
200
190
180
170
160
150
140
130
120
110
100
90
80
70
60
50
40
30
20
10
0
f1 (ppm)

CHO
F
N
PMP
Br
6e

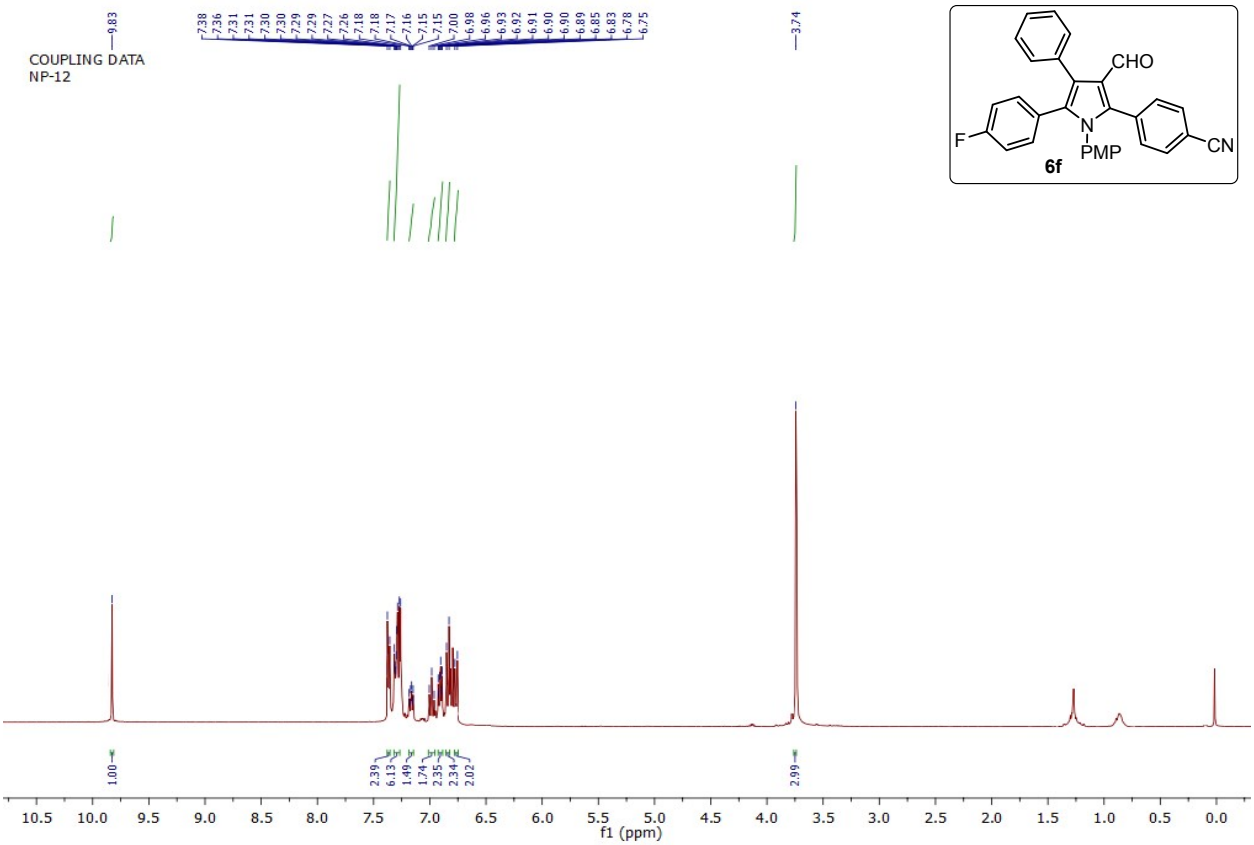
COUPLING DATA
NP-12
9.83
7.38
7.36
7.31
7.31
7.30
7.30
7.29
7.29
7.27
7.26
7.18
7.18
7.17
7.16
7.15
7.15
7.00
6.98
6.96
6.93
6.92
6.91
6.90
6.90
6.89
6.85
6.83
6.78
6.75
3.74
CHO
F
N
PMP
CN
6f
1.00
2.39
6.13
1.49
1.74
2.35
2.34
2.02
2.99
10.5
10.0
9.5
9.0
8.5
8.0
7.5
7.0
6.5
6.0
5.5
5.0
4.5
4.0
3.5
3.0
2.5
2.0
1.5
1.0
0.5
0.0
f1 (ppm)

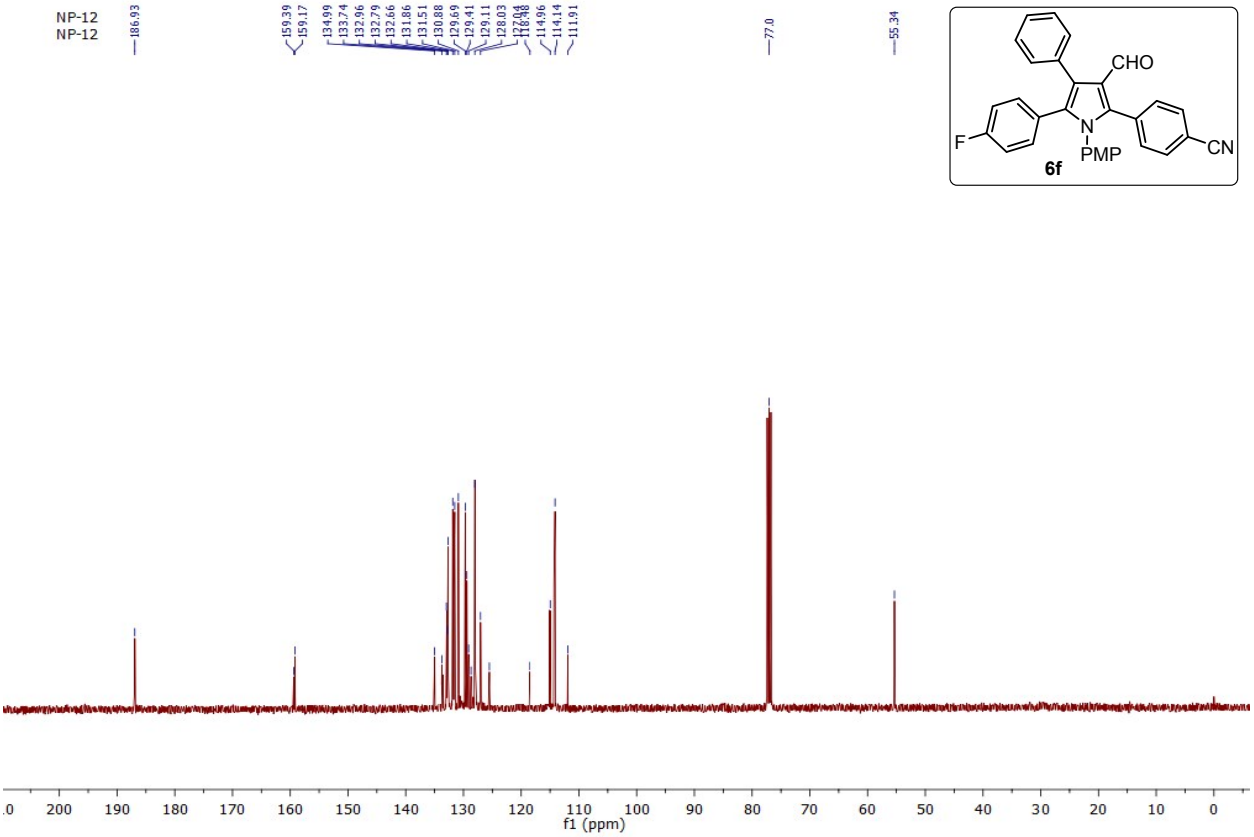
NP-12
NP-12
186.93
159.39
159.17
134.99
133.74
132.96
132.79
132.66
131.86
131.51
130.88
129.69
129.41
129.11
128.03
114.96
114.14
111.91
77.0
55.34
CHO
F
N
PMP
CN
6f
200
190
180
170
160
150
140
130
120
110
100
90
80
70
60
50
40
30
20
10
0
f1 (ppm)

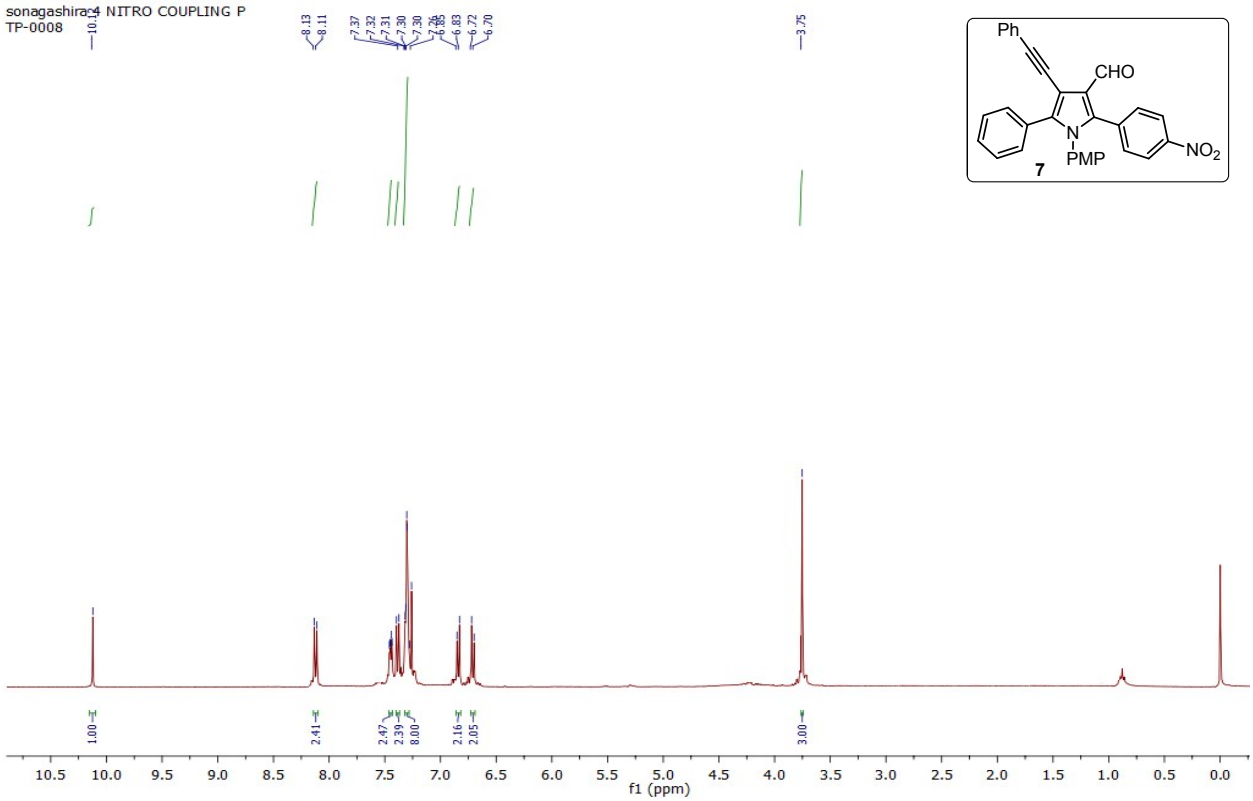
sonagashira 4 NITRO COUPLING P
TP-0008
10.14
8.13
8.11
7.37
7.32
7.31
7.30
7.30
7.26
6.85
6.83
6.72
6.70
3.75
Ph
CHO
N
PMP
NO2
7
1.00
2.41
2.47
2.39
8.00
2.16
2.05
3.00
f1 (ppm)

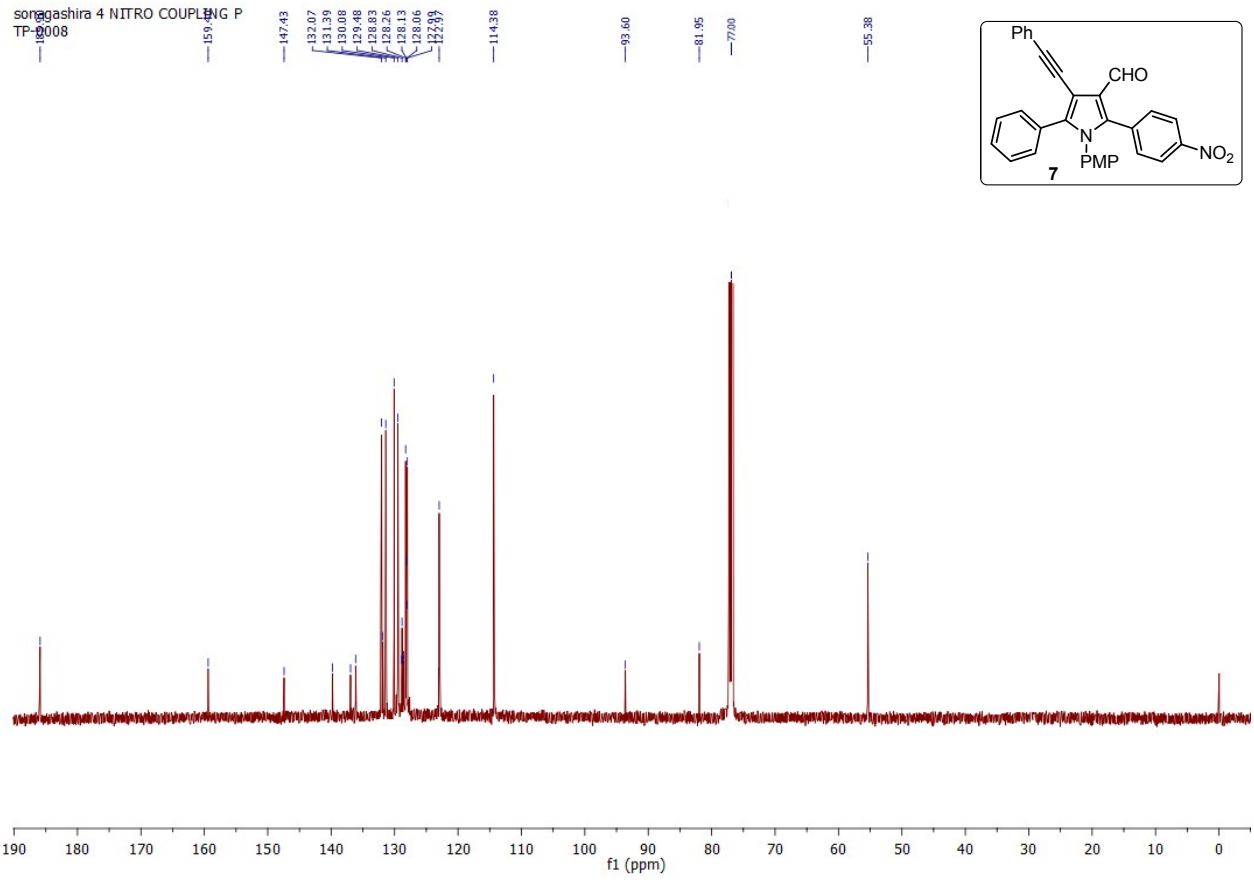
sonagashira 4 NITRO COUPLING P
TP-0008
159.42
147.43
132.07
131.39
130.08
129.48
128.83
128.26
128.13
128.06
114.38
93.60
81.95
77.00
55.38
Ph
CHO
N
PMP
NO2
7
f1 (ppm)

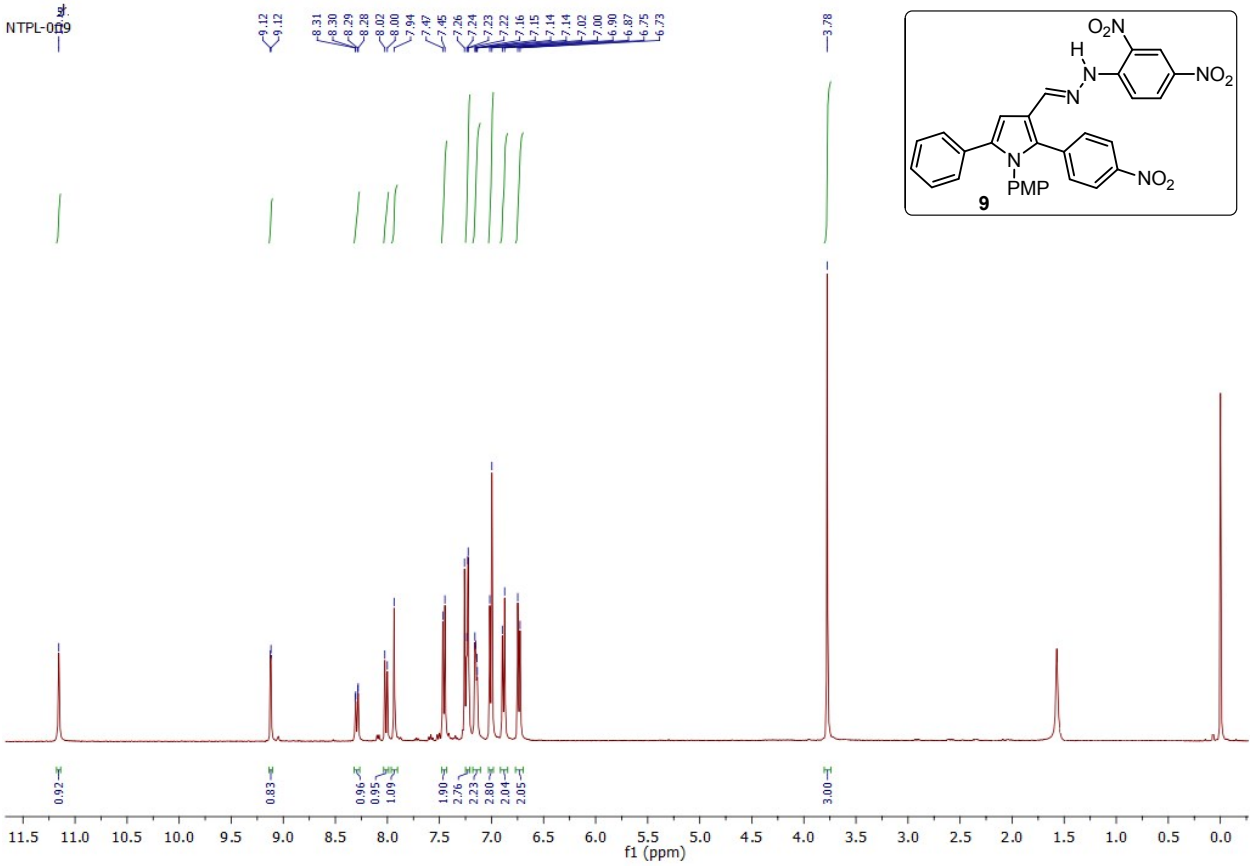
NTPL-009
9.12
9.12
8.31
8.30
8.29
8.28
8.02
8.00
7.94
7.47
7.45
7.26
7.24
7.23
7.22
7.16
7.15
7.14
7.14
7.02
7.00
6.90
6.87
6.75
6.73
3.78
0.92
0.83
0.96
0.95
1.09
1.90
2.76
2.23
2.80
2.04
2.05
3.00
11.5 11.0 10.5 10.0 9.5 9.0 8.5 8.0 7.5 7.0 6.5 6.0 5.5 5.0 4.5 4.0 3.5 3.0 2.5 2.0 1.5 1.0 0.5 0.0
f1 (ppm)
O2N
H
N
N
NO2
N
PMP
NO2
9

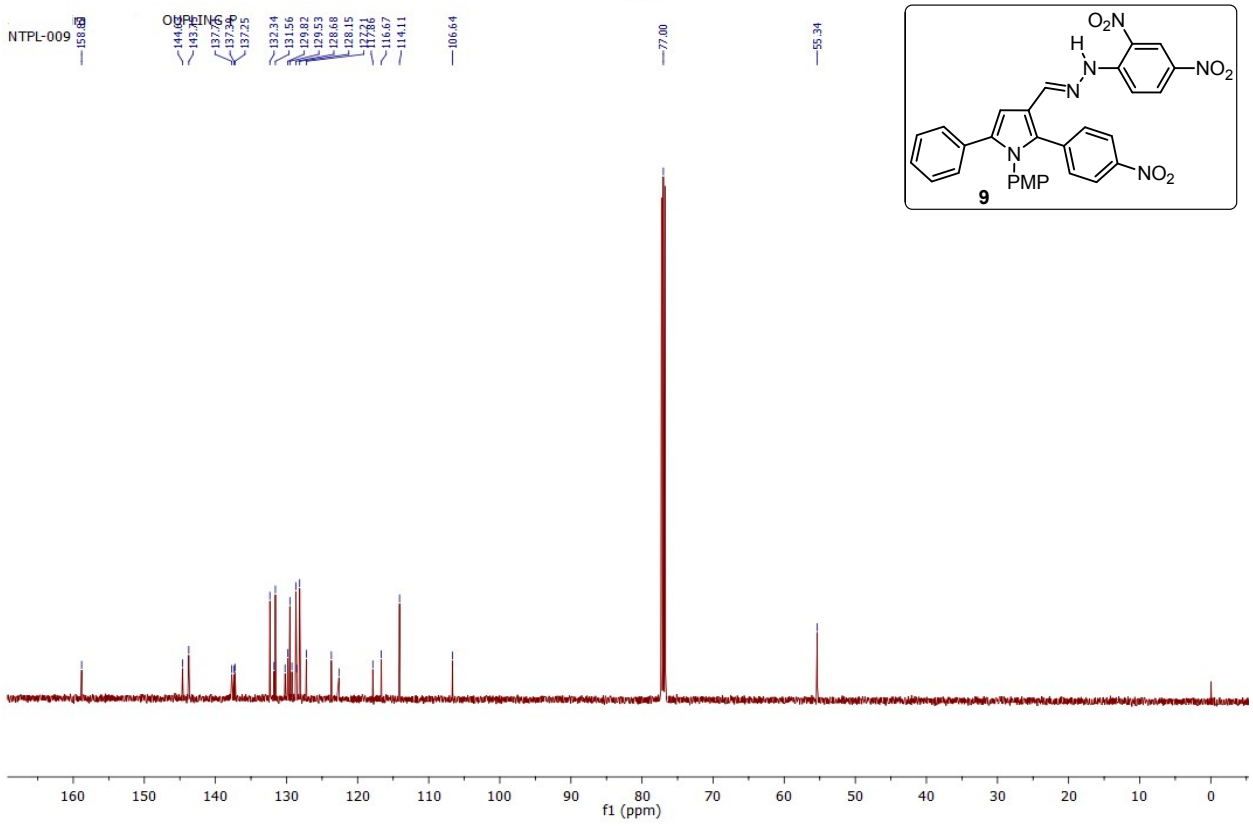
NTPL-009
158.68
144.01
143.71
137.74
137.34
137.25
132.34
131.56
129.82
129.53
128.68
128.15
117.21
117.86
116.67
114.11
106.64
77.00
55.34
160 150 140 130 120 110 100 90 80 70 60 50 40 30 20 10 0
f1 (ppm)
O2N
H
N
N
NO2
N
PMP
NO2
9

IndreshKumar-H1
4-No2-PyrolleAlcohol

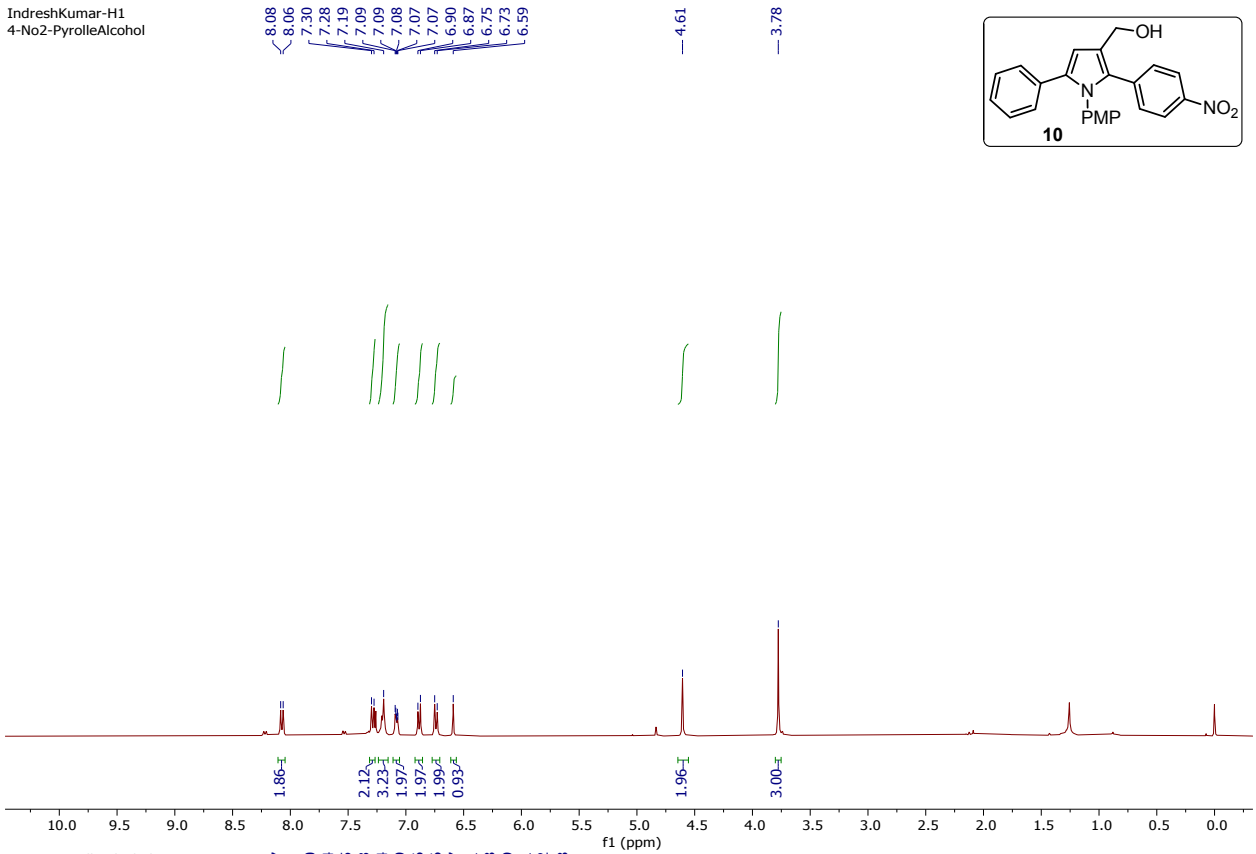

4-nitro-pyrolle alcohol_23 sep
4-NO2 Pyrole Alchohol

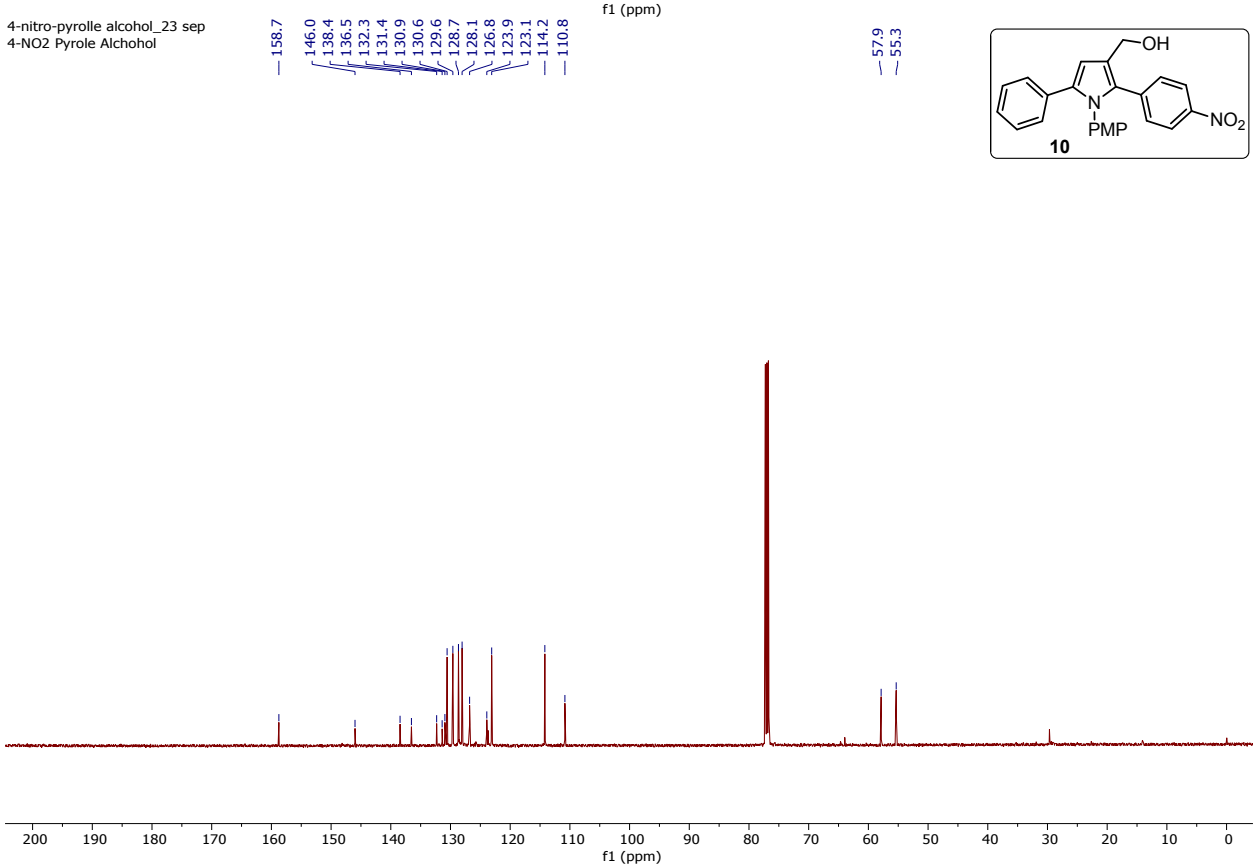

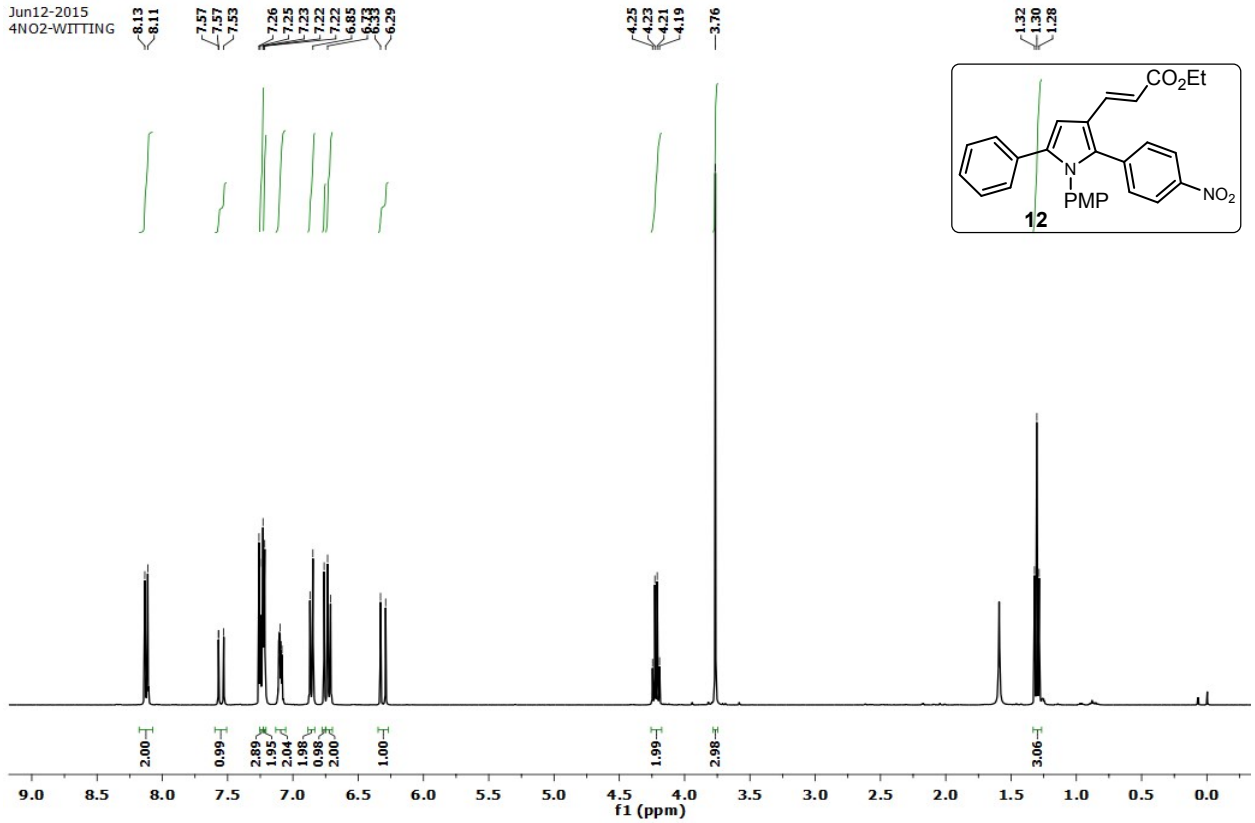
Jun12-2015
4NO2-WITTING
8.13
8.11
7.57
7.57
7.53
7.26
7.25
7.23
7.22
7.22
6.85
6.33
6.29
4.25
4.23
4.21
4.19
3.76
1.32
1.30
1.28
CO2Et
N
PMP
NO2
12
2.00
0.99
2.89
1.95
2.04
1.98
0.98
2.00
1.00
1.99
2.98
3.06
9.0
8.5
8.0
7.5
7.0
6.5
6.0
5.5
5.0
4.5
4.0
3.5
3.0
2.5
2.0
1.5
1.0
0.5
0.0
f1 (ppm)

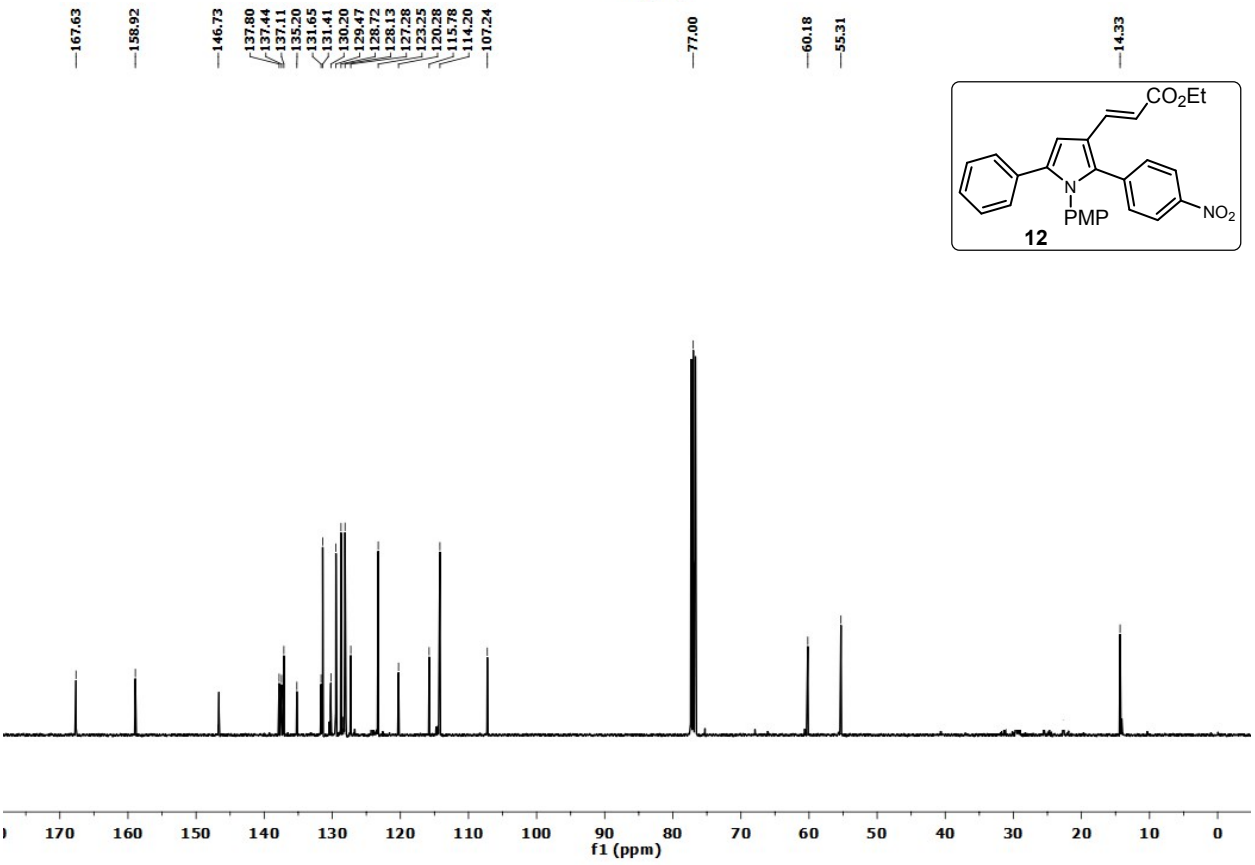
167.63
158.92
146.73
137.80
137.44
137.11
135.20
131.65
131.41
130.20
129.47
128.72
128.13
127.28
123.25
120.28
115.78
114.20
107.24
77.00
60.18
55.31
14.33
CO2Et
N
PMP
NO2
12
170
160
150
140
130
120
110
100
90
80
70
60
50
40
30
20
10
0
f1 (ppm)

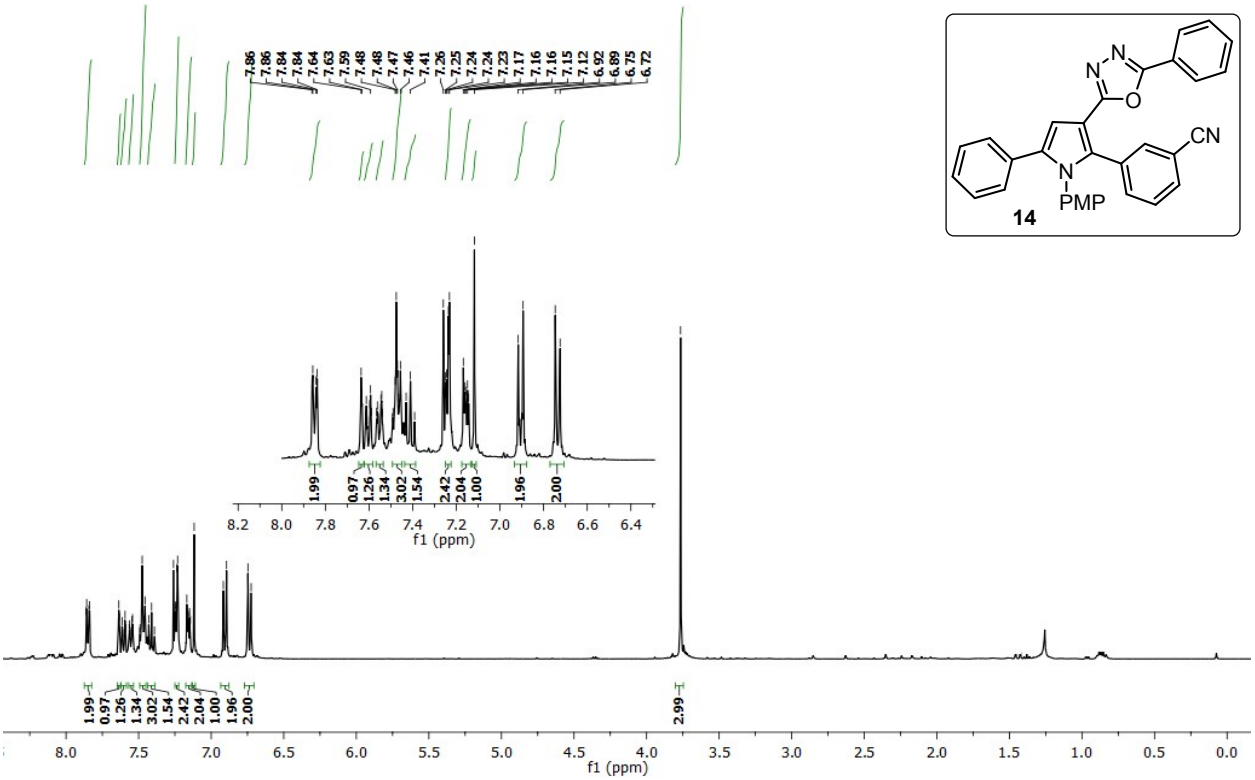
7.86
7.86
7.84
7.84
7.64
7.63
7.59
7.48
7.48
7.47
7.46
7.41
7.26
7.25
7.24
7.24
7.23
7.17
7.16
7.16
7.15
7.12
6.92
6.89
6.75
6.72
1.99
0.97
1.26
1.34
3.02
1.54
2.42
2.04
1.00
1.96
2.00
2.99
f1 (ppm)
N
N
O
CN
N
PMP
14

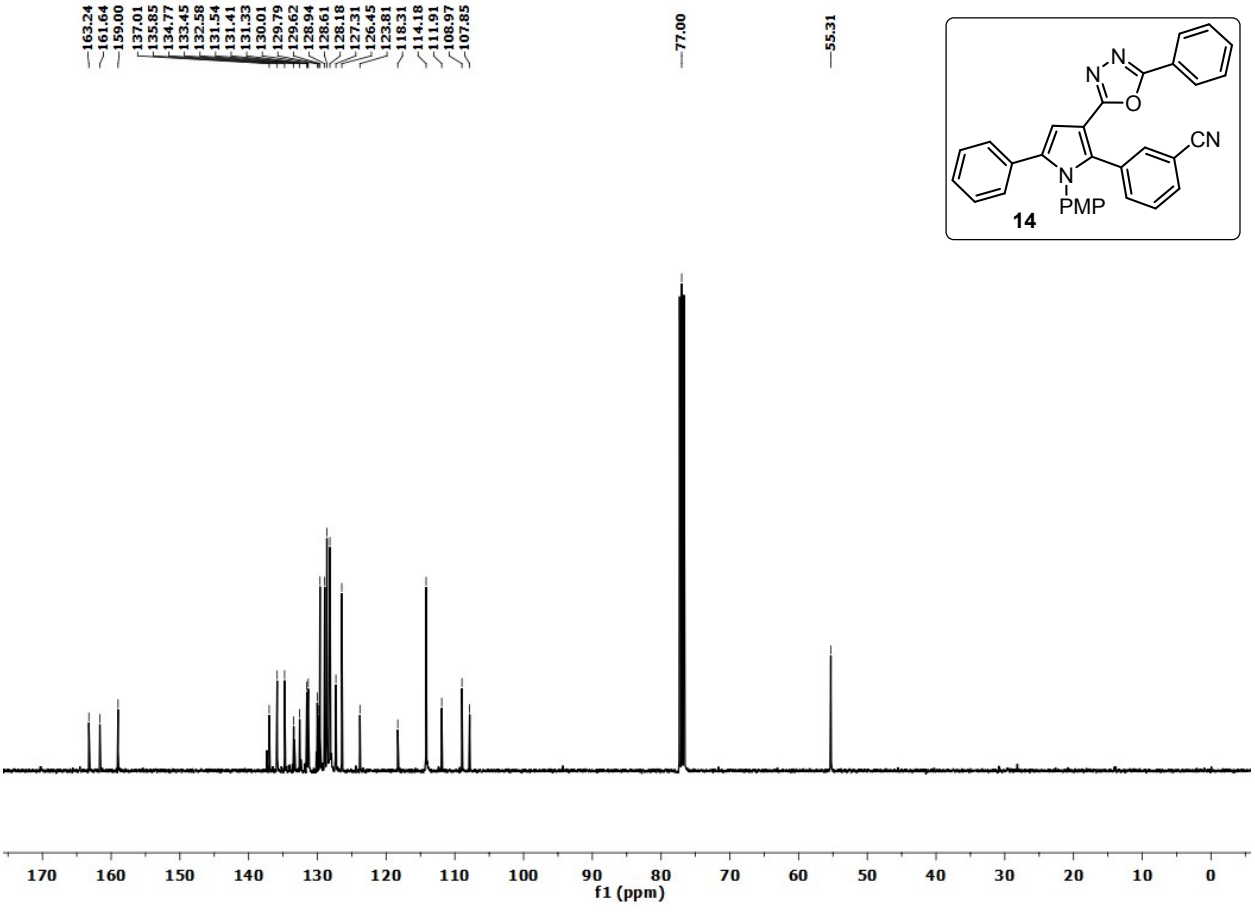
163.24
161.64
159.00
137.01
135.85
134.77
133.45
132.58
131.54
131.41
131.33
130.01
129.79
129.62
128.94
128.61
128.18
127.31
126.45
123.81
118.31
114.18
111.91
108.97
107.85
77.00
55.31
f1 (ppm)
N
N
O
CN
N
PMP
14

Crystal structure of 1-(4-methoxyphenyl)-2-(3-nitrophenyl)-5-phenyl-1H-pyrrole-3 carbaldehyde (5a) with CCDC No. 1400573

The compound 1-(4-methoxyphenyl)-2-(3-nitrophenyl)-5-phenyl-1H-pyrrole-3-carbaldehyde, $C_{24}H_{18}N_2O_4$, crystallizes in the monoclinic space group P 21/n with the unit-cell parameters: a= 23.3836(15), b= 7.8481(5), c= 24.1515(17) Å, β = 115.063(8) and Z = 4. The crystal structure was solved by direct methods using single-crystal X-ray diffraction data collected at room temperature and refined by full matrix least squares procedures to a final R-value of 0.0551 for 3359 observed reflections. X-ray intensity data of 15763 reflections (of which 7851 unique) were collected on *X'calibur* CCD area detector diffractometer equipped with graphite monochromated MoKα radiation (λ = 0.71073 Å). The crystal used for data collection was of dimensions 0.30 x 0.20 x 0.20 mm. The cell dimensions were determined by a least-squares fit of angular settings of 3935 reflections in the θ range 3.80 to 28.50°**.** The intensities were measured by ω scan mode for θ ranges 3.58 to 25.99°. 3359 reflections were treated as observed (I > 2σ (I)). Data were corrected for Lorentz, polarization and absorption factors. The structure was solved by direct methods using SHELXS97. All non-hydrogen atoms of the molecule were located in the best E-map. Full-matrix least-squares refinement was carried out using SHELXL97. The final refinement cycles converged to an R = 0.0551 and wR (F^2) = 0.0765 for the observed data. Residual electron densities ranged from -0.172 < Δρ < 0.152 eÅ^{-3}. Atomic scattering factors were taken from International Tables for X-ray Crystallography (1992, Vol. C, Tables 4.2.6.8 and 6.1.1.4). The crystallographic data are summarized in (**Table S6**). An ORTEP view of the compound with atomic labeling is shown in (**Figure S6**). The geometry of the molecule was calculated using the WinGX, PARST, and PLATON software.

Experimental

Crystal structure determination and refinement

X-ray intensity data of 15763 reflections (of which 7851 unique) were collected on *X'calibur* CCD area-detector diffractometer equipped with graphite monochromated MoKα radiation (λ = 0.71073 Å). The crystal used for data collection was of dimensions 0.30 x 0.20 x 0.20 mm. The cell dimensions were determined by least-squares fit of angular settings of 3935 reflections in the θ range 3.80 to 28.50°**.** The intensities were measured by ω scan mode for θ ranges 3.58 to 25.99°. 3359 reflections were treated as observed ($I > 2\sigma(I)$). Data were corrected for Lorentz, polarisation and absorption factors. The structure was solved by direct methods using SHELXS97.[1] All non-hydrogen atoms of the molecule were in the best E-map. Full-matrix least-squares refinement was carried out using SHELXL97.[1] The final refinement cycles converged to an R = 0.0551 and wR (F^2) = 0.0765 for the observed data. Residual electron densities ranged from $-0.172 < \Delta\rho < 0.152$ eÅ^{-3}. Atomic scattering factors were taken from International Tables for X-ray Crystallography (1992, Vol. C, Tables 4.2.6.8 and 6.1.1.4). The crystallographic data are summarized in Table S1.

Result and discussions

An ORTEP view of the compound with atomic labeling is shown in Figure S1.[2] The geometry of the molecule was calculated using the WinGX,[3] PARST[4] and PLATON [5] softwares.

References

1. Sheldrick GM (2008) Acta Cryst A64: 112
2. Farrugia LJ (1997) J Appl Cryst 30:565

3. Farrugia LJ (1999) J Appl Cryst 32:837
4. Nardelli M (1995) J Appl Cryst 28:659
5. Spek AL (2009) Acta Cryst D65: 148–155

Table S6: Crystal and experimental data for **5a**

Crystal description	white block
Crystal size	0.3 X 0.2 X 0.2 mm
Empirical formula	$C_{24}H_{18}N_2O_4$
Formula weight	398.40
Radiation, Wavelength	Mo *K*α, 0.71073 Å
Unit cell dimensions	a= 23.3836(15), b= 7.8481(5), c= 24.1515(17) Å, β = 115.063(8)
Crystal system	monoclinic
Space group	P 2_1/n
Unit cell volume	4014.9(5)
No. of molecules per unit cell, Z	8
Temperature	293(2) K
Absorption coefficient	0.091 mm^{-1}
F(000)	1664
Scan mode	ω scan
θ range for entire data collection	3.58 <θ< 25.99
Range of indices	h= -26 to 28, k= -9 to 9, l= -28 to 29

Reflections collected / unique	15763/ 7851
Reflections observed ($I > 2\sigma(I)$)	3359
R_{int}	0.0524
R_{sigma}	0.1111
Structure determination	Direct methods
Refinement	Full-matrix least-squares on F^2
No. of parameters refined	544
Final R	0.0551
wR (F^2)	0.0765
Weight	$1/[\sigma^2(F_o^2)+(0.0133P)^2 +0.0000P]$
	Where $P=[F_o^2 +2F_c^2] / 3$
Goodness-of-fit	0.894
Final residual electron density	$-0.172 < \Delta\rho < 0.152$ eÅ^{-3}
Measurement	*X'calibur system-Oxford diffraction make, U.K*
Software for structure solution:	SHELXS97 (Sheldrick, 2008)
Software for refinement:	SHELXL97 (Sheldrick, 2008)
Software for molecular plotting:	ORTEP-3 (Farrugia, 1997) PLATON
Software for geometrical calculation	PLATON (Spek, 2009) PARST
	(Nardelli, 1995)

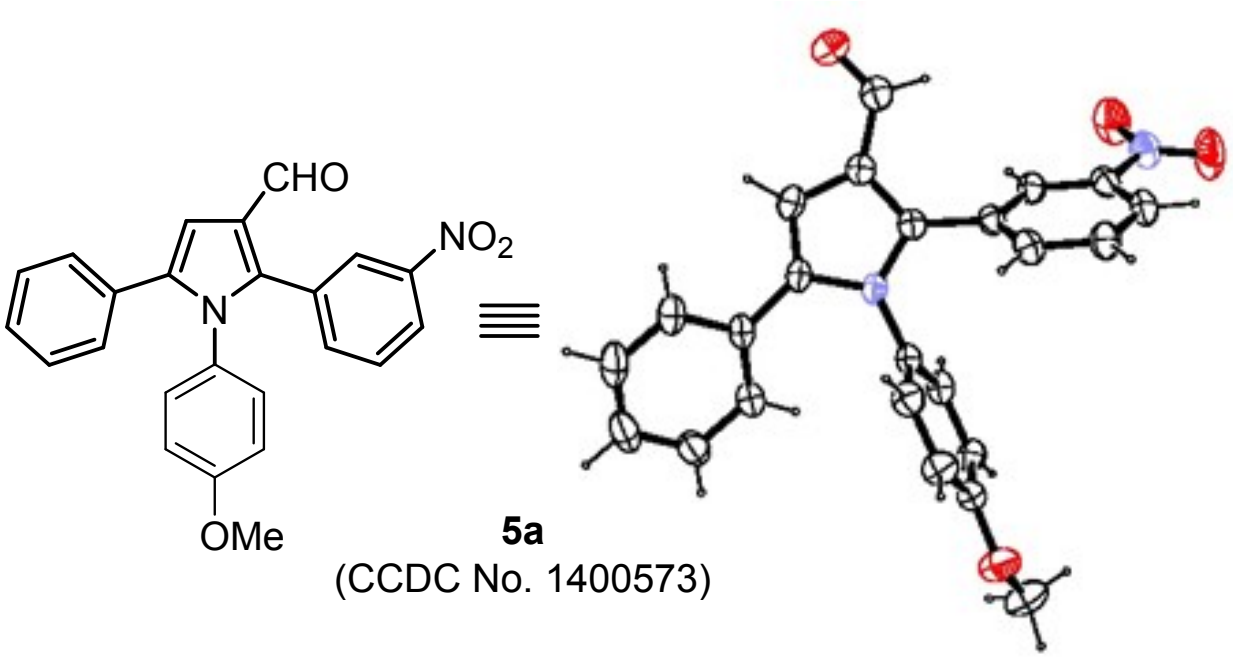

Figure S6. *ORTEP* view of the molecule with displacement ellipsoids drawn at 40%.

H atoms are shown as small spheres of arbitrary radii.